PB89-198253

Evaluation and Sensitivity Analyses Results of the MESOPUFF II Model with CAPTEX (Cross-Appalachian Tracer Experiment) Measurements

(U.S.) Environmental Protection Agency
Research Triangle Park, NC

Jun 89

U.S. Department of Commerce
National Technical Information Service
NTIS

PB89-198253

EPA/600/3-89/056
June 1989

EVALUATION AND SENSITIVITY ANALYSES RESULTS OF THE MESOPUFF II MODEL WITH CAPTEX MEASUREMENTS

by

James M. Godowitch
Atmospheric Sciences Modeling Division
Atmospheric Research and Exposure Assessment Laboratory
Research Triangle Park, North Carolina 27711

ATMOSPHERIC RESEARCH AND EXPOSURE ASSESSMENT LABORATORY
OFFICE OF RESEARCH AND DEVELOPMENT
U.S. ENVIRONMENTAL PROTECTION AGENCY
RESEARCH TRIANGLE PARK, NORTH CAROLINA 27711

REPRODUCED BY
U.S. DEPARTMENT OF COMMERCE
NATIONAL TECHNICAL INFORMATION SERVICE
SPRINGFIELD, VA. 22161

DISCLAIMER

The information in this document has been funded wholly or in part by the United States Environmental Protection Agency. It has been subject to the Agency's peer and administrative reviews, and has been approved for publication as an EPA document.

AFFILIATION

The author is on assignment to the Atmospheric Sciences Modeling Division, Atmospheric Research and Exposure Assessment Laboratory, from the National Oceanic and Atmospheric Administration, U.S. Department of Commerce.

ABSTRACT

The MESOPUFF II regional Lagrangian puff model has been evaluated and tested with the Cross-Appalachian Tracer Experiment (CAPTEX) data base. The model was applied to the six full-scale CAPTEX episodes in order to simulate the tracer plume formed from the 3-hour release of an inert, non-depositing perfluorocarbon tracer gas from either one of two selected sites. Surface tracer measurements were made at 3 hour or 6 hour intervals over an extensive sampling network of arcs downwind to 1100 km in the northeastern U. S. and southeastern Canada.

An operational evaluation was conducted by exercising the model transport and dispersion components with all default features set according to the user's guide. Transport in the model is simulated by a mixed-layer averaged wind field and an upper level wind field averaged from the mixing height to 700 mb level. Puff growth within 100 km downwind is governed by horizontal and vertical dispersion parameters derived from expressions fitted to the standard PGT curves, while time dependent formulas are applied at greater distances.

Model performance was quantitatively determined from standard statistical measures of difference and correlation between modeled and observed tracer concentrations paired in time and location. The model overpredicted peak and mean concentrations, whether paired in time and/or location. Modeled mean concentrations were within a factor of two of observed mean values in four of the experiments. The overpredictions are primarily attributed to an underestimation of vertical dispersion during neutral stability conditions which were specified during the afternoon hours after releases. Graphical maps and comparative tests between observed and modeled concentration pairs revealed that spatial displacements between the observed and modeled plumes contributed to the large scatter and low correlations found in the evaluation statistics. Analysis of plume centroid positions revealed that the greatest changes in the separation of the observed and modeled plumes occurred during the nocturnal periods. Revisions are suggested to better treat this source type in the model.

Diagnostic model test results with optional wind fields in the model (e.g. surface, 850 mb single level wind fields) and various dispersion options are compared to those from the operational model and the observed data. A surface wind field transported the modeled plume considerably slower and generally to the left of the observed plume while the single level 850 mb wind field consistently shifted the modeled plume to the right (clockwise) of the actual plume location. Model results with the mixed-layer averaged wind field displayed the best overall performance in comparisons of the position and time of impact of the peak concentration with the observed plume values at the 300 km arc.

The 24-h peak and plume average concentration results from model test runs, which focused on different options and variations in key parameters of the the dry deposition and chemical transformation modules, are compared to base case values. All model runs were performed with SO_x emissions from a realistic elevated point source. Peak SO_2 concentrations showed negligible variations when deposition or chemical transformation were omitted, however, mean SO_2 concentrations in the plume were more sensitive. Mean and peak sulfate concentrations were more sensitive than SO_2 by variations in the surface resistance and by changes in parameters controlling the chemical transformation rate.

CONTENTS

Abstract iii
Figures vi
Tables viii
Acknowledgements x

1. INTRODUCTION 1

2. DESCRIPTION OF MODEL COMPONENTS AND TECHNICAL FEATURES 4
   - Wind Fields and Related Meteorological Parameters 7
   - Dispersion Parameters 10
   - Dry Deposition and Chemical Transformation Methods 10
   - Model Grid System 12

3. MODEL EVALUATION DATA BASE 14
   - Description of the Field Measurement Program 14
   - Data Preparation for the Meteorological Processor 18

4. MODEL EVALUATION PROCEDURES AND RESULTS 30
   - Operational Model Evaluation Analyses and Results 33
     - Statistical Results for Mean and Peak Concentrations 33
     - Comparative Analyses of Plume Patterns and Positions 54
   - Diagnostic Model Test Results 64

5. MODEL SENSITIVITY RESULTS 82

6. SUMMARY AND CONCLUSIONS 93

REFERENCES 96

APPENDIX A Model test results for different puff release/sampling rates 99

Preceding page blank

LIST OF FIGURES

Number		Page
1	Flow diagram of the MESOPUFF II modeling system	5
2	Surface sampling network for the CAPTEX field program	16
3	Meteorological grid in MESOPAC II for the Dayton cases of the CAPTEX field program	19
4	Closest rawinsonde site (1 - 6) to each grid point in the MESOPAC II meteorological grid for Dayton cases	22
5	Surface meteorological stations considered in the MESOPAC II runs for the CAPTEX evaluation. Boundaries for meteorological grids are denoted (heavy solid and dashed lines)	23
6	Closest surface meteorological station (1 - 25) to each grid point in the MESOPAC II meteorological grid for Dayton cases during CAPTEX	25
7	Land use categories in the MESOPAC II meteorological grid for the Dayton cases during CAPTEX	29
8	Average concentrations obtained from sites with observed and modeled nonzero concentrations over the sampling periods during a) CAPTEX #1 and b) CAPTEX #2	41
	Same as 11a-b, except for c) CAPTEX #3 and d) CAPTEX #4	42
	Same as 11a-b, except for e) CAPTEX #5 and f) CAPTEX #7	43
9	Cumulative frequency distributions of the model and observed concentrations from the entire data set	44
10	Cumulative frequency distributions of model and observed concentrations for a) CAPTEX #1 and b) CAPTEX #2	46
	Same as 13a-b, except for c) CAPTEX #3 and d) CAPTEX #4	47
	Same as 13a-b, except for e) CAPTEX #5 and f) CAPTEX #7	48
11	Observed (O) and modeled (*) plume patterns depicted from sites with nonzero concentrations during; a) CAPTEX #1 and b) CAPTEX #2	56
	Same as 8a-b, except for c) CAPTEX #3 and d) CAPTEX #4	57
	Same as 8a-b, except for e) CAPTEX #5 and f) CAPTEX #7	58

Number | **Figures (continued)** | Page

12 Ratios of downwind distances of the model and observed plume centroid locations (D_p/D_o) and separation distance between centroid positions to the observed downwind distance (D_s/D_o) versus time of day starting from the day of release. Negative and positive values for D_s/D_o denote the model plume position is to the right and left of the observed plume, respectively. a) CAPTEX #1 and b) CAPTEX #2 results 61

Same as 9a-b, except for c) CAPTEX #3 and d) CAPTEX #4 62

Same as 9a-b, except for e) CAPTEX #5 and f) CAPTEX #7 63

13 a) Difference between the downwind distances of the centroid locations of the model (D_p) and observed (D_o) plume patterns versus time after release. b) Separation distance (D_s) between model and observed plume centroid locations versus time after release. Symbols in both figures denote events for each experiment; CAPTEX #1 (O), #2 (X), #3 (triangles), #4 (squares), #5 (stars), and #7 (diamonds) 65

14 Upper air wind speed (O) and wind direction (X) profiles at a) 18 GMT (i.e. 13 LST) and b) 00 GMT for CAPTEX #2 72

15 a) Wind speed (O) and wind direction (X) profiles and b) temperature profile at Dayton, Ohio from CAPTEX #3 74

16 Tracer concentration pattern from aircraft flight legs at different levels during the afternoon of October 3, 1983 during CAPTEX #3 75

17 Hourly variation of mixing height (Z_i) from the MESOPAC II meteorological processor for Dayton, Ohio during September 18-19, 1983 of CAPTEX #1 81

18 Average 24-h SO_2 concentration fields from the model base case run for a) Day 1 and b) Day 2. All values in units of $\mu g\ m^{-3}$ 85-86

19 Average 24-h sulfate concentration fields from the model base case for a) Day 1 and b) Day 2. All values in units of $\mu g\ m^{-3}$ 87-88

LIST OF TABLES

Number		Page
1	Calculation sequence of meteorological parameters in MESOPAC II	6
2	Computation sequence of the MESOPUFF II model code	8
3	Tracer release information for CAPTEX	15
4	Tracer sampling periods during each CAPTEX field experiment	15
5	Upper air measurements and specifications	21
6	Surface meteorological station information	24
7	Hourly surface observations and specifications	26
8	Land use categories and surface roughness lengths for MESOPAC II	28
9	Input control parameters and default features of MESOPAC II runs for CAPTEX episodes	31
10	Input parameters and specifications for MESOPUFF II runs	32
11	MESOPUFF II model evaluation results: observed and modeled concentrations paired in time and location	35
12	Test results of modeled and observed concentrations paired in time and location	37
13	Selected statistical evaluation results for each event of the CAPTEX experiments	39
14	Distribution of observed and modeled concentrations over the entire CAPTEX data set	49
15	Peak observed and model concentrations paired in location only	50
16	Peak observed and modeled concentrations paired in time only for the events of each CAPTEX experiments	52
17	High-25 observed and modeled concentrations unpaired in time and location for each CAPTEX experiment	53
18	Statistical results of observed and modeled concentrations paired in time and location from sampling arcs for CAPTEX #1-4	55
19	Peak observed and modeled concentrations unpaired in time and location for each arc from CAPTEX #1-4	55
20	Comparative results for different wind fields on peak concentration/plume transport at the 300 km arc for CAPTEX #1	67

TECHNICAL REPORT DATA
(Please read Instructions on the reverse before completing)

1. REPORT NO. EPA/600/3-89/056	2.	3. RECIPIENT'S ACCESSION NO. PB89-198253/AS
4. TITLE AND SUBTITLE EVALUATION AND SENSITIVITY ANALYSES RESULTS OF THE MESOPUFF II MODEL WITH CAPTEX MEASUREMENTS		5. REPORT DATE June 1989
		6. PERFORMING ORGANIZATION CODE
7. AUTHOR(S) James M. Godowitch		8. PERFORMING ORGANIZATION REPORT NO.
9. PERFORMING ORGANIZATION NAME AND ADDRESS Atmospheric Research and Exposure Assessment Laboratory Office of Research and Development U.S. Environmental Protection Agency Research Triangle Park, NC 27711		10. PROGRAM ELEMENT NO. A101/B/64 - 6083 (FY-89)
		11. CONTRACT/GRANT NO.
12. SPONSORING AGENCY NAME AND ADDRESS Atmospheric Research and Exposure Assessment Laboratory Office of Research and Development U.S. Environmental Protection Agency Research Triangle Park, NC 27711		13. TYPE OF REPORT AND PERIOD COVERED In-house (6/86-12/88)
		14. SPONSORING AGENCY CODE EPA/600/09

15. SUPPLEMENTARY NOTES

16. ABSTRACT

The MESOPUFF II regional Lagrangian puff model has been evaluated and tested against measurements from the Cross-Appalachian Tracer Experiment (CAPTEX) data base in an effort to assess its ability to simulate the transport and dispersion of a nonreactive, nondepositing tracer plume out to distances of over 1000 km. The model applied a mixed-layer averaged wind field to simulate boundary layer transport and Gaussian dispersion parameters to govern puff growth. The model was executed to simulate the plume formed by the 3-hour ground-level release of a perfluorocarbon tracer gas from either Dayton, Ohio or Sudbury, Ontario for six cases. Model performance was quantitatively determined from traditional statistical measures of difference and correlation between modeled and observed concentration pairs measured at 3-h or 6-h intervals. The model overpredicted peak and mean concentrations; modeled mean values were within a factor of two of observed values in four experiments. Graphical maps confirmed that the scatter among concentration pairs was primarily due to notable spatial displacements between observed and modeled tracer plumes. Analysis of plume centroid positions was employed to give quantitative information about the difference in downwind distances and separation between the observed and modeled plume patterns versus time. Diagnostic test run results, where optional single level wind fields and optional dispersion methods were exercised, are also compared to default model run results and to observed values. Sensitivity test runs focused on variations in the dry deposition and chemical transformation parameters for SO_x.

17. KEY WORDS AND DOCUMENT ANALYSIS

a. DESCRIPTORS	b. IDENTIFIERS/OPEN ENDED TERMS	c. COSATI Field/Group

18. DISTRIBUTION STATEMENT RELEASE TO PUBLIC	19. SECURITY CLASS *(This Report)* UNCLASSIFIED	21. NO. OF PAGES 109
	20. SECURITY CLASS *(This page)* UNCLASSIFIED	22. PRICE

EPA Form 2220-1 (Rev. 4-77) PREVIOUS EDITION IS OBSOLETE

Tables (continued)

Number		Page
21	Comparative results for different wind fields on peak concentration/plume transport at the 300 km arc for CAPTEX #2	68
22	Comparative results for different wind fields on at the 300 km arc for CAPTEX #3	69
23	Comparative results for different wind fields on at the 300 km arc for CAPTEX #4	70
24	Selected meteorological observations and model results at the release site for each CAPTEX experiment	71
25	Results of analysis of observed upper air wind profiles for the CAPTEX release days	77
26	Peak concentrations for CAPTEX #1 using various dispersion options	79
27	Comparison of observed and modeled mixing heights	79
28	Source characteristics and emission rates for all model sensitivity test runs	83
29	Results of model sensitivity runs: Comparisons with 24-h base case peak and mean concentrations	89
30	Results of sensitivity runs from variations in select key parameters in the model	91
A1	Differences in peak values at the initial arc for different puff release/sampling rates	99

ACKNOWLEDGEMENTS

The author wishes to extend his appreciation to Terry Clark, Norman Possiel, and Jerome Heffter for their thorough reviews and helpful suggestions which were incorporated into this final report. Thanks are also expressed to Terry Clark for providing a copy of the CAPTEX data base and for the useful discussions concerning regional model evaluation methods. Appreciation is also expressed to James Reagan for his assistance with the land use inventory.

SECTION 1

INTRODUCTION

The ability of a regional-scale air quality model to reproduce spatial pollutant concentration fields or deposition patterns on a short-term basis is strongly dependent upon its formulations for simulating the transport and dispersion processes. Models need to treat the important diurnal variations occurring in the mean and turbulent structure of the three-dimensional wind flow which directs the path of and impacts the spread of pollutant plumes. Thus, an evaluation of these crucial model components with field measurements is a critical element in establishing the credibity of any model. Although a comprehensive evaluation of all components in a model, including the chemical mechanism and removal methods, is highly desireable, the data necessary to undertake such an effort have been difficult to compile.

Experimental field studies with certain tracer gases have provided valuable meteorological and concentration measurements on regional scales, which allow evaluations to focus on the transport and dispersion components of models. One of the most recent tracer data sets available for this purpose is the Cross-Appalachian Tracer Experiment (CAPTEX). This field program was was specifically designed and conducted with the intent of acquiring an accurate tracer data set from an extensive surface sampling network with concurrent upper air meteorological measurements for use in transport and dispersion model evaluation efforts. During the CAPTEX episodes, a chemically inert, non-depositing perfluorocarbon tracer gas was released at ground-level over a 3-h period from either one of two selected sites. Uncertainties often existing in emissions were minimized as the tracer emission rate was highly controlled and concentrations were accurately measured above a relatively low background level. There was also no known interference from other sources to complicate the interpretation of the tracer measurements. The CAPTEX field program was conducted in the northeastern U.S. and southeastern Canada and the data base consists of a challenging set of seven experiments with measurements spanning up to two diurnal cycles in each episode.

The results from a few models which have been applied to particular cases or to the entire CAPTEX data set have already been reported. Lee (1987) applied a particle-in-cell numerical model to all CAPTEX cases and relied heavily on various graphical analyses to investigate model performance. Even though plots of modeled and observed plume patterns showed relatively good qualitative agreement in most cases, a scatter diagram of modeled and observed concentration pairs showed considerable variability and no correlation. In fact, the large number of zero concentrations for either the observed or predicted values indicated that notable spatial plume displacements must have existed during the course of each experiement.

The ARL (Air Resources Laboratory) Lagrangian puff model, which distributes mass vertically into different layers and transports the mass by different trajectories at each level, was evaluated in several ways with the CAPTEX data base by Draxler (1987). Several model runs were performed with various combinations of the meteorological surface and upper air data; some simulations applied finer spatial resolution and/or a more frequent temporal interval than the standard twice-daily profiles of the routine measurement network. Results were not conclusive as to whether improved spatial or temporal resolution in the input data produced more accurate model plume patterns. However, the best results for the plume trajectory were indeed found when both spatial and temporal resolutions were enhanced. Nevertheless, the predicted concentrations displayed order-of-magnitude differences from observed values when pairs were compared even when using the most highly-resolved input data. Thus, spatial plume displacements still were sufficient to produce large scatter and low correlations in concentration pairs in time and location.

Davis et al. (1986) demonstrated the ability of a Lagrangian puff model (MLAM), which allowed puffs to be vertically distributed and transported within seven vertical layers and also simulated decoupling from the surface, to explain the plume patterns in two CAPTEX episodes. While no statistical results were provided, the graphical displays showed the ability of this model to treat the considerable vertical direction shear present in one of the CAPTEX cases simulated.

Most recently, a four-dimensional data assimilation technique incorporated into a three dimensional hydrodynamic model was also applied to two CAPTEX cases by Kao and Yamada (1988), who utilized it with a random-particle diffusion model. Their graphical results of concentration pairs revealed notable scatter. Differences between observed and simulated wind components, which developed with time over the modeled plume history were mainly attributed for the discrepancies in plume centerline positions. Spatial displacements were found to be larger in the latter stages of each episode.

Clearly, the statistical and graphical analyses from these efforts revealed the difficulty that current models have in successfully replicating the three-dimensional wind flows and dispersion processes that characterize the observed data, as exemplified by concentration differences and plume pattern displacements between the models and observations.

In this report, the results of an evaluation and testing effort of the MESOPUFF II model (Scire et al., 1984a,b) with the CAPTEX data base are presented. MESOPUFF II is a second generation Lagrangian puff model which was designed to treat transport, dispersion, chemical transformation, and the removal (dry and wet) processes impacting pollutant emissions from elevated point and/or area sources on a regional scale for short-term applications. Although the chemical and deposition modules were specifically developed for sulfur oxides and nitrogen oxides, any non-reacting and/or non-depositing gaseous species may be modeled by electing not to simulate these processes during model execution. Thus, no significant changes in the mode code were needed for this evaluation effort.

The current operational version of MESOPUFF II (version 4.3) was applied and evaluated with the measurements obtained from six CAPTEX episodes. The model can take advantage of two different layer-averaged wind fields derived from surface and upper air data to transport a pollutant plume, while puff dispersion is treated with traditional dispersion parameters. Section 2 describes the model system and provides the pertinent details about the methods employed in the model to simulate these processes, while Section 3 discusses the CAPTEX data base and preparation of the various input data for the model runs.

Model performance was examined with various analyses techniques in order to investigate the model's ability to predict concentrations and plume patterns out to 1000 km from the tracer release sites. Thus, the analysis tools included, but were not limited to traditional statistical measures of difference and correlation between modeled and observed concentrations paired in time and/or location. While these statistical results provide useful quantitative information, the results of previous regional model evaluations with the CAPTEX data base have also shown the utility of various graphical analysis and more innovative quantitative measures, which helped clarify observed and modeled plume positions. Consequently, graphical displays are used to demonstrate qualitative spatial agreement between observed and simulated plumes, while analysis of plume centroid locations is the method applied to obtain quantitative measures of differences in the downwind position and separation of the respective plumes. In Section 4, all of these analysis techniques are employed in the evaluation process in order to obtain the best overall picture of the capabilities and limitations of the model for this particular application.

Uncertainty should be considered in the analysis of model predictions. The uncertainty is caused by errors in the measurements, model formulation and model input errors, as well as the inherent uncertainty associated with the stochastic nature of turbulence and diffusion of a plume. The uncertainty is not addressed directly within the evaluation analyses. However, any inadequacy in the input data is pointed out where it may contribute to model error. Particular attention in the analyses will focus on highlighting shortcomings in the model's simulation of the transport and dispersion processes.

Since the model evaluation with the CAPTEX data is limited to an assessment of the transport and dispersion components of the model system, a select group of model test runs was also undertaken to investigate the impact on pollutant concentrations from optional methods in the model or to changes to key technical parameters of the chemical transformation and dry deposition mechanisms. The model test runs simulated the SO_x emissions from a single, elevated point source and apply the same meteorological fields from one of the CAPTEX episodes. Section 5 discusses the results of model test runs from comparisons of 24-h peak and average plume concentrations from each test simulation to those of a base case run.

SECTION 2

DESCRIPTION OF MODEL COMPONENTS AND TECHNICAL FEATURES

The principal program components of the model system and their important input/output features are depicted in Figure 1. In particular, separate computer codes perform the specific functions for processing various meteorological data (READ56, MESOPAC II), for computing pollutant concentrations (MESOPUFF II), and for postprocessing operations with the calculated concentrations from receptor sites and/or grid points (MESOFILE II). All of these model components were exercised during this evaluation and testing effort. An overview of the attributes of the model components is given herein and the essential details of the methods used to compute the parameters relevant to the transport and dispersion processes, and treatments of dry removal and chemical transformation are also presented. This information provides some background to assist in the interpretation of the evaluation results and sensitivity test runs. Complete details about the various methods in the model programs can be found in Scire et al. (1984a) and complete instructions for applying the model system and optional features are contained in Scire et al. (1984b).

The READ56 processor program examines and reformats the twice-daily (i.e. 00 and 12 GMT) rawinsonde sounding measurements, and creates a formatted file of temperature and wind speed/direction profile data for each site. This program screens the profile measurements to determine if values at mandatory levels are missing. However, data quality assurance tests and inserting missing values must be performed by the user.

MESOPAC II is the primary meteorological processor program. It generates hourly gridded fields of meteorological parameters from hourly surface meteorological observations, the upper air data files produced by READ56, and land use category information. Precipitation measurements are necessary when modeling wet episodes, otherwise these data are optional. Precipitation measurements were not used in this model evaluation effort as dry conditions existed during the CAPTEX episodes. Table 1 shows the execution sequence of the MESOPAC II program code and the order of calculation of meteorological parameters. The processor program is highly modular in that each parameter is computed within a separate subroutine. A single output file of gridded meteorological parameters is produced by MESOPAC II, which serves as the primary input file to the model program.

Both processor programs were specifically designed to accept as input the various formatted meteorological data archived by the National Climatic Data Center in Ashville, North Carolina. The National Weather Service (NWS) upper air data (TDF5600 format) and hourly surface observations (CD1444 format) are the expected data sets for these programs, although comparable observed data can be substituted if all the necessary variables have been measured. Hourly measurements of ceiling height, cloud cover, and near-surface observations of temperature, pressure, wind speed and direction, and relative humidity are required.

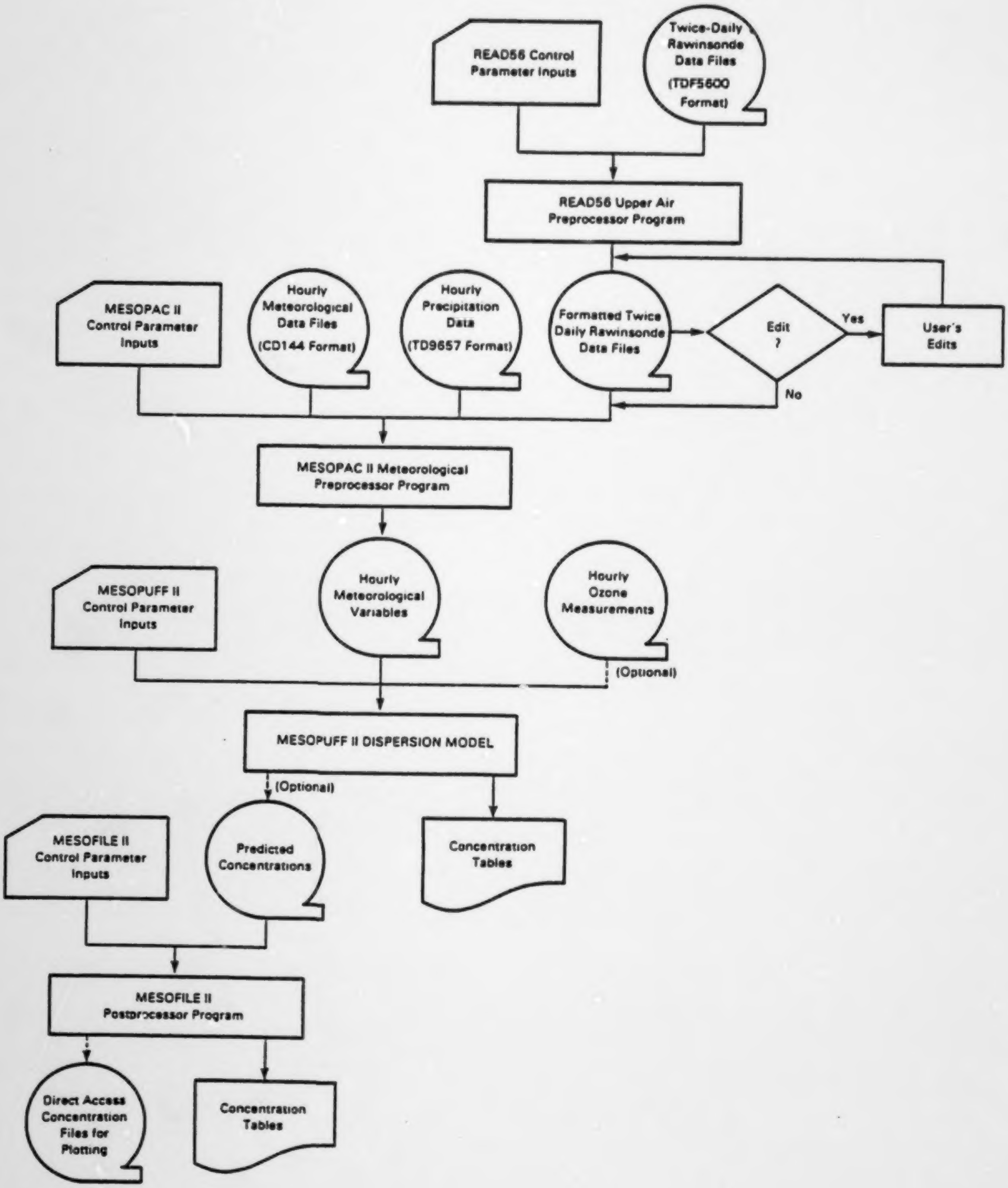
READ56 Control Parameter Inputs
Twice-Daily Rawinsonde Data Files (TDF5600 Format)
READ56 Upper Air Preprocessor Program
MESOPAC II Control Parameter Inputs
Hourly Meteorological Data Files (CD144 Format)
Hourly Precipitation Data (TD9657 Format)
Formatted Twice Daily Rawinsonde Data Files
Edit ?
Yes
No
User's Edits
MESOPAC II Meteorological Preprocessor Program
MESOPUFF II Control Parameter Inputs
Hourly Meteorological Variables
Hourly Ozone Measurements
(Optional)
MESOPUFF II DISPERSION MODEL
(Optional)
MESOFILE II Control Parameter Inputs
Predicted Concentrations
Concentration Tables
MESOFILE II Postprocessor Program
Direct Access Concentration Files for Plotting
Concentration Tables

Figure 1. Flow diagram of the MESOPUFF II modeling system. (Scire et al., 1984a)

TABLE 1

CALCULATION SEQUENCE OF METEOROLOGICAL PARAMETERS IN MESOPAC II

```
> READ USER INPUT FOR CONTROL AND TECHNICAL FEATURES
> READ UPPER AIR PROFILE DATA (00 AND 12 GMT FOR FIRST SIMULATION DAY)
     < ITERATE OVER DAY(S)
     * COMPUTE SUNRISE/SUNSET TIMES, HOURLY SOLAR ELEVATION ANGLES
     > READ PRECIPITATION DATA (OPTIONAL)
          < ITERATE OVER HOURS
             > READ HOURLY SURFACE METEOROLOGICAL STATION OBSERVATIONS
             > IF HOUR IS 00 GMT, READ NEXT 12 GMT UPPER AIR PROFILE
             > IF HOUR IS 12 GMT, READ NEXT 00 GMT UPPER AIR PROFILE
             * CALCULATE SURFACE WIND FIELD AT GRID POINTS
             * CALCULATE PGT STABILITY CLASS AT GRID POINTS
             * CALCULATE SENSIBLE HEAT FLUX (H) AT GRID POINTS
             * CALCULATE FRICTION VELOCITY ($U_*$) AT GRID POINTS
             * CALCULATE MIXING HEIGHT ($Z_i$) AT GRID POINTS
             * CALCULATE OBUKHOV LENGTH (L) AT GRID POINTS
             * CALCULATE CONVECTIVE VELOCITY ($W_*$) AT GRID POINTS
             * CALCULATE LOWER WIND FIELD AT EACH GRID POINT
             * CALCULATE UPPER WIND FIELD AT EACH GRID POINT
             * OUTPUT/STORE ALL GRIDDED METEOROLOGICAL PARAMETERS
          < END OF HOUR ITERATION
     < END OF DAY ITERATION
     * CLOSE FILES
     * END PROGRAM EXECUTION
```

MESOPUFF II computes hourly surface pollutant concentrations on a Cartesian grid and/or at user-specified, nongridded receptor sites. The model applies a Gaussian puff superposition technique to simulate a continuous plume by a series of individual puffs. The puff release and sampling rates, and source and emission information must be supplied by the user. Each puff is individually transported and its mass is subjected to dispersion, deposition (dry and/or wet) and chemical transformation. Table 2 reveals the overall execution sequence of the MESOPUFF II code and the order of simulation of the physical processes. Options exist that permit one or more of the removal mechanisms to be omitted or for input values to override default values of key technical parameters.

The MESOFILE II postprocessor package is capable of performing various analyses of individual or multiple concentration files produced by the model. Time-averaging of concentrations may be performed in an evaluation effort or statistical results can be computed to investigate variations in concentration fields produced by different model runs. The latter function is particularly useful when conducting model sensitivity studies in a comparison of different results to a base case.

WIND FIELDS AND RELATED METEOROLOGICAL PARAMETERS

Two different layer-averaged wind fields are generated by MESOPAC II in the default mode. A mixed-layer averaged wind field is determined from hourly surface observations and twice-daily upper air profile data in order to represent the mean boundary layer flow pattern between the surface and mixing height (Z_i). An upper wind field is determined over the layer from Z_i to the 700 mb height. The user may override these default fields by selecting alternate wind fields according to particular input specifications (see Scire et al., 1984b). Optional wind fields include; a single level wind field for surface, 850 mb, 700 mb, or 500 mb levels, or vertically averaged winds from Z_i to 850 mb or to 500 mb. A single wind field model is also possible by specifying the same wind field selection as the lower and upper level wind fields.

The methodology to determine the layer-averaged wind fields consists of several steps. Surface wind components (u_s, v_s) are determined at each grid point from the hourly surface station observations with the inverse distance-squared ($1/d^2$) technique. An alignment weighting factor is also applied which gives greater consideration to measurements at sites more directly upwind or downwind of a grid point. The 00 GMT and 12 GMT rawinsonde profiles are assumed to be representative of neutral/unstable conditions and stable conditions, respectively. With the appropriate rawinsonde profile, layer-averaged wind speed and direction are computed from all measurements between the surface and the current Z_i. Then the ratio of the layer-averaged and surface wind speeds (R_{ws}), and the angular difference between the layer-averaged and surface wind directions ($d\theta$) at the rawinsonde site are determined. Finally, the mixed-layer averaged horizontal wind components (U_{ml},V_{ml}) at a grid point for a particular hour are computed by applying R_{ws} and $d\theta$ from the closest rawinsonde site to the spatially-interpolated surface wind speed and direction, respectively, at that grid point.

The layer-averaged upper wind field is determined by linear interpolation in time between soundings and averaging all data over the layer from Z_i

TABLE 2

COMPUTATION SEQUENCE OF THE MESOPUFF II MODEL CODE

```
> READ INPUTS FOR TECHNICAL OPTIONS, GRID SIZE, SOURCES/EMISSIONS

> READ THE GRIDDED WIND FIELDS FOR INITIAL HOUR OF SIMULATION

  < ITERATE OVER THE HOURS FOR THE SIMULATION

    > READ OTHER GRIDDED METEOROLOGICAL PARAMETERS FOR CURRENT HOUR

    > READ GRIDDED WIND FIELDS FOR NEXT HOUR

    * INITIALIZE CONCENTRATION ARRAYS

     < PERFORM PUFF ITERATIONS

     * FOR NEW EMITTED PUFF - COMPUTE PLUME RISE

        < PERFORM PUFF SAMPLING ITERATIONS

        * TRANSPORT THE PUFF

        * COMPUTE AND APPLY DISPERSION PARAMETERS TO PUFF, AND
          TRANSFER MASS IF IN 3-LAYER MODE

        * CALCULATE AND APPLY CHEMICAL TRANSFORMATION RATE(S)

        * CALCULATE AND APPLY WET REMOVAL

        * CALCULATE AND APPLY DRY DEPOSITION

        * SAMPLE PUFF TO COMPUTE CONCENTRATION CONTRIBUTION
          AT GRID POINTS/NONGRIDDED RECEPTOR LOCATIONS

        < END PUFF SAMPLING ITERATIONS

      < END PUFF ITERATIONS

    * CALCULATE PUFF CONCENTRATIONS FOR NEXT HOUR'S CHEMISTRY

    * CALCULATE MULTI-HOUR AVERAGE CONCENTRATIONS, IF SPECIFIED

    * PRINT/STORE MODELED CONCENTRATIONS

  < END HOUR ITERATIONS

  * END PROGRAM EXECUTION
```

to the 700 mb height. The upper level wind components (U_{ul}, V_{ul}) are derived at each grid point by the $1/d^2$ method with the summation of contributions over the rawinsonde sites.

The appropriate wind field for puff transport is automatically selected by a comparison of the puff center height (Z_p) and the current Z_i on an hourly basis The source height and any plume rise are summed to obtain Z_p. For $Z_p<Z_i$, a puff is advected with the lower level wind field. If $Z_p>Z_i$, the upper wind field is used to transport the puff and its growth is governed by stability class 5 (i.e. PGT class E by default). Puff splitting is not performed by this model. However, when the multi-layer model feature is exercised, puff mass can be transferred between the mixed-layer and upper layer. For example, the amount of mass removed from the mixed-layer depends on the fractional change of Z_i since its peak value. This model feature is usually selected with the surface depletion method for dry deposition in an attempt to account for the large difference of boundary layer resistance to mixing at night compared to daylight hours.

The mixing height has particularly important roles in this model because it is involved in both transport, as just discussed, and in dispersion processes. Since Z_i is the demarcation level defining the vertical extent of the mixed-layer averaged wind field and the starting height of averaging for the upper level wind field, variations in Z_i can lead to possibly notable differences in puff transport, especially when strong vertical shears in speed and/or direction exist. As in many models, Z_i is also the critical height scale in vertical dispersion calculations. Thus, it is essential to model performance that the temporal behavior and spatial variations of Z_i be simulated realistically.

During the daylight hours, convective and mechanical mixing heights are computed with the greater of the two values being selected as Z_i at each grid point. The convective mixing height (Z_{ic}) is strongly controlled by the surface sensible heat flux ($H = w'T'$) and the temperature structure aloft. The behavior of H is highly dependent on the incoming solar radiation and the observed cloud cover. Eqs. (1) and (2) are used to compute Z_{ic} and the temperature discontinuity (ΔT) at the mixed-layer top, respectively, at the next hour (t+1) over an hourly time step (dt).

$$Z_{ic_{t+1}} = \left(Z_{ic_t}^{2} + 2H(1+E)dt/\psi - 2\Delta T_t Z_{ic_t}/\psi\right)^{1/2} + \Delta T_{t+1}/\psi \tag{1}$$

$$\Delta T_{t+1} = (2\, E\, \psi\, H\, dt)^{1/2} \tag{2}$$

The potential temperature lapse rate (ψ) is determined over a 200 m layer (default) above Z_{ic}. An entrainment coefficient (E) is included in an effort to parameterize an additional contribution to Z_{ic} growth from downward transport of warmer air with a default value for E of 0.15.

A daytime mechanical mixing height (Z_{im}) is computed from the surface friction velocity (U_*) and the Brunt-Väisälä frequency (N_b) according to;

$$Z_{im} = 2U_*^{1/2}/(fN_b) \tag{3}$$

where f is the Coriolis parameter. During nocturnal hours, the mixing height is defined solely by Z_{im}, which has an even stronger dependency on U_* according to the empirical expression in Eq. 4.

$$Z_{im} = C\ U_*^{3/2} \tag{4}$$

The current default value for C is 2400.

The friction velocity is a function of the surface wind speed, surface roughness length (Z_o), and a stability adjustment factor (Scire et al.,1984a). The land use type for each grid point should be accurately specified because Z_o is assigned internally based on representative values for the broad land use types of Sheih et al. (1979).

DISPERSION PARAMETERS

Each puff in the model is horizontally symmetric with a Gaussian distribution. Puff growth is governed by the horizontal and vertical dispersion parameters, σ_y and σ_z. Values of these parameters are computed by power law functions which were derived from fits of the Turner (1970) curves. The form of these functions is given by;

$$\sigma = A\ X^b \tag{5}$$

where A and b vary with stability class and are different for σ_y and σ_z (Scire et al., 1984b). Eq. (5) is applied to puff growth out to downwind distances (X) of 100 km (default). Thereafter, puff growth is determined with the time-dependent formulas of Heffter (1965). The crossover distance where the change in methods occurs may be overidden. An optional feature in the model uniformly disperses puffs throughout the mixed-layer depth immediately after being released.

The stability class for each grid point is determined each hour according to the Turner (1964) method. Since these PGT stability classes are defined according to cloud cover, ceiling height, solar elevation angle, and the surface wind speed, values can vary across the model grid each hour. Stability classes range from 1 (A - very unstable) to 6 (F - moderately stable).

DRY DEPOSITION AND CHEMICAL TRANSFORMATION METHODS

Although the tracer gas which is the subject of this evaluation effort is nondepositing and chemically inert, the methodologies that simulate dry removal processes and determine the transformation rates in MESOPUFF II are described because the results of the sensitivity analyses in Section 5 are obtained from variations to the default methods.

Both of these physical processes are highly complex in the atmosphere and revisions to model formulations are often performed as new experimental information becomes available. Methods to simulate these processes must be species dependent. While MESOPUFF II is capable of simulating SO_x and NO_x simultaneously, the information contained in this overview is limited to this model's treatment of SO_2 and a secondary product, fine sulfate (SO_4).

Dry deposition has received greater recognition over the past decade as an important removal process of pollutants over regional and larger scales. Consequently, more resources have been devoted to obtaining experimental dry deposition measurements of certain pollutants (Hales et al., 1987), which has provided more information to improve our understanding of deposition processes and has advanced the development of deposition parameterization methods. There has also been a notable evolution in the treatment of dry deposition in models from the simple technique of specifying a constant deposition velocity of a specific pollutant, as in the first generation of MESOPUFF (Benkley and Bass, 1979) to a physically realistic method which attempts to account for the spatial and temporal variations in meteorological parameters and surface features that influence dry removal processes. Currently, atmospheric and surface resistances are commonly employed to compute spatially-averaged deposition velocities for grid cells by consideration of the proportion of various land use types within each cell (Walcek, et al., 1986).

The dry deposition method in MESOPUFF II is also parameterized by a deposition velocity (V_d). In this scheme the removal processes consist of the vertical turbulent diffusion of pollutants through a turbulent atmospheric surface layer and a laminar sublayer, which is followed by uptake into the vegetative or surface material. Individual resistances are used to represent the ability of a species to transfer through the atmosphere and surface cover. The deposition velocity is computed as the inverse of the sum of individual resistances according as follows;

$$V_d = (r_a + r_b + r_s)^{-1} \tag{6}$$

where r_a is the aerodynamic resistance, r_b is the quasi-laminar boundary layer resistance in the proximity of the canopy or surface interface and r_s is the surface resistance. Values of r_a and r_b are temporally and spatially variable since both are dependent upon the meteorological conditions and land use. These aerodymamic resistances are computed from;

$$r_a = (k\,U_*)^{-1}(\ln(z/Z_o) - Sh \tag{6a}$$

$$r_b = (kU_*)^{-1}kB^{-1} \tag{6b}$$

where Sh is a stability correction factor and B is a surface transfer function. The value of kB^{-1} for SO_2 is 2.6. However, r_b is assumed to have a constant value of 1000 s/m for SO_4. Specifications for other modeled pollutants are given in the user guide (Scire et al., 1984b).

Surface resistances for SO_2 are a function of land use and stability class. The default values are specified internally in the module for summer conditions only and are the same as those in Sheih et al. (1979). For SO_4, the total resistance is determined by the sum of r_a and r_b because r_s is currently assigned to be zero in the module.

In the multi-layer mode of the model, only puff mass within the mixed layer is subjected to dry deposition. In contrast, the source depletion method is exercised when the single layer mode of the model is selected.

The treatment of chemical transformation in the atmosphere has also shown great advances. There is a hierarchy of methods to simulate chemical reactions and their rates that vary from the linear treatments with fixed transformation rates to sophisticated chemical mechanisms containing numerous reactions which require considerable computer resources.

Chemical conversion of SO_2 to SO_4 in MESOPUFF II is controlled by a transformation rate which is computed from a parameterized expression. Scire et al. (1984a) described the photochemical model mechanism and analyses of the model simulation results which lead to defining the primary variables that dominated the transformation rates. Expressions for transformation rates were developed from statistical regression analyses of many photochemical model run results for a range of conditions. In particular, the hourly transformation rate (k) for SO_2 to sulfate for the daytime period is computed from;

$$k = 36R^{0.55}O_3^{0.71}S^{-1.29} + 3x10^{-8}RH^4 \qquad (7)$$

where R is total solar radiation (kwatt/m^2), O_3 is the background ozone concentration (ppm), S is the stability class, and RH is relative humidity (%). These parameters were found to be the dominant variables from regression analysis of the photochemical model results. Thus, chemical conversion of SO_2 is enhanced in the model under conditions of high solar radiation, strong dispersion, high background O_3, and high humidity. The default background O_3 concentration in the model is currently 80 ppb, although the model is capable of accepting measured O_3 concentrations at sites within the model domain. Model run results in Scire et al. (1984a) indicated values for k were 2-3% per hour during the daytime, which were comparable to existing experimental results from field studies (Wilson, 1981). During the nocturnal period, the SO_2 oxidation rate is set to 0.2% h^{-1}. Equations comparable to (7) have also been developed for NO_x transformation rates.

GRID SYSTEM

The grids for MESOPAC II and MESCPUFF II are based on a Cartesian coordinate reference frame. Since it is not constructed on a latitude-longitude framework, alignment differences between N-S grid lines and the true N-S direction lines defined by longitude can become serious for grid domains larger than a few hundred kilometers, especially at middle and high latitude regions. An approach used to minimize the impact of this effect on the grid system for the CAPTEX region will be noted later.

A meteorological grid defines the set of grid points where the meteorological parameters are computed by MESOPAC II. Currently, the computer code limits the size to 40 x 40 grid indices. The computational grid in MESOPUFF II can be defined to be the same size as the meteorological grid or a subset of it. When a puff travels beyond the computational grid, it is eliminated from further consideration in concentration calculations. A sampling grid defines the set of gridded receptor points where concentrations are computed and this grid may be identical to or a subset of the computational grid. The model is also capable of computing concentrations at so-called nongridded receptor locations. This model feature can be particularly useful in a model evaluation, such as in this application to the CAPTEX tracer sampling sites, since measurement networks are not designed according to a uniformly spaced grid. Model execution time is also reduced significantly by restricting concentration calculations to the nongridded receptor locations with an option to omit calculations for the sampling grid. The grid size and grid point spacing must be defined by the user in each application. Additional details and an example configuration of the model grid systems are presented in Scire et al. (1984b).

SECTION 3

MODEL EVALUATION DATA BASE

DESCRIPTION OF THE FIELD MEASUREMENT PROGRAM

The field study phase of CAPTEX consisted of seven individual tracer releases from either Dayton, Ohio or Sudbury, Ontario over the period from mid-September to late October 1983. Information about each tracer experiment is given in Table 3. With the exception of experiment #6, which was very short to permit the start up of the next release from Sudbury, the amount of tracer gas emitted for these experiments was comparable. All releases were from ground level and a constant emission rate is assumed over a 3-hour period during each full-scale experiment.

The first four tracer releases were undertaken from Dayton and the release periods were during afternoon hours (Table 3). In contrast, both Sudbury releases were conducted at night. Nevertheless, the meteorological conditions at both sites permitted strong vertical mixing and the prevailing wind pattern in each case provided the desired transport of the tracer plume across the study region. Dayton releases were performed when the region was under the influence of large high pressure systems. At the release site, wind flows were from the southwest or west and mostly fair or partly cloudy sky conditions existed. The Sudbury releases occurred after cold front passages with northwesterly winds and mostly cloudy skies. Brown et al. (1985) provides detailed synoptic maps and discusses the weather conditions for each CAPTEX episode.

The field study region during CAPTEX encompassed the northeastern U. S. and southeastern Canada. The surface sampling network shown in Figure 2 was designed to encompass this area. It consisted of an array of individual arcs deployed at approximately 100 km intervals extending from 300 km to about 1100 km from of Dayton. Each sampling site was designated by a 3-digit number (e.g. 302); the leading digit (3) signifying the arc number in hundreds of kilometers and the next two digits (02) representing a site's relative position along each arc with numbers increasing from south to north.

The experimental measurement plan was to commence sampling concurrently at all sites along a given arc prior to the expected arrival of the tracer plume and to obtain measurements over the entire duration of plume passage. Each site was equipped with an automatic sequential sampler that was preset to collect tracer concentrations over a prescribed period. The tracer sampling system is described by Ferber et al. (1986). Tracer sampling began at the nearest arc soon after the start of a release, and at 3-h or 6-h intervals later at subsequent arcs. The sampling interval was set to 3-h at sites on the 300-km arc for Dayton releases and at some Canadian sites after the Sudbury releases to provide better temporal resolution near the release point. All other measurements were generally made over 6-h intervals. A maximum of six consecutive samples were obtained at each site,

TABLE 3

TRACER# RELEASE INFORMATION FOR CAPTEX

EXPT (#)	SITE	DATE (1983)	TIME (LST)	AMOUNT RELEASED (kg)	RATE (g/s)
1	DAYTON*	9/18	1200-1500	208	19.26
2	DAYTON	9/25	1205-1505	201	18.61
3	DAYTON	10/2	1400-1700	201	18.61
4	DAYTON	10/14	1100-1400	199	18.44
5	SUDBURY	10/25-6	2245-0145	180	16.67
6	DAYTON	10/28	1030-1100	32	2.96
7	SUDBURY	10/29	0100-0400	183	16.94

* Released from Wright-Patterson Air Force Base, otherwise at Dayton International Airport (DAY).

# Tracer used was perfluoromonomethylcyclohexane (C_7H_{14})

TABLE 4

TRACER SAMPLING PERIOD FOR EACH CAPTEX FIELD EXPERIMENT

EXPT (#)	START SAMPLING (DATE-TIME (LST)	STOP SAMPLING$ (DATE/TIME (LST)	DURATION (hours)
1	9/18-1400	9/20-0800	42
2	9/25-1300	9/28-0400	63
3	10/02-1600	10/04-1900	51
4	10/14-1300	10/16-1000	45
5	10/26-0300	10/28-0300	48
6*	10/28-1100	10/29-0800	21
7**	10/28-0100	10/30-0800	33

$ Sampling end time for most sites up through the 1000 km arc.
* Canadian sites were not put in operation in anticipation of #7.
** One site continued sampling until 11-31/1500

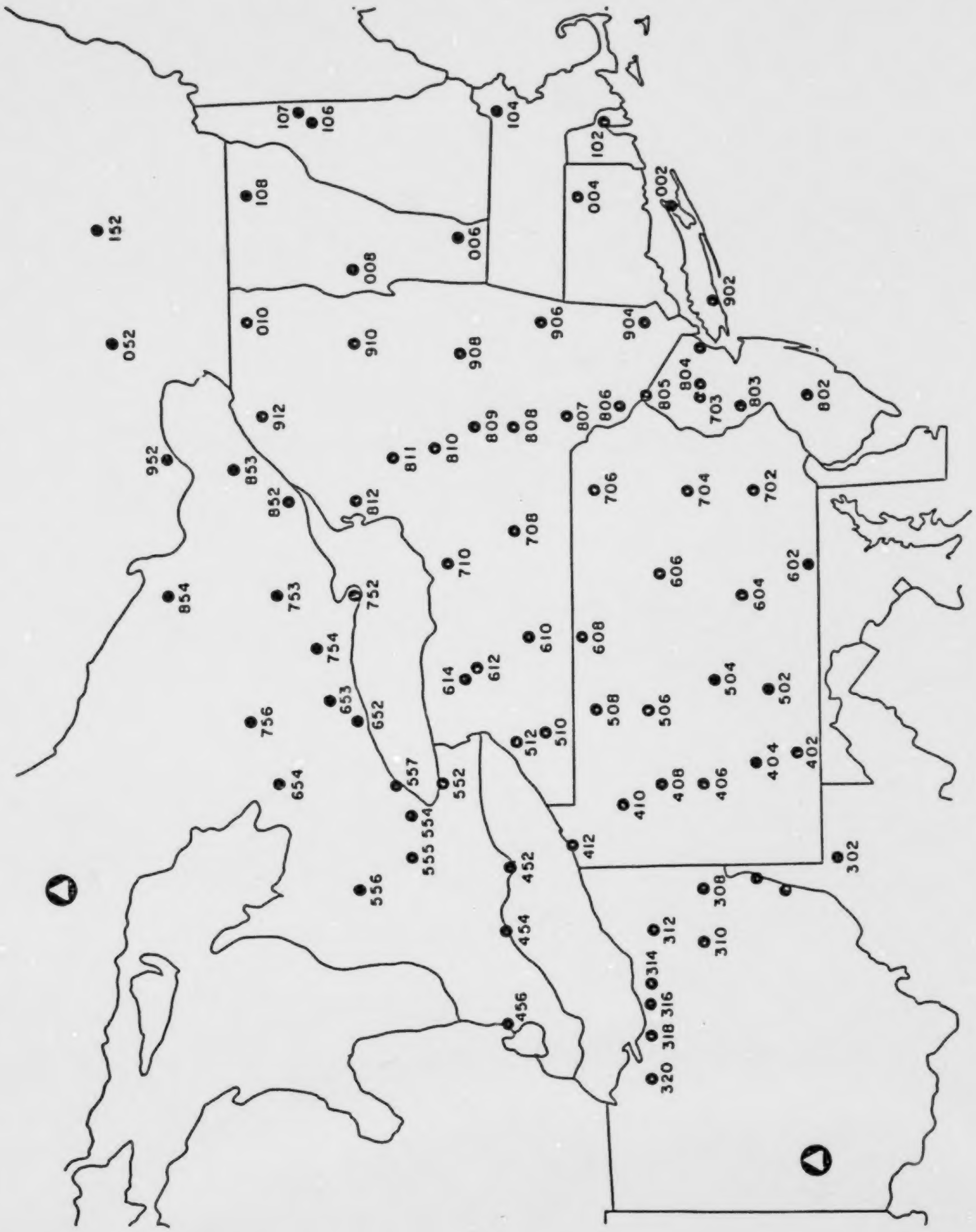
152
052
107
106
108
008
010
104
006
910
908
906
102
004
002
904
902
912
952
853
852
811
810
809
808
807
806
805
804
703
803
802
812
706
704
702
854
753
752
710
708
606
602
604
754
610
608
614
612
653
652
756
508
506
504
502
512
510
654
557
552
410
408
406
404
402
555
554
412
302
556
452
308
454
310
312
314
316
318
320
456

Figure 2. Surface sampling network for the CAPTEX field program.

so measurements spanned either 18 or 36 hours. In most cases this sampling strategy was successful since the arrival and departure times of the tracer plume, and peak concentrations could be determined at each arc to within the averaging interval of the measurements. Table 4 lists the start time and most common ending time of sampling to reveal the overall duration of each experiment. Measurements at a few sites on the most distant arcs continued even later than those posted in Table 4. The sampling period for all experiments, with the exception of #6, extended over at least one diurnal cycle. Measurement periods for the four Dayton experiments covered episodes of approximately two full days before the actual tracer plume departed the sampling network.

The acquisition of upper air meteorological data on more frequent temporal and finer spatial scales was also an important ingredient of the CAPTEX field program. During the experimental periods the National Weather Service rawinsonde sites in the CAPTEX region launched four rawinsondes daily at 6-hour intervals, instead of the routine twice-daily soundings. These supplemental soundings were made at 06 and 18 GMT. Even though the meteorological processor was not designed to accept these profiles as input, Z_i observations from these soundings may be compared to modeled values and the intermediate wind profiles are also useful in diagnosing and interpreting the causes of model variations. There were 10 additional upper air sites deployed in the region during this experimental program to provide greater spatial density of the rather sparse NWS rawinsonde network. Rawinsonde soundings were also performed during the tracer release periods at both release sites.

Several research aircraft were specially-equipped with modified tracer samplers for the CAPTEX studies. Sampling flights were conducted to obtain the horizontal dimensions of the tracer plume at various levels at different downwind distances and aircraft soundings were conducted to investigate the vertical distribution of tracer. The aircraft flight paths for each experiment and listings of the tracer concentrations measured along each flight path are provided by Ferber et al. (1986). Since the aircraft tracer measurements represented spatially-averaged concentrations sampled over several minutes along a flight path at various heights above ground, these measurements will not be directly used in the quantitative statistical analysis of the model results. However, the aircraft measurements provided valuable information about the tracer plume position, and its spatial dimensions at various times and distances from the release point. The aircraft data can be helpful in an examination of modeled and observed plume locations and in qualitative assessments of modeled and observed concentrations when possible. Results of analyses of the horizontal and vertical distribution of the aircraft tracer data have been presented by Raynor et al. (1984) and Stunder et al. (1986), respectively.

The tracer measurements collected at each sampling site were subjected to quality assurance audits and tests (Lagomarsino et al., 1987). Tracer concentrations were provided in units of femtoliters per liter (fl l^{-1}) which is equivalent to parts per 10^{15}. According to Ferber et al. (1986), an ambient background concentration of 3.4 fl l^{-1} was subtracted from all tracer measurements. The final data base contained concentrations to the nearest 1 fl l^{-1} at each site with accompanying date/time (GMT) information, and sampling interval (3 or 6 hours). The data base contained no entries for sampling periods when tracer concentrations were not collected at a site or when measurements were rejected by quality assurance procedures. A conversion factor of 1 fl $l^{-1} = 1.56x10^{-11}$ g m^{-3} was applied to modeled concentrations for their evaluation against observations.

DATA PREPARATION FOR THE METEOROLOGICAL PROCESSOR PROGRAM

Prior to the selection of surface stations and data preparation for the model evaluation runs, a meteorological grid for MESOPAC II was designed with sufficient size and adequate resolution to cover the CAPTEX region. It was also decided to use different grid sizes for the Dayton and Sudbury cases. The meteorological grid was set to 30 x 19 for the Dayton cases and 30 x 24 for both Sudbury releases. However, the grid point spacing of 37 km was the same for both grids. Therefore, the grid domain covered an 1100 km x 700 km area for the Dayton cases and an 1100 km X 888 km region for the Sudbury cases. The selection of the grid point spacing was partly based on the resolution of the land use inventory which will be discussed later. This combination of grid size and the grid point spacing provided sufficient coverage and spatial resolution of the study region. Figure 3 shows the meteorological grid for the Dayton cases. The release site is situated a sufficient distance from grid boundaries and the domain extends eastward to include the 1000 km arc. The northern boundary of the grid extended to 47°N for the Sudbury cases. These grid sizes appeared to stretch the applicability of this model grid system to a maximum limit due to the convergence of longitude lines with latitude. Differences in alignment of grid and longitude lines, taking the overall domain into consideration, were minimized by defining the N-S grid lines in the middle of the model domain to be parallel with longitude lines. Thus, alignment differences increased slowly toward the E-W boundaries.

A magnetic tape of the CAPTEX data base contained the rawinsonde data, surface tracer concentrations, aircraft tracer data, ancillary meterological measurements from several towers, and terrain heights over the CAPTEX region according to the format specifications documented in Ferber et al. (1986).

The rawinsonde sounding measurements at the release sites and the regular NWS upper air network sites were processed for input to MESOPAC II. Since a survey of the rawinsonde measurements from the 10 additional sounding sites revealed that winds were consistently missing for many levels within the boundary layer, these sites were not included in the meteorological processor runs. The wind and temperature records for each sounding were combined from separate blocks on the tape. An additional complication was that the significant wind and temperature reporting levels did not necessarily correspond, as temperatures were often detected at fewer levels. Consequently, an upper air profile with temperatures and winds at common levels up to 500 mb was constructed by deriving values by linear interpolation at heights where the other parameter was measured. The formatted upper air data files were reviewed to insure that soundings existed at 00 and 12 GMT for all days in the simulation period required to model each experiment. These files were also examined to make sure values existed at all mandatory levels (i.e. 1000, 850, 500 mb) because the MESOPAC II code ceases execution when an upper air profile or data are missing. Table 5

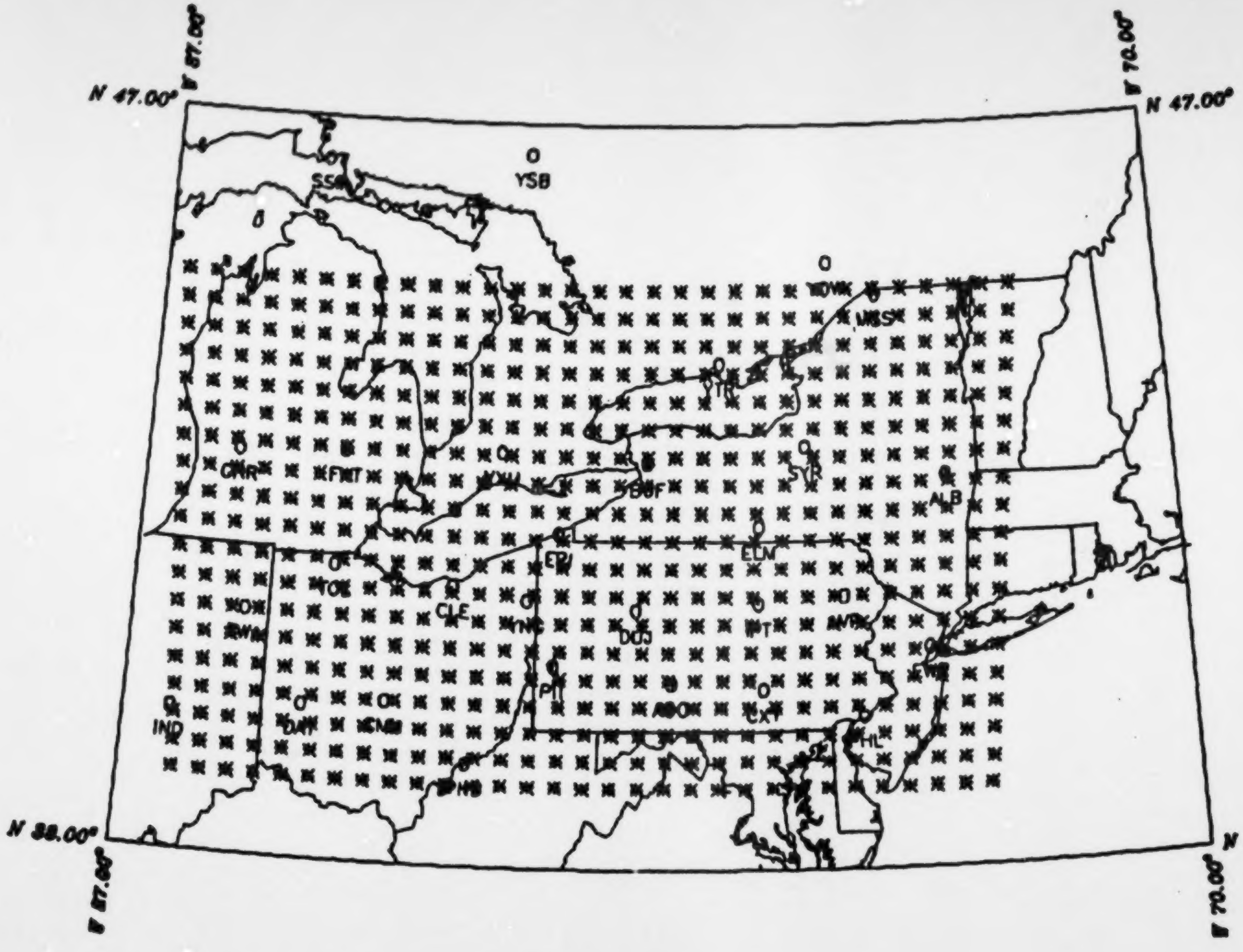
N 47.00°
W 87.00°
W 70.00°
N 47.00°
N 38.00°
W 87.00°
N 38.00°
W 70.00°
YSB
SSM
GRR
FNT
BUF
YTR
SYR
ALB
MSS
ERI
ELM
TOL
CLE
YNG
DUJ
IPT
AVP
EWR
PIT
AOO
CXY
PHL
IND
DAY
CMH
HTS

Figure 3. Meteorological grid in MESOPAC II for the Dayton cases of the CAPTEX field program.

contains information about the upper air measurements required as input to MESOPAC II. These upper air data were subjected to various quality control/assurance tests during processing and archival procedures (Ferber et al., 1986). Figure 4 displays the closest rawinsonde station to each grid point by a number from 1 to 6. There were six rawinsonde sites available for the Dayton cases. It is evident from Figure 4 that each site is assumed to represent a rather large section of the model grid, ranging from 300 km to over 400 km in most directions.

The hourly surface meteorological observations at all regularly reporting stations in the northeastern United States and for several stations in Ontario were also obtained, as the processor cannot compute fields of meteorological parameters without hourly surface measurements. Since the number of stations available was much greater than MESOPAC II's limit of 25 sites, a single group of stations was selected and their observations were prepared for model input. Figure 5 shows the full set of stations selected for the model evaluation. These sites were chosen in order to cover the entire CAPTEX region and to also provide a relatively uniform intersite spacing across the region. The hourly observations at each release site were included as input for the experiments with a release from that site. Table 6 lists the entire group of stations whose observations were use as input for the model runs. A set of 25 stations was used in all cases, however, a few sites were only used in the Dayton experiments and other stations were substituted for the Sudbury cases. In particular, stations closer to a release location were selected in an attempt to provide better definition of the flow pattern around the time of release. For example, two stations in Indiana and one in Michigan were included in the Dayton cases, but these stations were excluded from the model runs for the Sudbury releases in lieu of sites closer to Sudbury. Although the dimensions of arrays in the program code could be easily increased to accommodate data at additional stations, the purpose of the operational evaluation was to exercise the code as specified in the user guide. Figure 6 reveals that the greater number of surface sites is translated into finer spatial resolution than that for the upper air stations.

There are notable elevation differences among the stations in Table 6. The relatively level terrain across Ohio and Ontario gives way to higher elevations and complex terrain variations among the stations across Pennsylvania and New York. Nevertheless, elevation data are not required by MESOPAC II since flat terrain is assumed by this model.

The MESOPAC II code contains no provisions for missing data and execution stops if it detects missing data or an error occurs in the date/time information. Therefore, it is also imperative that the hourly surface observation files be carefully scrutinized for missing data and that editting corrections be performed before model execution. Fortunately, only a small fraction of observations were missing from the 25 selected sites. In most cases a single hour of observations was missing, although 2 or 3 consecutive hours of missing data occurred occasionally. In all instances, values were estimated by linear interpolation from observations taken immediately before and after the missing hour(s). Table 7 presents the surface meteorological variables required as input to MESOPAC II. The information about each variable is taken from CD144 (Card Deck 144) format specifications. The files of hourly observations were also reviewed and values were derived when a single variable was missing.

TABLE 5

UPPER AIR MEASUREMENTS AND SPECIFICATIONS#

VARIABLE	UNITS	RESOLUTION
Pressure	mb	0.1 mb
Height	m, MSL*	1 m
Temperature	degrees (°K)	0.1°
Wind speed	m/s	0.1 m/s
Wind direction	degrees (°)	1 °

# Units and resolution of the format requirements in MESOPAC II.
* altitude above mean sea level

```
STATION NUMBER OF CLOSEST RAWINSONDE STATION TO EACH GRID POINT

MULTIPLY ALL VALUES BY 10 **    0

19 \  6  6  6  6  6  6  6  6  6  6  6  6  5  5  5  5  5  5  5  5  5  5  5  3  3  3  3  3  3  3
   \  +  +  +  +  +  +  +  +  +  +  +  +  +  +  +  +  +  +  +  +  +  +  +  +  +  +  +  +  +  +
18 \  6  6  6  6  6  6  6  6  6  6  6  6  5  5  5  5  5  5  5  5  5  5  5  3  3  3  3  3  3  3
   \  +  +  +  +  +  +  +  +  +  +  +  +  +  +  +  +  +  +  +  +  +  +  +  +  +  +  +  +  +  +
17 \  6  6  6  6  6  6  6  6  6  6  6  6  5  5  5  5  5  5  5  5  5  5  5  3  3  3  3  3  3  3
   \  +  +  +  +  +  +  +  +  +  +  +  +  +  +  +  +  +  +  +  +  +  +  +  +  +  +  +  +  +  +
16 \  6  6  6  6  6  6  6  6  6  6  6  6  5  5  5  5  5  5  5  5  5  5  5  3  3  3  3  3  3  3
   \  +  +  +  +  +  +  +  +  +  +  +  +  +  +  +  +  +  +  +  +  +  +  +  +  +  +  +  +  +  +
15 \  6  6  6  6  6  6  6  6  6  6  6  6  5  5  5  5  5  5  5  5  5  5  5  3  3  3  3  3  3  3
   \  +  +  +  +  +  +  +  +  +  +  +  +  +  +  +  +  +  +  +  +  +  +  +  +  +  +  +  +  +  +
14 \  6  6  6  6  6  6  6  6  6  6  6  6  5  5  5  5  5  5  5  5  5  5  5  3  3  3  3  3  3  3
   \  +  +  +  +  +  +  +  +  +  +  +  +  +  +  +  +  +  +  +  +  +  +  +  +  +  +  +  +  +  +
13 \  6  6  6  6  6  6  6  6  6  6  6  6  5  5  5  5  5  5  5  5  5  5  5  3  3  3  3  3  3  3
   \  +  +  +  +  +  +  +  +  +  +  +  +  +  +  +  +  +  +  +  +  +  +  +  +  +  +  +  +  +  +
12 \  6  6  6  6  6  6  6  6  6  6  6  6  5  5  5  5  5  5  5  5  5  5  5  3  3  3  3  3  3  3
   \  +  +  +  +  +  +  +  +  +  +  +  +  +  +  +  +  +  +  +  +  +  +  +  +  +  +  +  +  +  +
11 \  6  6  6  6  6  6  6  6  6  6  6  6  5  5  5  5  5  5  5  5  5  5  5  3  3  3  3  3  3  3
   \  +  +  +  +  +  +  +  +  +  +  +  +  +  +  +  +  +  +  +  +  +  +  +  +  +  +  +  +  +  +
10 \  6  6  6  6  6  6  6  6  6  6  6  4  4  4  5  5  5  5  5  5  5  5  5  3  3  3  3  3  3  3
   \  +  +  +  +  +  +  +  +  +  +  +  +  +  +  +  +  +  +  +  +  +  +  +  +  +  +  +  +  +  +
 9 \  6  6  6  6  6  6  6  6  6  5  4  4  4  4  4  4  5  5  5  5  5  5  5  3  3  3  3  3  3  3
   \  +  +  +  +  +  +  +  +  +  +  +  +  +  +  +  +  +  +  +  +  +  +  +  +  +  +  +  +  +  +
 8 \  1  1  1  1  1  1  1  1  6  4  4  4  4  4  4  4  4  4  4  5  5  5  5  3  3  3  3  3  3  3
   \  +  +  +  +  +  +  +  +  +  +  +  +  +  +  +  +  +  +  +  +  +  +  +  +  +  +  +  +  +  +
 7 \  1  1  1  1  1  1  1  1  1  4  4  4  4  4  4  4  4  4  4  4  2  2  2  2  3  3  3  3  3  3
   \  +  +  +  +  +  +  +  +  +  +  +  +  +  +  +  +  +  +  +  +  +  +  +  +  +  +  +  +  +  +
 6 \  1  1  1  1  1  1  1  1  1  1  4  4  4  4  4  4  4  4  4  2  2  2  2  2  2  3  3  3  3  3
   \  +  +  +  +  +  +  +  +  +  +  +  +  +  +  +  +  +  +  +  +  +  +  +  +  +  +  +  +  +  +
 5 \  1  1  1  1  1  1  1  1  1  1  4  4  4  4  4  4  4  4  4  2  2  2  2  2  2  2  2  3  3  3
   \  +  +  +  +  +  +  +  +  +  +  +  +  +  +  +  +  +  +  +  +  +  +  +  +  +  +  +  +  +  +
 4 \  1  1  1  1  1  1  1  1  1  1  4  4  4  4  4  4  4  4  2  2  2  2  2  2  2  2  2  2  3  3
   \  +  +  +  +  +  +  +  +  +  +  +  +  +  +  +  +  +  +  +  +  +  +  +  +  +  +  +  +  +  +
 3 \  1  1  1  1  1  1  1  1  1  1  4  4  4  4  4  4  4  2  2  2  2  2  2  2  2  2  2  2  2  2
   \  +  +  +  +  +  +  +  +  +  +  +  +  +  +  +  +  +  +  +  +  +  +  +  +  +  +  +  +  +  +
 2 \  1  1  1  1  1  1  1  1  1  1  4  4  4  4  4  4  4  2  2  2  2  2  2  2  2  2  2  2  2  2
   \  +  +  +  +  +  +  +  +  +  +  +  +  +  +  +  +  +  +  +  +  +  +  +  +  +  +  +  +  +  +
 1 \  1  1  1  1  1  1  1  1  1  1  1  4  4  4  4  4  2  2  2  2  2  2  2  2  2  2  2  2  2  2
   \  +  +  +  +  +  +  +  +  +  +  +  +  +  +  +  +  +  +  +  +  +  +  +  +  +  +  +  +  +  +
    ------------------------------------------------------------------------------------------
      1  2  3  4  5  6  7  8  9 10 11 12 13 14 15 16 17 18 19 20 21 22 23 24 25 26 27 28 29 30
```

Figure 4. Closest rawinsonde site (1 - 6) to each grid point in the MESOPAC II meteorological grid for Dayton cases.

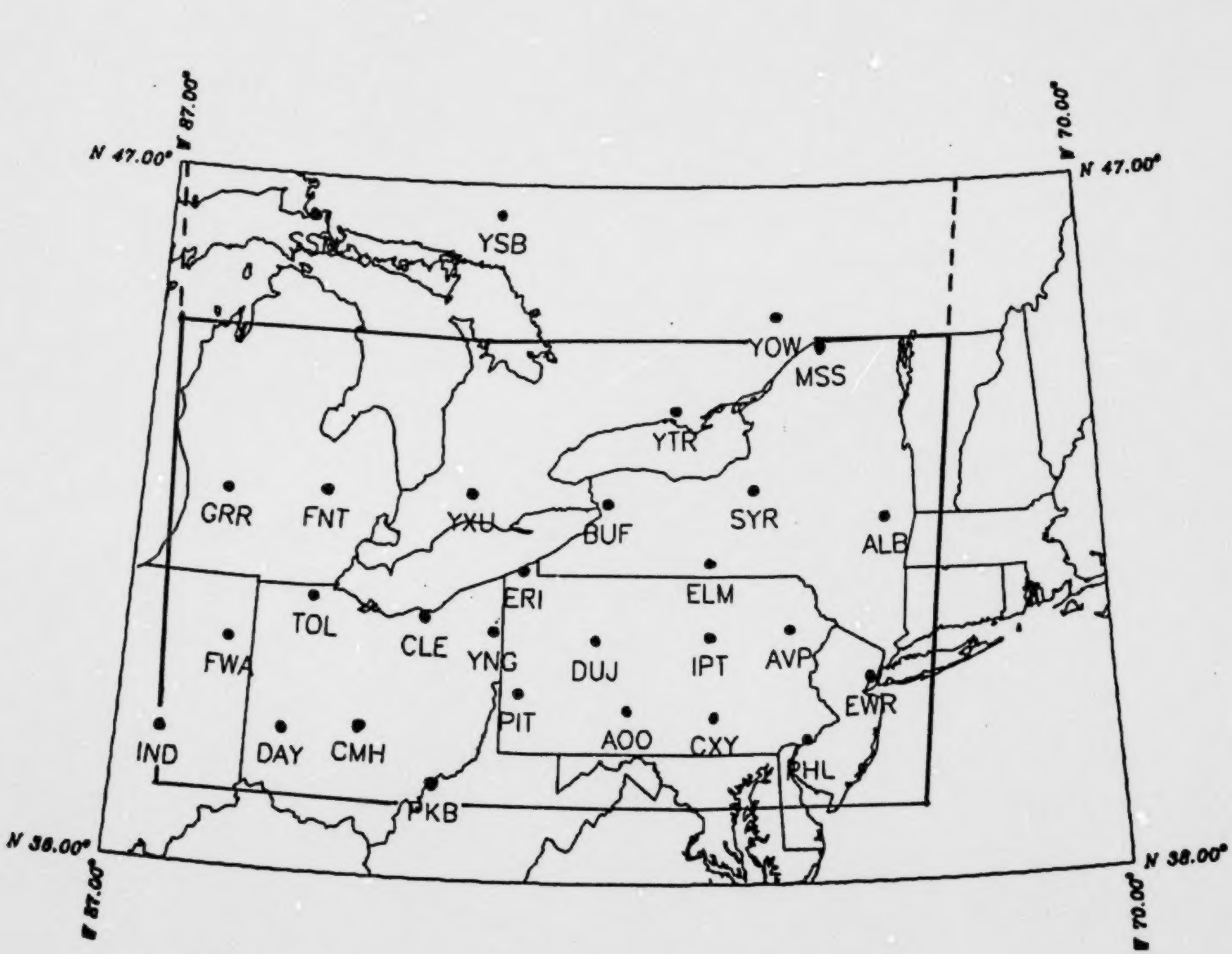
N 47.00°
W 87.00°
W 70.00°
N 47.00°
YSB
SSM
YOW
MSS
YTR
GRR
FNT
YXU
BUF
SYR
ALB
ERI
ELM
TOL
CLE
YNG
DUJ
IPT
AVP
FWA
EWR
PIT
AOO
CXY
IND
DAY
CMH
PHL
PKB
N 38.00°
W 87.00°
N 38.00°
W 70.00°

Figure 5. Surface meteorological stations considered in the MESOPAC II runs for the CAPTEX evaluation. Boundaries for meteorological grids are denoted (heavy solid and dashed lines).

TABLE 6

SURFACE METEOROLOGICAL STATION INFORMATION

LOCATION	SITE ID	LATITUDE (DEG. N)	LONGITUDE (DEG. W)	ELEVATION (m ASL)
Albany, NY	ALB	42.75	73.80	89.
Altoona, PA	AOO	40.30	78.32	448.
Avoca, PA	AVP	41.33	75.53	289.
Buffalo, NY	BUF	42.93	78.73	215.
Cleveland, OH	CLE	41.42	81.87	245.
Dayton, OH	DAY	39.90	84.20	306.
Dubois, PA	DUJ	41.18	78.90	556.
Elmira, NY	ELM	42.17	76.90	291.
Erie, PA	ERI	42.08	80.18	225.
Flint, MI	FNT	42.97	83.75	234.
Ft. Wayne, IN	FWA	41.00	85.20	252.
Grand Rapids,MI	GRR	42.90	85.50	245.
Harrisburg, PA	CXY	40.22	76.85	107.
Indianapolis,IN	IND	39.75	86.25	246.
Messina, NY	MSS	44.93	74.85	65.
Newark, NJ	EWR	40.70	74.17	9.
Philadelphia, PA	PHL	39.88	75.25	8.
Pittsburgh, PA	PIT	40.50	80.22	374.
Parkerburg, WV	PKB	39.27	81.57	194.
*Sault Ste Marie,MI	SSM	46.47	84.37	221.
Syracuse, NY	SYR	43.12	76.12	124.
Toledo, OH	TOL	41.60	83.80	211.
Williamsport, PA	IPT	41.25	76.92	160.
Youngtown, OH	YNG	41.27	80.67	362.
Canadian Sites:				
London, ONT.	YXU	43.05	81.09	278.
*Ottawa, ONT.	YOW	45.32	75.67	126.
*Sudbury, ONT.	YSB	46.62	80.80	348.
Trenton, ONT.	YTR	44.12	77.53	81.
Alternate Site:				
#Columbus, OH	CMH	40.00	82.88	254.

* applied in the Sudbury cases only in place of FWA, IND, YNG

# Substituted for DAY in a test case only

```
                                        MESOPUFF   VERSION  4.0    LEVEL 870421
********************************************************************************************************************************

STATION NUMBER OF CLOSEST SURFACE MET. STATION TO EACH GRID POINT

MULTIPLY ALL VALUES BY 10 **   0

19 \  14  14  14  14  12  12  12  12  12  25  25  25  25  25  24  24  24  24  24  24  24  24  17  17  17  17  17  17  17  17
   \   +   +   +   +   +   +   +   +   +   +   +   +   +   +   +   +   +   +   +   +   +   +   +   +   +   +   +   +   +   +
18 \  14  14  14  14  12  12  12  12  12  25  25  25  25  25  25  24  24  24  24  24  24  24  24  17  17  17  17  17  17  17
   \   +   +   +   +   +   +   +   +   +   +   +   +   +   +   +   +   +   +   +   +   +   +   +   +   +   +   +   +   +   +
17 \  14  14  14  14  12  12  12  12  12  25  25  25  25  25  25  24  24  24  24  24  24  24  24  17  17  17  17  17  17  17
   \   +   +   +   +   +   +   +   +   +   +   +   +   +   +   +   +   +   +   +   +   +   +   +   +   +   +   +   +   +   +
16 \  14  14  14  14  12  12  12  12  12  25  25  25  25  25  25   4   4  24  24  24  24  24  24  21  21  17  17  17   1   1
   \   +   +   +   +   +   +   +   +   +   +   +   +   +   +   +   +   +   +   +   +   +   +   +   +   +   +   +   +   +   +
15 \  14  14  14  14  12  12  12  12  12  25  25  25  25  25  25   4   4   4  24  24  24  24  21  21  21  21   1   1   1   1
   \   +   +   +   +   +   +   +   +   +   +   +   +   +   +   +   +   +   +   +   +   +   +   +   +   +   +   +   +   +   +
14 \  14  14  14  14  12  12  12  12  12  25  25  25  25  25  25   4   4   4   4   4  24  21  21  21  21  21   1   1   1   1
   \   +   +   +   +   +   +   +   +   +   +   +   +   +   +   +   +   +   +   +   +   +   +   +   +   +   +   +   +   +   +
13 \  14  14  14  14  14  12  12  12  12  25  25  25  25  25  25   4   4   4   4   4  21  21  21  21  21  21   1   1   1   1
   \   +   +   +   +   +   +   +   +   +   +   +   +   +   +   +   +   +   +   +   +   +   +   +   +   +   +   +   +   +   +
12 \  14  14  14  14  14  12  12  12  12  25  25  25  25  25  10  10   4   4   4   4   9   9  21  21  21  21   1   1   1   1
   \   +   +   +   +   +   +   +   +   +   +   +   +   +   +   +   +   +   +   +   +   +   +   +   +   +   +   +   +   +   +
11 \  14  14  14  14  14  12  12  12  12   5  25  25  10  10  10  10   4   4   4   9   9   9   9   9  21   3   1   1   1   1
   \   +   +   +   +   +   +   +   +   +   +   +   +   +   +   +   +   +   +   +   +   +   +   +   +   +   +   +   +   +   +
10 \  14  14  14  14  22  22  22  22  22   5   5   5  10  10  10  10  10   8   8   9   9   9   9   9   3   3   3   1   1   1
   \   +   +   +   +   +   +   +   +   +   +   +   +   +   +   +   +   +   +   +   +   +   +   +   +   +   +   +   +   +   +
 9 \  13  13  13  13  22  22  22  22   5   5   5   5  23  23  10  10   8   8   8  16  16  16  16   3   3   3   3   3  11  11
   \   +   +   +   +   +   +   +   +   +   +   +   +   +   +   +   +   +   +   +   +   +   +   +   +   +   +   +   +   +   +
 8 \  13  13  13  13  13  22  22  22   5   5   5   5  23  23  23   8   8   8   8  16  16  16  16   3   3   3   3  11  11  11
   \   +   +   +   +   +   +   +   +   +   +   +   +   +   +   +   +   +   +   +   +   +   +   +   +   +   +   +   +   +   +
 7 \  13  13  13  13  13  22  22  22   5   5   5   5  23  23  23   8   8   8   8   2  16  16  16   3   3   3  11  11  11  11
   \   +   +   +   +   +   +   +   +   +   +   +   +   +   +   +   +   +   +   +   +   +   +   +   +   +   +   +   +   +   +
 6 \  13  13  13  13  13   7   7  22   5   5   5   5  19  19  19  19   8   8   2   2   6   6   6   6   3   3  11  11  11  11
   \   +   +   +   +   +   +   +   +   +   +   +   +   +   +   +   +   +   +   +   +   +   +   +   +   +   +   +   +   +   +
 5 \  15  15  13  13   7   7   7   7   7   5   5  19  19  19  19  19   2   2   2   2   6   6   6   6  18  18  18  11  11  11
   \   +   +   +   +   +   +   +   +   +   +   +   +   +   +   +   +   +   +   +   +   +   +   +   +   +   +   +   +   +   +
 4 \  15  15  15   7   7   7   7   7   7  20  20  20  19  19  19  19   2   2   2   2   6   6   6   6  18  18  18  18  11  11
   \   +   +   +   +   +   +   +   +   +   +   +   +   +   +   +   +   +   +   +   +   +   +   +   +   +   +   +   +   +   +
 3 \  15  15  15   7   7   7   7   7  20  20  20  20  20  19  19  19   2   2   2   2   6   6   6   6  18  18  18  18  18  11
   \   +   +   +   +   +   +   +   +   +   +   +   +   +   +   +   +   +   +   +   +   +   +   +   +   +   +   +   +   +   +
 2 \  15  15  15   7   7   7   7   7  20  20  20  20  20  20  20  19   2   2   2   2   6   6   6  18  18  18  18  18  18  18
   \   +   +   +   +   +   +   +   +   +   +   +   +   +   +   +   +   +   +   +   +   +   +   +   +   +   +   +   +   +   +
 1 \  15  15  15   7   7   7   7   7  20  20  20  20  20  20  20  20   2   2   2   2   6   6   6  18  18  18  18  18  18  18
   \   +   +   +   +   +   +   +   +   +   +   +   +   +   +   +   +   +   +   +   +   +   +   +   +   +   +   +   +   +   +
    --------------------------------------------------------------------------------------------------------------------------

       1   2   3   4   5   6   7   8   9  10  11  12  13  14  15  16  17  18  19  20  21  22  23  24  25  26  27  28  29  30
```

Figure 6. Closest surface meteorological station (1-25) to each grid point of the MESOPAC II meteorological grid for Dayton cases during CAPTEX.

TABLE 7

HOURLY SURFACE OBSERVATIONS AND SPECIFICATIONS

VARIABLE	UNITS	RESOLUTION
Wind speed	knots	1
Wind direction	degrees (°)	10°
Temperature	F°	1
Pressure (station)	Inches Hg	0.01
Relative humidity	%	1
Cloud cover	Tenths (x10)	1
Ceiling height	Ft, AGL#	100
Weather code (Precip. type)*	-----	-----

* Card Deck 1444 specifications
# height above ground level

However, no quality assurance tests were performed on the surface observations since various quality control procedures are routinely conducted during the data archival process by the National Climatic Data Center.

It should also be stated that these surface observations do not represent actual time-averaged measurements over 1-hour periods. The hourly observations are actually taken over a relatively short interval prior to each hour. It is particularly notable that wind direction is recorded only to the nearest 10°. There is no random number technique in MESOPAC II to generate a value for the units place and observed directions are multiplied by 10 in the model. While wind speed is reported to the nearest 1 knot, observed wind speeds less than 3 knots are rare due to instrument response limitations. These light wind conditions are usually reported as calm (i.e. zero wind speed).

The land use type must also be provided at each grid point in the meteorological domain. A list of the land use categories and their associated surface roughness lengths built into the preprocessor code are given in Table 8. Since land use information was not part of the CAPTEX data base, land use types were obtained from an existing in-house land use inventory (Page,1980). Briefly, this inventory contained the percentage contributions of 12 different land use types for cells covering 1/6° latitude by 1/4° longitude areas (i.e. approximately 18.5 km square grids). The land use cell whose coordinates were closest to each grid point was determined and the land use type exhibiting the largest percentage was selected to represent the land use at each grid point. At most grid points, a single land use type was dominant with percentages greater than 70%. There were a few cases when the agriculture (Category 1) and forest (Category 4 or 5) categories were the major land use types and exhibited nearly equivalent percentages. Category 2 (see Table 8) was selected as a representative compromise in these situations because only one land use category could be specified for each grid point. It is acknowledged that this is a simplification to the real-world where the landscape usually exhibits various land uses on subgrid scale of this model.

Figure 7 displays the grid for Dayton experiments with the land use categories. The principal water bodies (12) include the Great Lakes and Atlantic Ocean. Agricultural cropland (1) dominates Ohio while forested (5) regions cover central Pennsylvania, and parts of New York state and Ontario. There are a few grid points defined as urban land use (11). The spatial pattern in Figure 7 was also found to closely correspond with the coarser grid scale land use map presented by Sheih et al. (1979).

TABLE 8

LAND USE CATEGORIES AND SURFACE ROUGHNESS LENGTHS FOR MESOPAC II

CATEGORY	LAND USE DESCRIPTION	ROUGHNESS LENGTH Z_o (m)
1*	crops and pasture	0.20
2*	crops, woodland, and grazing land	0.30
3	irrigated crops	0.05
4	grazed forest and woodland	0.90
5*	ungrazed forest and woodland	1.00
6	subhumid grassland and semiarid grazing land	0.10
7	open woodland grazed	0.20
8	desert shrubland	0.30
9	swamp	0.20
10	marshland	0.50
11*	urban	1.00
12*	water	0.0001

NOTE:
Contents of table taken from Sheih et al. (1979)
* land use types input at grid points in the model domain

```
                                        MESOPAC   VERSION  1.1   LEVEL 860328
**************************************************************************************************************

LAND USE CATEGORIES FOR EACH GRID POINT

MULTIPLY ALL VALUES BY 10 **    0

19 \  12  12  12   2   2   2   5   5  12  12  12  12  12  12  12   5   5   5   5   5   5   5   5   1   1   1   1   5   5   1
   \   +   +   +   +   +   +   +   +   +   +   +   +   +   +   +   +   +   +   +   +   +   +   +   +   +   +   +   +   +   +
18 \  12   2   2   2   2   5   5  12  12  12  12  12   2  12  12   5   5   5   5   5   5   5   5   1   1   2   2   5  12   2
   \   +   +   +   +   +   +   +   +   +   +   +   +   +   +   +   +   +   +   +   +   +   +   +   +   +   +   +   +   +   +
17 \  12   2   2   2   2   5   5  12  12  12  12   1   1   1   1   1  12   1   1   2   2   2   2   2   2   5   5   5   2   5
   \   +   +   +   +   +   +   +   +   +   +   +   +   +   +   +   +   +   +   +   +   +   +   +   +   +   +   +   +   +   +
16 \   2   2   2   2   2   2   2  12  12  12  12   1   1   1   1   1   1   1   1   1   1  12   1   1   5   5   5   5   5   5
   \   +   +   +   +   +   +   +   +   +   +   +   +   +   +   +   +   +   +   +   +   +   +   +   +   +   +   +   +   +   +
15 \   2   2   2   2   2   2  12   1   1  12  12   1   1   1   1   1   1  12  12  12  12  12  12   2   5   5   5   5   5   5
   \   +   +   +   +   +   +   +   +   +   +   +   +   +   +   +   +   +   +   +   +   +   +   +   +   +   +   +   +   +   +
14 \   2   2   2   2   2   2   1   2   1  12  12   1   1   1   1  12  12  12  12  12  12  12   2   5   5   5   5   5   5   5
   \   +   +   +   +   +   +   +   +   +   +   +   +   +   +   +   +   +   +   +   +   +   +   +   +   +   +   +   +   +   +
13 \  12   2   2   2   2   2   2   2   1  12   1   1   1   1   1   2   2   1   1   1   2   2   2   2   2   1   5   5   5   2
   \   +   +   +   +   +   +   +   +   +   +   +   +   +   +   +   +   +   +   +   +   +   +   +   +   +   +   +   +   +   +
12 \  12   1   1   1   1   1   1   1   1   1   1   1   1   1  12  12  12   2   2   1   2   1   2   2   2   2   2   2   2   5
   \   +   +   +   +   +   +   +   +   +   +   +   +   +   +   +   +   +   +   +   +   +   +   +   +   +   +   +   +   +   +
11 \   1   1   1   1   1   1   1  11  12   1   1  12  12  12  12  12   2   2   2   2   2   1   1   2   2   2   2   2   2   5
   \   +   +   +   +   +   +   +   +   +   +   +   +   +   +   +   +   +   +   +   +   +   +   +   +   +   +   +   +   +   +
10 \   1   1   1   1   1   1   1  11   1  12  12  12  12  12   2   2   2   2   2   2   2   2   2   2   2   2   5   5   2   5
   \   +   +   +   +   +   +   +   +   +   +   +   +   +   +   +   +   +   +   +   +   +   +   +   +   +   +   +   +   +   +
 9 \   1   1   1   1   1   1   1  12  12  12  12  12   2   2   1   5   5   5   5   5   5   2   1   1   2   5   5   2   2   5
   \   +   +   +   +   +   +   +   +   +   +   +   +   +   +   +   +   +   +   +   +   +   +   +   +   +   +   +   +   +   +
 8 \   1   1   1   1   1   1   1   1  12  12  11   2   2   2   2   5   5   5   5   5   5   5   5   5   2   2   5   2   2   2
   \   +   +   +   +   +   +   +   +   +   +   +   +   +   +   +   +   +   +   +   +   +   +   +   +   +   +   +   +   +   +
 7 \   1   1   1   1   1   1   1   1   1   1   1   2   2   2   2   2   2   2   5   5   5   5   2   2   5   5   2   2   5   2
   \   +   +   +   +   +   +   +   +   +   +   +   +   +   +   +   +   +   +   +   +   +   +   +   +   +   +   +   +   +   +
 6 \   1   1   1   1   1   1   1   1   1   1   1   2   2   2   2   2   2   5   5   5   2   2   2   2   5   1   2  11  11  11
   \   +   +   +   +   +   +   +   +   +   +   +   +   +   +   +   +   +   +   +   +   +   +   +   +   +   +   +   +   +   +
 5 \   1   1   1   1   1   1   1   1   1   2   1   2   2   2  11   2   2   5   5   5   5   2   2   2   1   1   1  11  12  12
   \   +   +   +   +   +   +   +   +   +   +   +   +   +   +   +   +   +   +   +   +   +   +   +   +   +   +   +   +   +   +
 4 \   1   1   1   1   1   1   1   1   1   2   1   2   2   2   1   2   2   2   2   5   2   1   1   1   2  11   2   2  12  12
   \   +   +   +   +   +   +   +   +   +   +   +   +   +   +   +   +   +   +   +   +   +   +   +   +   +   +   +   +   +   +
 3 \   1   1   1   1   1   1   1   1   1   2   1   1   2   2   1   2   5   5   5   2   1   1   1   2   2  11   5   5  12  12
   \   +   +   +   +   +   +   +   +   +   +   +   +   +   +   +   +   +   +   +   +   +   +   +   +   +   +   +   +   +   +
 2 \   1   1   1   1   1   1   1   1   5   5   2   2   5   5   1   5   5   5   5   5   1   1   2   2   2   2   5  12  12  12
   \   +   +   +   +   +   +   +   +   +   +   +   +   +   +   +   +   +   +   +   +   +   +   +   +   +   +   +   +   +   +
 1 \   1   1   1   1   1   1   2   5   5   5   2   2   5   5   1   5   5   2   2   1   1   1   5   1   1  12   5  12  12  12
   \   +   +   +   +   +   +   +   +   +   +   +   +   +   +   +   +   +   +   +   +   +   +   +   +   +   +   +   +   +   +
  -----------------------------------------------------------------------------------------------------------------------
       1   2   3   4   5   6   7   8   9  10  11  12  13  14  15  16  17  18  19  20  21  22  23  24  25  26  27  28  29  30
```

Figure 7. Land use categories in the MESOPAC II meteorological grid for the Dayton cases during CAPTEX.

SECTION 4

MODEL EVALUATION PROCEDURES AND RESULTS

The MESOPUFF II modeling system was applied to the six full-scale CAPTEX experimental cases. Experiment #6 was omitted in this model evaluation effort because it was limited to a half-hour release with few nonzero measured concentrations over the sampling network. All model runs and data analyses were performed on a Sperry Univac 1182 computer system.

The important input variables and standard features specified in the MESOPAC II processor runs are given in Table 9. All MESOPAC II runs began at hour 00 EST (midnight, Eastern Standard Time) of a release day and the number of simulation hours was sufficient to cover the entire sampling period of each experiment. All technical default features in the operational model runs were applied according to the user guide (Scire et al., 1984b). The data files of hourly surface observations from 25 selected stations, the maximum number permitted, were input in each case and data files of upper air measurements for 6 and 7 rawinsonde sites were used for Dayton and Sudbury cases, respectively. The gridded meteorological fields generated by the processor were stored on a single disk file in each case and an output file was also produced with results printed at two hour intervals for use in analysis and interpretation of model results. The MESOPAC II program required about 400,000 bytes of computer core during execution and computational times varied from 400 to 600 seconds for these episodes spanning two to three simulation days.

The input values and specifications for the MESOPUFF II model runs are presented in Table 10. Due to the conservative nature of the tracer, the wet/dry deposition and transformation processes were not simulated. The computational grid in the model was defined to be identical to the meteorological grid. The emission rate (g s^{-1}) was slightly different in each case as individual rates were computed from the actual amount of tracer emitted over the release period (see Table 3). The tracer gas existed under ambient temperature and exhibited neutral bouyancy. Thus, no plume rise occurred. The height of the release nozzle was specified to be 1 m above the surface in all model runs.

The selection of rates for puff release and puff sampling is an important element for any puff model because sufficient puff overlap must occur under all wind speeds encountered in an application for the model to properly simulate plumes. The results of several model test runs conducted with various combinations of rates are listed in Appendix A. Results showed that individual peak concentrations at 300 km arc sites differed by 3% or less from the average peak value computed over all test runs. Since these results indicated that modeled concentrations were not sensitive to combinations of rates between 2 and 12 puffs h^{-1} at the nearest arc, the puff release rate and puff sampling rate were both set to 4 h^{-1} in all model runs. However, an optional feature was selected for these model runs which allowed the puff sampling rate to increase, if necessary, in order to insure sufficient puff overlap. The start time for

TABLE 9

INPUT CONTROL PARAMETERS AND DEFAULT FEATURES OF MESOPAC II RUNS FOR CAPTEX EPISODES

FEATURE	SPECIFICATION
METEOROLOGICAL GRID	30 x 19 (Dayton), 30 x 24 (Sudbury)
GRID POINT SPACING	37 km
TIME STEP	1 hour
SIMULATION PERIOD	VARIABLE - start at 00 EST on the day of release and go to end of sampling period (e.g. range from 56 to 87 h)
REFERENCE TIME ZONE	Eastern Standard Time (EST)
METEOROLOGICAL STATIONS	25 hourly surface sites
UPPER AIR STATIONS	6 - Dayton , 7 - Sudbury cases
WIND FIELDS (default)	Mixed-layer average (Sfc. to Z_i), upper layer average (Z_i to 700 mb)
OUTPUT FIELDS	Storage on disk file, printer output at 2-hour intervals
COMPUTER REQUIREMENTS	400,000 bytes; 10 minutes CPU time on a Sperry Univac 1182 computer

TABLE 10

INPUT PARAMETERS AND SPECIFICATIONS FOR MESOPUFF II RUNS

TRACER EMISSIONS	3-hour release at constant rate Source Height - 1 m; neutral buoyancy
COMPUTATIONAL GRID	IDENTICAL TO METEOROLOGICAL GRID
TIME STEP	1 hour
PUFF RELEASE RATE	4 per hour
PUFF SAMPLING RATE	4 per hour
WET/DRY DEPOSITION/CHEMICAL TRANSFORMATION	PROCESSES NOT SIMULATED
PUFF DISPERSION	σ_y and σ_z according to PGT curves to 100 km;time dependent expressions of Heffter (1965) at greater distances
SAMPLING GRID CALCULATIONS	deactivated; calculations at nongridded site coordinates only
COMPUTATION REQUIREMENTS	400,000 bytes of core

model execution corresponded with the beginning hour for each release.

The model code was modified slightly to stop new puffs from being emitted after 3 hours. Thereafter, only existing puffs were tracked and sampled during the remainder of the simulation period. Hourly tracer concentrations (g/m^3) were computed at the coordinates of all operational tracer measurement sites in the model domain, instead of at sampling grid points. This feature reduced the execution time of individual model runs to less than two minutes for this application.

In order to compare the modeled results with the surface tracer measurements, the MESOFILE II postprocessor program was applied in order to compute 3-h or 6-h average concentrations from the model output file over the same time periods as the measurements and modeled concentrations were also converted into the same units as the measurements (fl l^{-1}).

OPERATIONAL MODEL EVALUATION ANALYSES AND RESULTS

Sets of statistical measures of differences (residuals) and correlation between observed and modeled concentration pairs are presented from time and/or space pairings in order to provide quantitative evidence of model performance. Concentration pairs with both observed and modeled values equal to zero were excluded in the calculation of the statistical measures because neither the observed nor the modeled plumes had an impact in these cases; 1088 out of 1895 pairs were in this category. In addition, analyses of observed plume concentration patterns at individual time periods revealed a large number of concentrations of 1-2 fl l^{-1}; some at sites separated from the main plume distribution by adjacent sites which exhibited zero concentrations. Specifically, measurements at these isolated locations were believed to be anomolous since there was considerable uncertainty as to whether a measured concentration so close to the natural background really indicated an actual impact by the tracer plume. Potential error in the analytical procedures used to determine concentrations might be attributed for some of these values above background (Ferber et al., 1986). However, instead of eliminating all such extremely low values, a screening procedure redefined 73 values to be zero where an observed concentration of ≤ 2 fl l^{-1} occurred at any outlying site separated from the tracer plume pattern. Other observed concentrations ≤ 2 fl l^{-1} at sites next to locations with nonzero tracer concentrations were not changed in the data set since it was deemed reasonable to assume that the tracer plume had indeed impacted such locations. Therefore, the final evaluation data set contained all paired values that formed the union of both the perceived actual and predicted plumes. As a consequence of applying these screening criteria, the full data set was composed of 734 concentration pairs from the six modeled experiments.

Statistical Results For Mean and Peak Concentrations

Statistical results were computed from observed and modeled concentration pairs matched in time and location for each experiment and over the entire data set. These criteria provide a stringent test of model performance and a critical test of model skill as each predicted concentration was compared to the measured value at the same site and for the same time period.

The results in Table 11 reveal that MESOPUFF II overpredicted mean concentrations in each case. Nevertheless, the predicted mean concentration (P) was within a factor of two of the observed mean value (O) in experiments #2,#4, and #7 and for the entire data set. The overall mean residual (d) was -33.8 fl 1^{-1}, while individual values ranged from -58.3 fl 1^{-1} for CAPTEX #1 to a low of -12.8 fl 1^{-1} in CAPTEX #2. The most significant model overprediction occurred in CAPTEX #3 as P was five times greater than O; however, the observed mean concentration in CAPTEX #3 was considerably lower than the mean values of the other experiments. Results of additional analyses will be presented later in an effort to explain this large discrepancy.

Since no absolute standards have been established for defining acceptable model performance, statistical results like those in Table 11 are primarily useful in an intercomparison of different models. However, comparable statistics for other models have yet to appear. Nevertheless, results of several statistical measures in Table 11 did indicate that considerable scatter existed among the paired concentrations. The standard deviations of the residuals (SD_d) are much larger than the observed mean concentrations. Furthermore, there is greater variability in the modeled results as exemplified by the standard deviations of the modeled concentrations (SD_p), which are greater than corresponding standard deviations for observed values (SD_o). The results for the average absolute residual (AAR) and root mean square error (RSME), when compared to observed concentrations, also indicate that notable scatter exists between modeled and observed concentrations. In addition, the Pearson correlation coefficient (R) is also generally near zero which reveals no linear relationship among the concentration pairs for these individual data sets and over the entire data set.

Similar results for the statistical measures were also obtained by Policastro et al. (1986) when the predicted results of eight regional models, including MESOPUFF II, were evaluated in time and space against measurements from two different tracer field studies. Large scatter and low correlations were generally found between model and observed results, and most models also displayed a tendency to overpredict mean concentrations. Consequently, scatter plots of observed versus modeled concentrations showed many pairs where either the observed or the predicted value was zero (Policastro et al., 1986; Draxler, 1987; Lee, 1987). Thus, it was evident that the modeled plume was either displaced away from particular sites where the actual tracer was measured or modeled concentrations impacted the particular sites at different times that the observed plume. Some statistical measures were strongly sensitive to these circumstances and the ensuing results reflected situations when plume displacements occurred. In particular, significant scatter (e.g. large values for d, AAR, and RMSE) and low correlations were obtained when observed and modeled plumes exhibit little or no overlap, even though modeled mean concentrations may have compared favorably with observed mean values (Policastro, et al., 1986). However, the statistical measures could only provide partial information concerning regional model performance and more innovative analyses, to be shown, are certainly required to provide better quantitative information to assist in assessing and understanding the causes of model/measured differences.

TABLE 11

MESOPUFF II MODEL EVALUATION RESULTS: OBSERVED AND MODELED CONCENTRATIONS PAIRED IN TIME AND LOCATION

STATISTIC$	CAPTEX EXPERIMENT						
	#1	#2	#3	#4	#5	#7	ALL
N	143	247	124	96	68	56	734
$\overline{O}$	22.6	45.7	10.0	54.9	41.7	79.7	38.6
SD_o	±138.1	±172.0	±31.4	±172.2	±112.7	±135.4	±143.3
$\overline{P}$	80.9	58.5	49.9	90.5	86.0	113.5	72.4
SD_p	±252.8	±231.1	±163.2	±226.5	±166.8	±214.8	±218.6
d	-58.3	-12.8	-39.9	-35.7	-44.4	-33.8	-33.8
SD_d	±165.5	±295.5	±168.2	±294.6	±178.4	±283.0	±244.6
AAR	71.8	95.7	57.1	123.6	103.2	185.5	95.7
RMSE	174.9	295.2	172.2	295.2	182.6	282.5	246.7
R	0.80	-0.05	-0.07	-0.08	0.23	-0.27	0.14

$ - units are fl/l, except for N and R
N - number of concentration pairs

$\overline{O}$ - mean observed concentration ; $\overline{P}$ - mean modeled concentration
SD - standard deviation about the mean

d - average residual = O - P
AAR - average absolute residual
RMSE - root mean square error
R - Pearson correlation coefficient

Objective tests between the concentration pairs were performed in order to provide additional quantitative comparative results which could provide a better overall picture of the model's capabilities to simulate the spatial plume pattern over the time frame of these experiments. In particular, comparative test results that demonstrate the relative amount of correspondence between modeled and observed plumes could provide relevant information about the abilities of the transport and dispersion components of the model to simulate the movement and growth experienced by the tracer plume. Table 12 contains results in the form of percentages for certain comparative tests on the concentration pairs. One of the interesting tests is the percentage of pairs where both observed and modeled values are nonzero (T1). High percentages for T1 demonstrates that a substantial overlap must have existed between the modeled and observed plumes for the sampling periods of an experiment, which also suggests the overall speed and path, and growth of the plume was accurately simulated. Conversely, low percentages would reveal that the area of intersection between the respective plumes was rather small which implies inadequate treatment of plume transport/dispersion by the model. The percentages for T1 in Table 12 vary among these cases with the highest being 46.9% for CAPTEX #4. T1 was less than 20% for experiments #1, #3, #5, and #7 which indicated rather small areas of intersection for the observed and modeled plumes during these cases.

Additional evidence of spatial displacements between the respective plumes is provided by test results showing the percentages when either the observed (T2) or the predicted (T3) concentration was zero while its counterpart was nonzero. Low percentages for T2 and T3 would suggest a strong spatial correspondence of the respective tracer plumes. However, these results show a notable number of pairs where either the observed or predicted concentration was zero. In fact, results indicate that either T2 or T3 was greater than 50% in some experiments with most values for T2 and T3 above 30%. The best combination of T2 and T3 is found for CAPTEX #4, which also displayed the highest value for T1. Finally, the results for T4, the percentage of cases where observed concentrations were greater than modeled values, vary with values ranging from about 35% to 54%. Results from the T4 test are sometimes used as indicators of the performance of dispersion in a model. For example, when T4 is significantly greater than 50%, it might be suggested that the modeled plume exhibited less horizontal spread than the observed plume. Nevertheless, T4 results are difficult to interpret in this manner and are also complicated by the potential effects from both transport and dispersion. Even though the model certainly overpredicted the mean concentrations, as shown by the earlier statistical results, spatial displacements due to differences in the speed and/or the directional components of transport between the model and observed plumes are believed to be the principal factors responsible for the variations in T4 results among these cases.

Mean concentrations and selected statistical measures for each experiment are presented in Table 13 to illustrate model behavior on an event by event basis. An examination of Table 13 indicates that observed mean concentrations generally exhibited an increase with time and then gradually decreased toward the last sampling period. This temporal trend reflects the arrival of the tracer plume accompanied by generally high concentrations

TABLE 12

TEST RESULTS OF MODELED AND OBSERVED CONCENTRATIONS PAIRED IN TIME AND LOCATION

TEST	CAPTEX EXPERIMENT #1	#2	#3	#4	#5	#7	ALL
N	143	247	124	96	68	56	734
T1 (%) (P&O >0)	16.8	33.6	16.1	46.9	19.1	16.1	26.4
T2 (%) (O=0, P>0)	52.4	32.0	33.9	27.1	48.5	37.5	37.6
T3 (%) (P=0, O>0)	30.8	34.4	50.0	26.0	32.4	46.4	36.0
T4 (%) (O>P)	35.7	53.0	54.0	44.8	35.3	48.2	46.7

TABLE 13

SELECTED STATISTICAL EVALUATION RESULTS FOR EACH EVENT OF THE CAPTEX EXPERIMENTS

EXPT	MM/DD-HR (LST)	N	O (fl/l)	P (fl/l)	d (fl/l)	AAR (fl/l)	NN_o	NN_p	T1 (%)	T4 (%)
1	9/18-14	4	5.8	59.0	-53.2	53.2	2	0	25.	0.
1	9/18-17	5	552.2	1012.8	-460.5	615.5	0	1	75.	50.
1	9/18-20	15	23.7	155.9	-131.3	140.7	3	4	53.	40.
1	9/18-23	4	0.8	29.0	-28.2	29.8	2	2	0.	50.
1	9/19-02	21	16.6	61.8	-45.1	75.5	8	10	14.	52.
1	9/19-05	3	0.	118.7	-118.7	118.7	3	0	0.	0.
1	9/19-08	26	4.5	49.2	-44.7	52.5	16	6	8.	31.
1	9/19-14	26	3.2	38.1	-34.8	41.3	17	9	0.	35.
1	9/19-20	26	2.0	36.6	-34.6	38.1	17	7	8.	31.
1	9/20-02	14	2.4	13.0	-10.6	15.0	7	5	7.	36.
2	9/25-13	4	0.2	51.0	-50.8	51.2	3	1	0.	25.
2	9/25-16	5	0.2	827.6	-827.4	827.8	4	1	0.	20.
2	9/25-19	6	45.7	419.0	-373.3	464.0	3	2	17.	33.
2	9/25-22	14	130.4	155.8	-25.4	285.9	5	8	7.	57.
2	9/26-01	8	311.6	118.8	192.9	421.4	4	2	25.	38.
2	9/26-04	24	125.6	33.3	92.3	150.1	6	13	21.	71.
2	9/26-10	33	32.6	32.7	-0.1	50.0	9	13	30.	70.
2	9/26-16	36	21.0	33.6	-12.6	42.3	10	10	42.	47.
2	9/26-22	37	17.8	17.2	0.6	23.1	9	11	43.	54.
2	9/27-04	32	17.7	8.6	9.1	21.9	8	13	31.	59.
2	9/27-10	25	11.7	8.7	3.0	16.7	6	8	36.	52.
2	9/27-16	10	5.1	9.7	-4.6	13.8	6	1	30.	40.
3	10/02-16	1	1.0	0.	1.0	1.0	0	1	0.	100.
3	10/02-19	4	18.0	1.5	16.5	17.5	2	2	0.	50.
3	10/02-22	6	50.8	257.5	-206.7	308.0	4	1	0.	17.
3	10/03-01	16	3.6	118.8	-115.1	122.4	7	9	0.	56.
3	10/03-04	4	5.0	5.5	-0.5	10.5	1	3	0.	75.
3	10/03-07	29	6.9	39.5	-32.6	45.2	11	14	10.	48.
3	10/03-13	27	6.7	28.9	-22.3	32.8	8	10	30.	48.
3	10/03-19	15	12.3	49.1	-36.9	49.1	5	5	27.	40.
3	10/04-01	12	12.6	4.7	7.9	12.6	4	7	8.	67.
3	10/04-07	5	12.0	0.	12.0	12.0	0	5	0.	100.
3	10/04-13	5	1.8	0.	1.8	1.8	0	5	0.	100.

TABLE 13 (CONTINUED)

EXPT	DATE/TIME	N	O	P	d	AAR	NN_o	NN_p	T1	T4
4	10/14-13	1	0.	67.0	-67.0	67.0	1	0	0.	0.
4	10/14-16	7	133.9	167.6	-33.7	301.4	5	2	0.	29.
4	10/14-19	5	276.6	521.0	-244.4	784.4	3	1	20.	20.
4	10/14-22	16	47.8	230.0	-72.2	138.7	3	7	38.	62.
4	10/15-01	9	30.1	77.0	-46.9	102.0	3	3	33.	33.
4	10/15-04	24	58.8	51.8	7.1	70.1	4	5	58.	50.
4	10/15-07	6	27.0	62.3	-35.3	69.0	3	0	33.	17.
4	10/15-10	16	9.6	33.2	-23.6	26.3	5	0	69.	19.
4	10/15-16	8	13.2	11.2	2.0	14.0	2	3	38.	62.
4	10/15-22	9	8.8	7.3	1.5	7.2	1	4	44.	67.
4	10/16-04	10	0.	0.			10	10		
5	10/26-03	4	86.2	0.	86.2	86.2	0	4	0.	100.
5	10/26-09	9	181.1	176.8	4.3	181.1	2	4	33.	56.
5	10/26-15	14	57.5	118.5	-61.0	175.1	6	5	14.	43.
5	10/26-21	12	2.8	130.5	-127.7	128.7	6	2	33.	17.
5	10/27-03	13	0.6	74.5	-73.8	74.2	10	1	8.	8.
5	10/27-09	10	0.6	2.0	-1.4	2.4	7	2	0.	20.
5	10/27-15	3	1.3	0.	1.3	1.3	0	3	0.	100.
5	10/27-21	1	1.	0.	1.	1.	0	1	0.	100.
7	10/28-23	0	0.	0.						
7	10/29-02	3	1.	0.	1.	1.	0	3	0.	100.
7	10/29-05	3	35.7	190.7	-155.0	155.0	2	0	33.	0.
7	10/29-08	14	25.6	220.8	-195.2	234.6	8	2	21.	14.
7	10/29-11	4	179.5	8.0	171.5	187.5	1	3	0.	75.
7	10/29-14	16	75.9	107.3	-31.4	179.7	6	6	25.	44.
7	10/29-20	11	196.0	63.2	132.8	259.2	2	9	0.	82.
7	10/30-02	3	32.7	83.3	-50.7	116.0	2	1	0.	33.

NN_o, NN_p - number of observed , predicted zero concentrations.
T1 - P and O both > 0
T4 - O > P

at the closest arc or sites a few hours after release, and this peak was followed by an general decrease in the mean concentration due to the plume being dispersed as it traveled across the sampling region. Modeled concentrations also exhibited a similar temporal pattern, although the time variation of mean model values was often out of phase with the time series of observed mean values. The residuals were usually negative as the model appears to overpredict in most events. The largest biases were usually found during an early time period when concentrations also happen to be highest. Differences in the time and location of impact of the peak concentration are attributed for these significant departures between the observed and modeled mean concentrations. The results for the number of observed (N_o) and predicted (N_p) concentrations being zero coupled with the low T1 results indicate important spatial plume displacements. In fact, during some events there was no intersection of the respective plumes (i.e. T1 = 0). Low values of T1 were more common during the early events and also near the end of an experiment. Differences in the time of initial impact of the respective plumes at the first arc (or closest sites for the Subdury cases) can produce low T1 values soon after release. At the later stages of an experiment a more rapid departure of the observed plume from the sampling region or large spatial displacements between the plume patterns existing on the sampling domain was also believed to lead to small fractions in T1.

Averaged concentrations for each event were also computed separately from observed and modeled concentrations (excluding any zero values) to assess differences in magnitude between the plumes with time. The results are presented as a function of time after release in Figure 8a-f. For CAPTEX #1-4 (Figures 8a-d), the highest observed and modeled average plume concentration occurred within 12 h after release as a result of plume impact at the 300 km arc sites. The modeled values (X) replicated the time history and magnitudes of observed (O) concentrations best in #2 and #4. For a few events there were very few or no observed nonzero concentrations, which was responsible for the values near or on the abscissa. These results also show the overall decrease in average plume concentrations with time. Concentration standard deviations were comparable to mean values for most events. The results for CAPTEX #5 and #7 (Fig. 8e-f) did not exhibit concentrations at early periods as high as the Dayton cases; probably because the plumes did not intersect sites or an arc as close to release point as in the Dayton cases. Despite the log scale for concentration, it appeared that average modeled concentrations from these calculations were more often higher than average observed values, which suggests that peak concentrations were overpredicted, although more definitive information about model performance at peak concentration levels will be presented later.

Cumulative frequency distributions were determined to establish the relative agreement between the observations and predicted values across the range of concentrations. Although frequency distributions do not demonstrate information about model skill, since values are not paired in time or location, the results can provide evidence about how well the modeled concentrations replicate the magnitude and overall distribution of observed values. The results from the entire data set in Figure 9 concur with the earlier tests that large numbers of either observed or modeled concentrations in the evaluation data set were zero. The cumulative frequency curve for observed concentrations lies above that for the modeled values. The

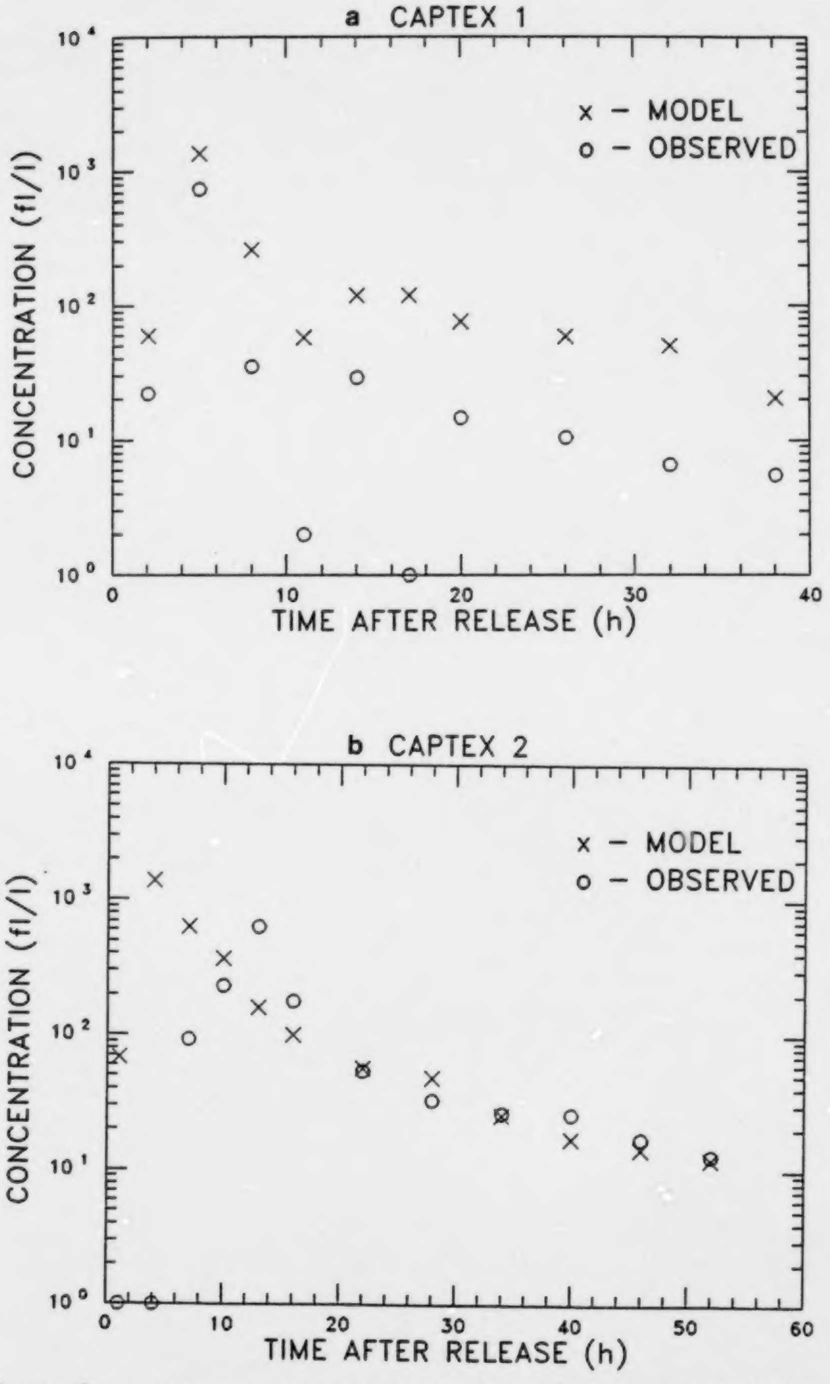

Figure 8. Average concentrations obtained from sites with observed and modeled nonzero concentrations over the sampling periods during a) CAPTEX #1 and b) CAPTEX #2.

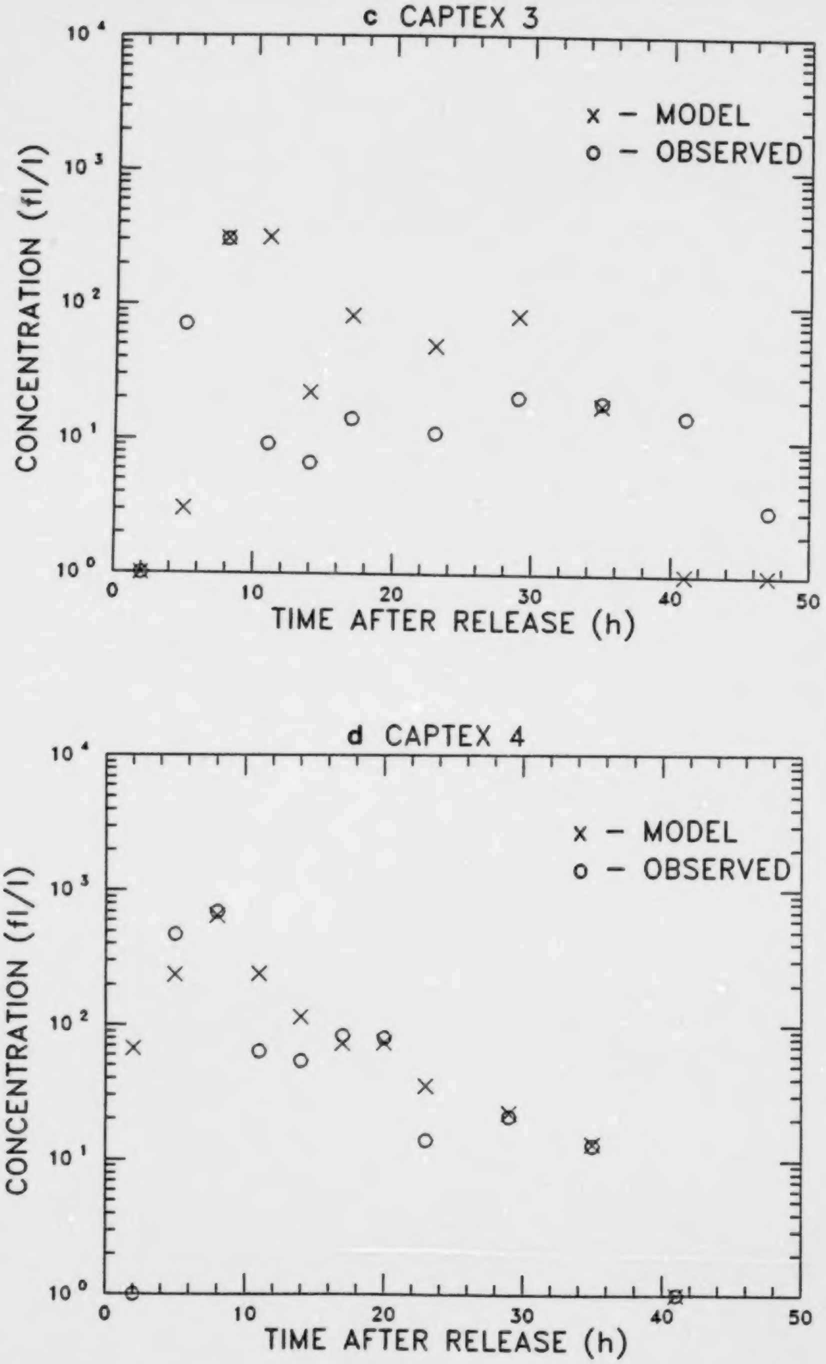

Figure 8. Same as 8a-b, except for c) CAPTEX #3 and d) CAPTEX #4.

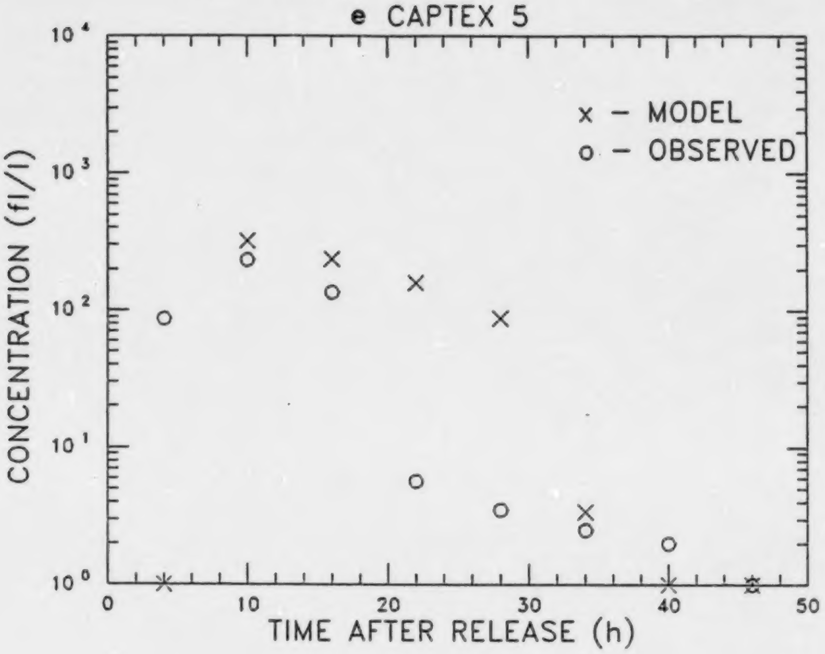

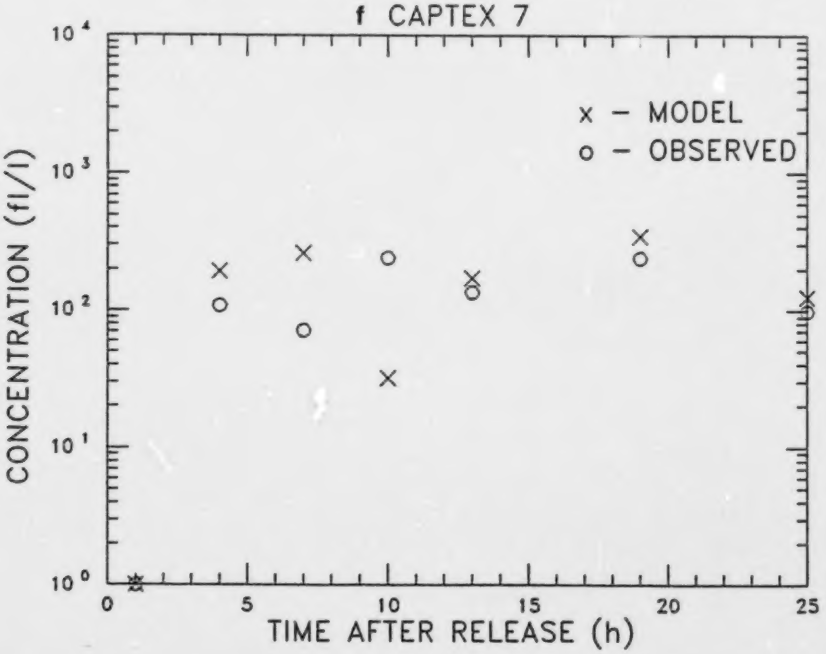

Figure 8. Same as 8a-b, except for e) CAPTEX #5 and f) CAPTEX #7.

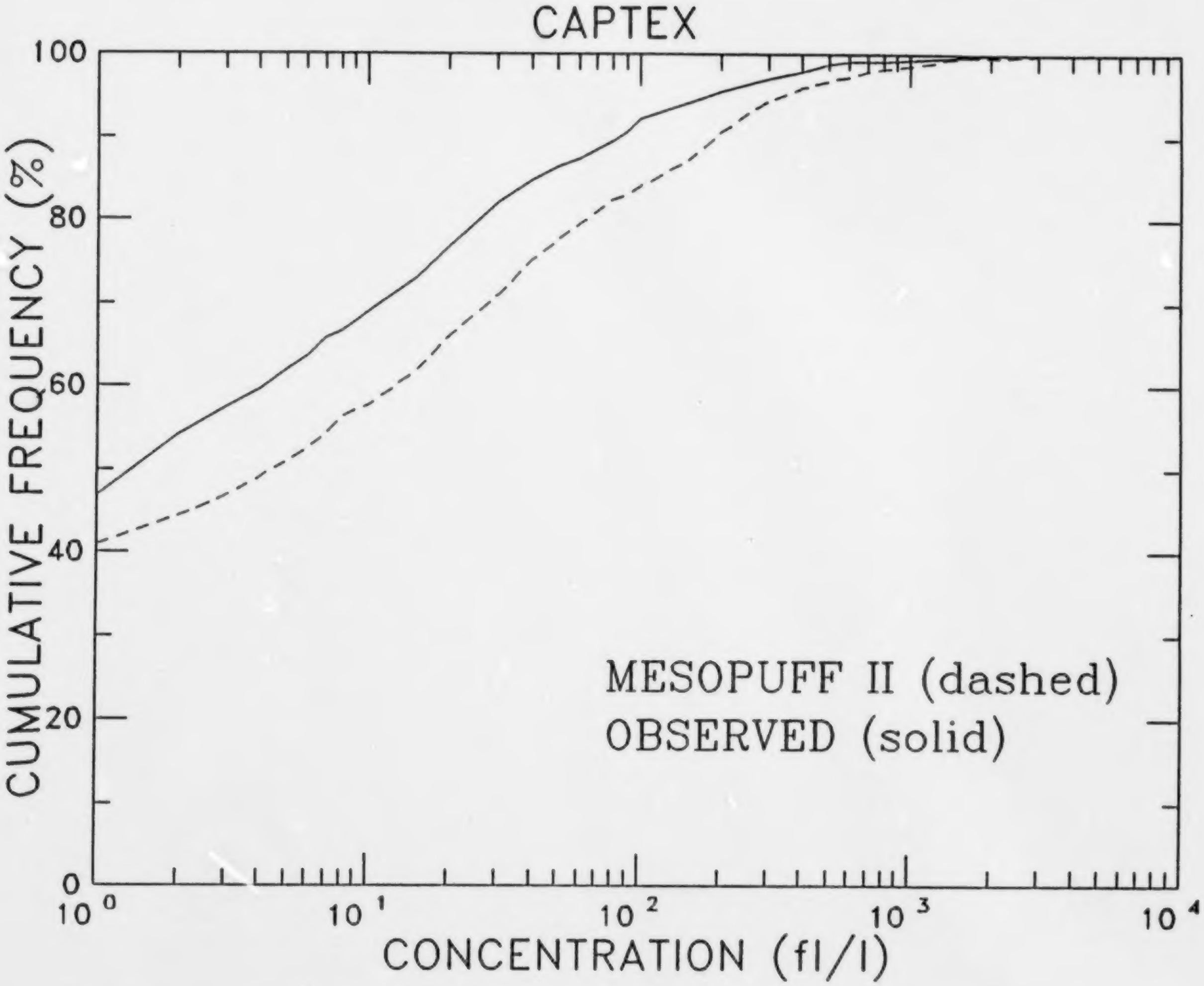

Figure 9. Cumulative frequency distributions of the model and observed concentrations from the entire data set.

separation between the curves increased from 1 to 10 fl l^{-1}, which indicated that a greater number of observed values exist at these low concentrations compared to modeled results. The separation remains about the same between 10 and 100 fl l^{-1}. However, the gap between the curves closed rapidly above 100 fl l^{-1} as a relatively greater number of modeled values occur at higher concentrations.

Individual cumulative concentration distributions are shown in Figures 10a-f to illustrate the variability in the distributions among these experiments. The best overall agreement between the cumulative distribution curves of observed and modeled concentrations appeared in experiments #2,4, and #7. CAPTEX #2 and #4 also happened to exhibit the best results for plume overlap (i.e. highest T1 values in Table 13) among these experiments.

The frequency distribution results of observed and modeled values in Table 14 quantitatively reinforce the previous cumulative distribution findings. These results that reveal a relatively large number of observed concentrations still existed at 1 fl l^{-1}, however, there was no basis to eliminate or modify these values since all were found at sites on the edge of the observed plume. These results also verify that larger numbers of observed values occurred at low concentrations. A crossover point appeared at about 25 fl l^{-1}, as the frequencies of modeled values were greater at higher concentrations. In fact, these results provided strong evidence that the model overpredicted the highest concentrations because twice as many modeled values are found in the intervals above 100 fl l^{-1} observed values.

The ability of a model to predict the highest concentration should certainly be an important aspect of an evaluation effort, since models are often applied in order to assess peak concentrations in regulatory situations. In the evaluation for peak concentrations, results were determined from observed and modeled values paired in time only or location only. In fact, there were very few cases where the modeled peak concentration occurred at the same site and time as the observed peak concentration, which is not unexpected in view of the spatial plume displacements reported earlier.

Table 15 contains the results for peak observed and modeled concentrations paired in location only. This evaluation framework allows peak observed and modeled concentrations to occur at different time periods at a given site. These results show that the model overpredicted peak concentrations for all experiments. Except for CAPTEX #3, the peak modeled concentrations were within a factor of two of peak observed values. The smallest negative residuals are found in CAPTEX #2 and #4. In these experiments, the results for T1 in Table 12 indicated that plume overlap was higher and the other test results were more favorable than in the other cases. The largest overpredictions of peak concentrations occurred in CAPTEX #1 and #3. As reported earlier, the mean observed concentration for CAPTEX #3 was unusually low in relation to the other cases. Results of analysis of peak concentrations at the 300 km sites, where the highest observed concentrations occurred for the Dayton cases, revealed that the main portion of the observed plume did indeed pass to the west of the 300 km arc in this case. This explains the low observed peak and mean concentrations for this experiment and the reason for the significant

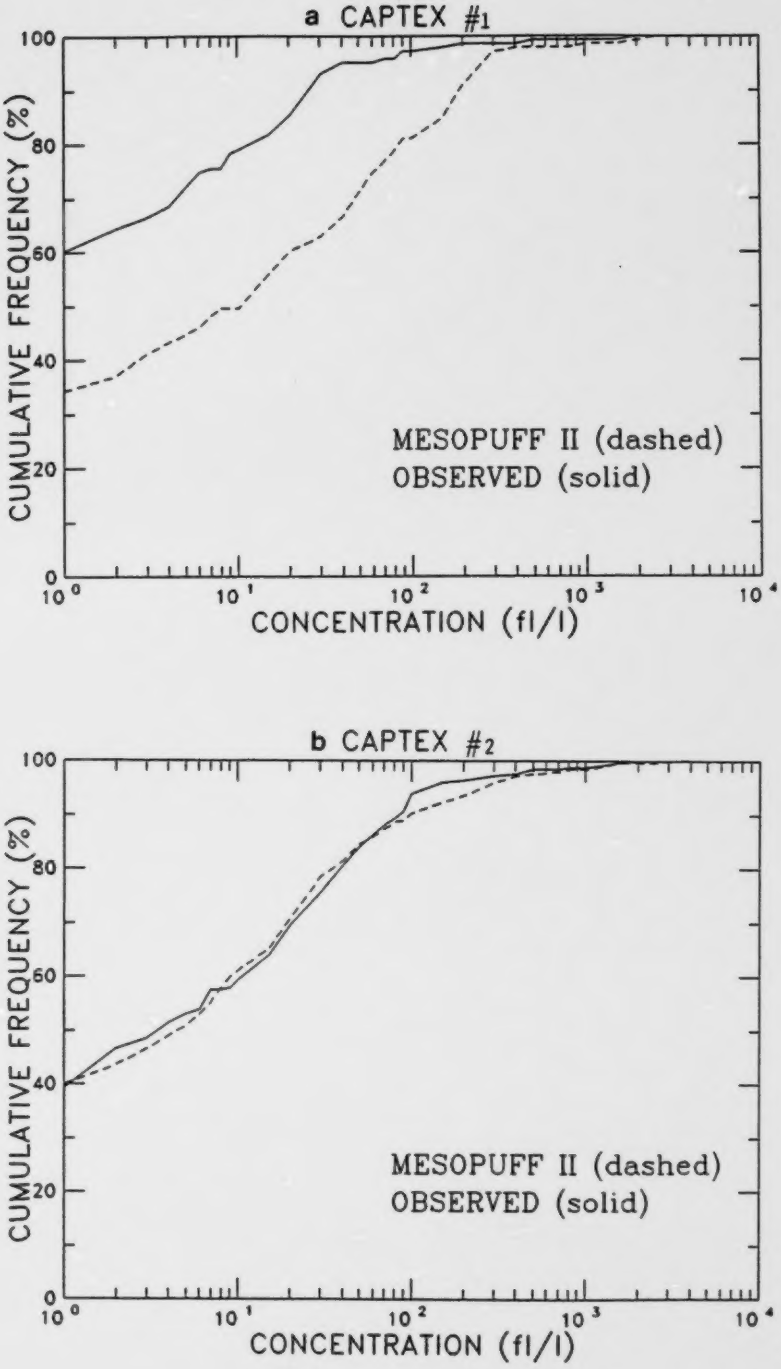

Figure 10. Cumulative frequency distributions of model and observed concentrations for a) CAPTEX #1 and b) CAPTEX #2.

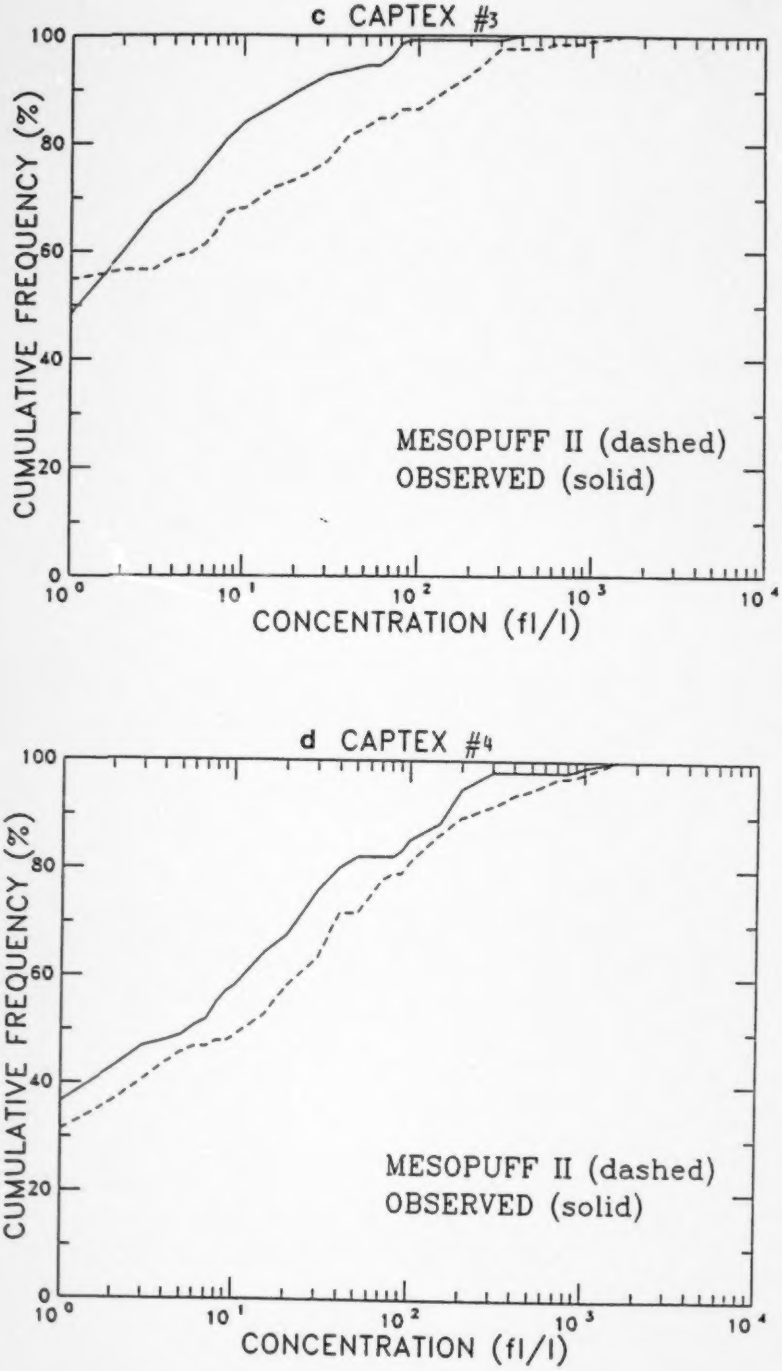

Figure 10. Same as 10a-b, except for c) CAPTEX #3 and d) CAPTEX #4.

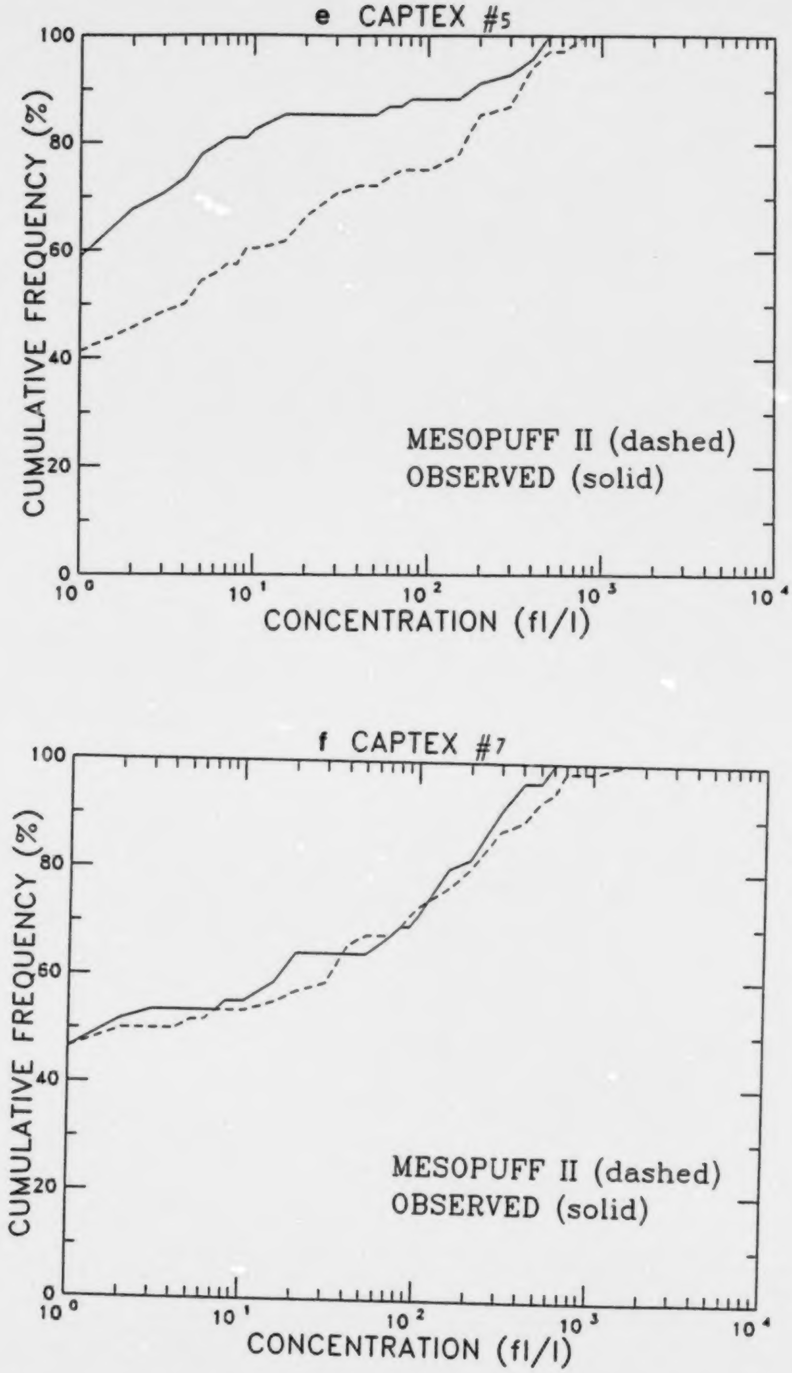

Figure 10. Same as 10a-b, except for e) CAPTEX #5 and f) CAPTEX #7.

TABLE 14

DISTRIBUTION OF OBSERVED AND MODELED CONCENTRATIONS FOR ENTIRE CAPTEX DATA SET

CONCENTRATION OR INTERVAL (f1/1)	NUMBER OF VALUES			
	OBSERVED		MODELED	
0	1437		1425	
1	68		36	
2	53	50.4%	25	34.8%
3-5	57		49	
5-10	53		50	
11-15	29		30	
16-25	51	36.9%	49	40.9%
26-50	47		67	
50-100	42		46	
100-150	14		24	
151-200	11		25	
201-250	8	10.7%	16	20.2%
251-300	3		12	
301-400	7		12	
401-500	6		6	
501-600	2		4	
601-701	0		4	
701-800	1	0.9%	2	2.8%
801-900	0		3	
900-1000	1		0	
1001-2001	5	1.1%	8	2.1%
>2001	0		2	

TABLE 15

PEAK OBSERVED AND MODELED CONCENTRATIONS PAIRED IN LOCATION ONLY

EXPT #	N	$\overline{O}$ (fl/l)	$\overline{P}$ (fl/l)	d (fl/l)	AAR (fl/l)	RMSE (fl/l)	R	T4 (O>P) (%)
1	42	66.1 ±251.2	176.4 ±427.0	-110.3 ±257.6	141.3	277.4	0.83	31.0
2	58	86.3 ±229.3	133.2 ±406.2	-46.9 ±84.5	180.6	482.6	-0.09	60.3
3	43	17.7 ±48.6	109.0 ±231.7	-91.4 ±242.2	115.4	256.2	-0.11	34.9
4	26	111.0 ±262.6	151.7 ±345.8	-40.7 ±458.8	208.7	451.8	-0.12	57.7
5	25	95.2 ±169.0	178.8 ±225.4	- 83.6 ±181.4	126.0	196.4	0.61	20.0
7	28	111.3 ±171.5	173.9 ±263.2	-62.6 ±344.7	236.5	344.2	-0.22	42.9
ALL	69	197.4 ±315.7	391.1 ±526.3	-193.6 ±550.6	326.0	579.9	0.22	29.0

overpredictions was because the modeled plume directly intercepted this arc. Other results in Table 15 also reveal large scatter and low correlations between peak pairs matched in space. The absolute value of residuals and RMSE are large relative to observed peak values and correlation coefficients are generally small and negative.

A comparative analysis of peak concentrations was also performed for observed and modeled values paired in time only. With this framework, the highest observed concentration is compared with the peak modeled value from any site for the same time period. Table 16 contains the results for the events of each experiment. Travel time is also given as the number of hours from the start time of release to the beginning hour of each sampling interval. Clearly, in most of the events the modeled peak concentrations were greater than observed values, as exemplified by the large number of negative residuals. An encouraging result, however, is that the highest modeled concentration within an experiment occurred at the same time as the corresponding observed peak value in #1,#4, and #5. This result suggests that there was apparently good agreement in the transport speed and direction between the modeled and actual plumes during the initial hours after release. On the otherhand, highest modeled peak concentrations for experiments #2 and #7 occurred much earlier than the observed highest values in these cases. Since these results are unpaired in space, it is also interesting to note that a survey of all 60 events revealed that in only 3 cases the observed and modeled peak concentrations during a particular event were found at the same site. However, there were 21 events where the peak values occurred at different sites along the same arc. Larger displacements obviously existed in another 25 events where the peak observed and modeled values were located at sites on different arcs. Finally, the relative positions of peak concentration pairs in the remaining 11 cases were indeterminant since either the observed or modeled value was zero. These results also reveal that the model generally overpredicted peak values and notable time and/or spatial displacements also existed between observed and modeled peak concentrations.

Statistical results in Table 17 were computed over the high-25 observed and modeled concentrations fully unpaired in time and location for each experiment and for the overall data set. These results are also not unexpected based on the previous analyses of the peak concentrations and frequency distributions. The model consistently overpredicted for this group of concentrations even when values are completely unpaired. The absolute values of the bias were less than the average peak observed concentrations for experiments #2, #4, and #7. Since time and location constaints are irrelevant in this comparison, the peak concentration differences given in Table 17 were not likely attributed to transport speed and direction variations of the observed and modeled plumes. These results and those in previous tables for peak concentrations suggest that dispersion of the modeled plumes may not be as great as that experienced by the actual tracer plumes. Results of analysis of additional model runs to be discussed later will attempt to confirm this hypothesis and identify the underlying cause(s).

The configuration of the sampling network presented an opportunity to investigate the four Dayton experimental results separately from the Sudbury cases. Consequently, a statistical analysis was performed on this

TABLE 16
PEAK OBSERVED AND MODELED CONCENTRATIONS PAIRED IN TIME FOR EACH EVENT OF THE CAPTEX EXPERIMENTS

	EVENT 1	2	3	4	5	6	7	8	9	10	11	12	AVE ± SD
CAPTEX #1													
DATE/TIME (DD/HR)	18/14	18/17	18/20	18/23	19/02	19/05	19/08	19/14	19/20	20/02			
TIME FROM RELEASE (h)	2	5	8	11	14	17	20	26	32	38			
Peak Obs. (fl/l)	22	1586	121	2	89	0	47	16	14	12			191 ± 492
Peak Modeled (fl/l)	153	2367	862	67	283	224	224	242	197	60			468 ± 668
RESIDUAL (O_p - P_p)	-131	-781	-741	-65	-194	-224	-177	-226	-183	-48			-277 ± 262
CAPTEX #2													
DATE/TIME (DD/HR)	25/13	25/16	25/19	25/22	26/01	26/04	26/10	26/16	26/22	27/04	27/10	27/16	
TIME FROM RELEASE (h)	1	4	7	10	13	16	22	28	34	40	46	52	
Peak Obs. (fl/l)	1	1	228	1348	1575	1399	200	96	73	96	43	44	425 ± 618
Peak MODELED (fl/l)	156	2767	1430	1020	381	413	245	214	144	50	27	26	573 ± 779
RESIDUAL (O_p - P_p)	-155	-2766	-1202	328	1194	986	-45	-118	-71	46	16	18	-148 ± 1017
CAPTEX #3													
DATE/TIME (DD/HR)	02/16	02/19	02/22	03/01	03/04	03/07	03/13	03/19	04/01	04/07	04/13		
TIME FROM RELEASE (hrs)	2	5	8	11	14	17	23	29	35	41	47		
Peak Obs. (fl/l)	1	71	304	21	15	63	68	162	79	28	3		74 ± 89
Peak MODELED (fl/l)	0	4	874	1416	22	264	201	294	28	0	0		282 ± 426
RESIDUAL (O_p - P_p)	1	67	-570	-1395	-7	-201	-133	-132	51	28	3		-208 ± 433
CAPTEX #4													
DATE/TIME (DD/HR)	14/13	14/16	14/19	14/22	15/01	15/04	15/07	15/10	15/16	15/22	16/04		
TIME FROM RELEASE (h)	2	5	8	11	14	17	20	23	29	35	41		
Peak Obs. (fl/l)	0	935	1350	248	216	210	156	40	37	28	0		293 ± 439
Peak MODELED (fl/l)	67	830	1448	687	491	392	221	147	51	35	0		397 ± 426
RESIDUAL (O_p - P_p)	-67	105	-98	-439	-275	-182	-65	-107	-14	-7	0		-104 ± 142
CAPTEX #5													
DATE/TIME (DD/HR)	26/03	26/09	26/15	26/21	27/03	27/09	27/15	27/21					
TIME FROM RELEASE (h)	4	10	16	22	28	34	40	46					
Peak Obs. (fl/l)	167	460	384	33	125	10	2	1					148 ± 181
Peak MODELED (fl/l)	0	794	478	382	272	5	0	0					241 ± 277
RESIDUAL (O_m - P_m)	167	-334	-94	-349	-147	5	2	1					- 93 ± 178
CAPTEX #7													
DATE/TIME (DD/HR)	28/23	29/02	29/05	29/08	29/11	29/14	29/20	30/02					
TIME FROM RELEASE (h)	-2	1	4	7	10	13	19	25					
Peak Obs. (fl/l)	1	1	107	309	277	546	553	98					236 ± 224
Peak MODELED (fl/l)	0	0	299	1041	32	578	652	230					354 ± 351
RESIDUAL (O_p - P_p)	1	1	-192	-732	245	-32	- 99	-132					-118 ± 280

TABLE 17

HIGH-25 OBSERVED AND MODELED CONCENTRATIONS UNPAIRED IN TIME AND LOCATION FOR EACH CAPTEX EXPERIMENT

EXPT	O_{25} (fl/l)	P_{25} (fl/l)	P25/O25	d (fl/l)
1	121 ± 311	379 ± 502	3.1	-259 ± 237
2	341 ± 437	470 ± 578	1.4	-129 ± 240
3	43 ± 59	230 ± 300	5.3	-187 ± 246
4	196 ± 293	319 ± 352	1.6	-123 ± 146
5	113 ± 161	230 ± 204	2.0	-117 ± 86
7	178 ± 152	253 ± 258	1.4	- 75 ± 118
ALL	637 ± 436	1010 ± 559	1.6	-373 ± 222

± one standard deviation

subset of concentration pairs to compare observed and modeled concentrations for each arc from Dayton cases. The results for mean concentrations in Table 18 were derived from paired values at all sites along each arc from CAPTEX #1-4. These results confirm that the largest overpredictions occurred at the closest arc with the largest negative residuals at the 300 and 400 km arcs. The mean observed concentration at the 300 km arc was significantly greater than values at other arcs by as much as a factor of 10. Another notable result is that observed mean values appear to display no strong trend with downwind distance between the 400 km and 1000 km arc over these cases. The modeled mean concentrations, on the otherhand, definitely exhibit a gradual decrease with distance. The most significant differences between the respective mean values existed from the 400 km to 600 km arcs.

The results for the peak concentrations in Table 19 are similar to those for mean values over these arcs. The peak observed and modeled values were computed from the highest concentration at each of the sites along the arcs for these cases. These results show that model overpredictions of peak concentrations were also certainly largest at the 300 km arc. While the peak observed concentration at the 300 km arc is considerably larger than peak values at any of the other arcs, there is also an indication of a secondary peak in the results for the 700 km arc. This feature was believed to be attributable to fumigation of elevated tracer material to the ground during the radid growth of the mixing height to higher levels over the morning period of the day after release.

Comparative Analyses of Plume Patterns and Positions

The graphical results in Figure 11a-f are shown to give qualitative displays of the overall observed and simulated plume patterns for each of the modeled CAPTEX experiments. The overall spatial patterns of the observed and modeled plumes are depicted by symbol(s) at the sites that experienced a nonzero observed (O) and/or modeled (*) concentration(s) during any sampling event of an experiment. The sites where both nonzero observed and predicted concentrations occurred represent an overlap region of the actual and modeled tracer plumes over the entire course of a particular experiment.

During CAPTEX #1-4 (Figures 11a-d) with releases from Dayton, both modeled and observed plumes crossed the 300 km arc in northern Ohio, although some spatial displacement in the positions of plume impact are evident even at this arc. The modeled plume appeared to overlap the observed tracer plume very well at the 300 km arc during CAPTEX #1 (Figure 11a), however, the observed plume traveled north of the modeled plume as it passed across Lake Ontario and upper New York state before exiting the sampling region. The modeled plume during CAPTEX #2 (Figure 11b) intercepted the 300 km arc to the left (i.e. counterclockwise) of the observed plume, however, there appears to be better overall spatial agreement in the plume patterns farther downwind in this case.

In contrast, the modeled plumes were shifted to the right (clockwise) of the observed plumes at the 300 km arc during CAPTEX #3 and #4 in Figures 11c and 11d, respectively. The spatial discrepancies between the respective plumes are particularly noticeable from the 300 km to 500 km arcs during CAPTEX #3. In fact, the observed plume nearly missed the 300 km arc

TABLE 18

STATISTICAL RESULTS OF OBSERVED AND MODELED CONCENTRATIONS PAIRED IN TIME AND LOCATION FROM SAMPLING ARCS FOR CAPTEX #1-4

ARC	N (SITES)	NN (PAIRS)	$\overline{O}$ (fl/l)	$\overline{P}$ (fl/l)	d (fl/l)	AAR (fl/l)	T4 (O>P) (%)
300	16	91	140.8	230.3	-89.5	321.8	41.8
400	9	71	12.0	110.7	-98.7	109.5	23.9
500	12	75	18.7	55.4	-36.7	53.7	30.7
600	10	78	15.2	34.3	-19.2	41.5	41.0
700	10	93	18.8	27.0	-8.2	39.3	55.9
800	13	112	16.8	14.1	2.7	27.0	67.5
900	8	63	12.2	12.5	-0.3	22.1	60.3
1000	3	27	13.7	13.4	0.3	17.6	63.0

TABLE 19

PEAK OBSERVED AND MODELED CONCENTRATIONS UNPAIRED IN TIME AND LOCATION FROM CAPTEX #1-4

ARC	N	NN	O_p (fl/l)	P_p (fl/l)	d (fl/l)	AAR (fl/l)	T4 (%)
300	12	12	439.0 ±658.2	1041.7 ±924.8	-602.7 ±1136.8	983.5	16.7
400	8	8	61.1 ±69.8	386.1 ±328.6	-307.0 ±354.8	307.0	0.0
500	9	9	71.7 ±59.1	170.4 ±95.7	-98.8 ±94.2	107.7	22.2
600	9	9	75.2 ±63.6	113.3 ±78.9	-38.1 ±65.6	64.6	22.2
700	9	9	84.8 ±74.2	135.2 ±82.6	-50.4 ±132.6	123.6	33.3
800	12	12	71.0 ±41.4	59.3 ±53.5	11.7 ±75.2	53.5	58.3
900	6	6	62.5 ±34.3	70.7 ±111.5	-8.2 ±125.5	80.8	50.0
1000	2	2	55.5 ±37.5	123.0 ±73.5	-67.5 ±36.1	67.5	0.0

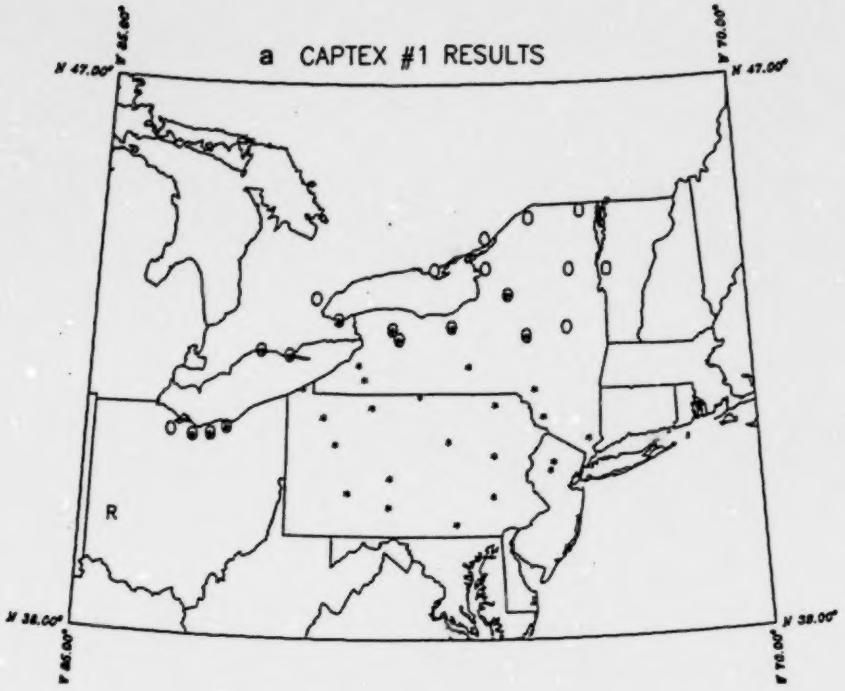
a CAPTEX #1 RESULTS
N 47.00°
W 85.00°
W 70.00°
N 47.00°
R
N 38.00°
W 85.00°
N 38.00°
W 70.00°

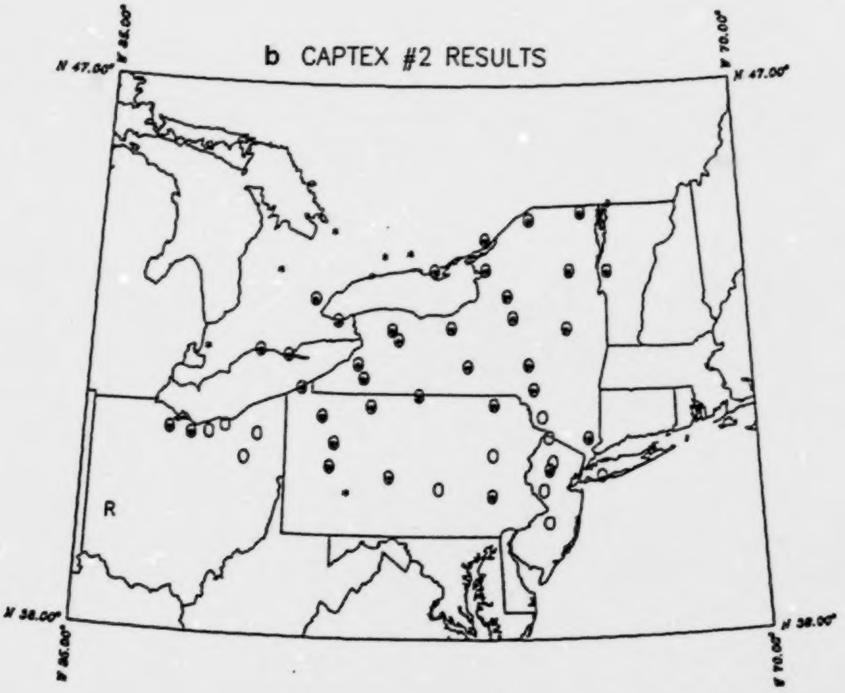
b CAPTEX #2 RESULTS
N 47.00°
W 85.00°
W 70.00°
N 47.00°
R
N 38.00°
W 85.00°
N 38.00°
W 70.00°

Figure 11. Observed (O) and modeled (*) plume patterns depicted from sites with nonzero concentrations during a) CAPTEX #1 and b) CAPTEX #2.

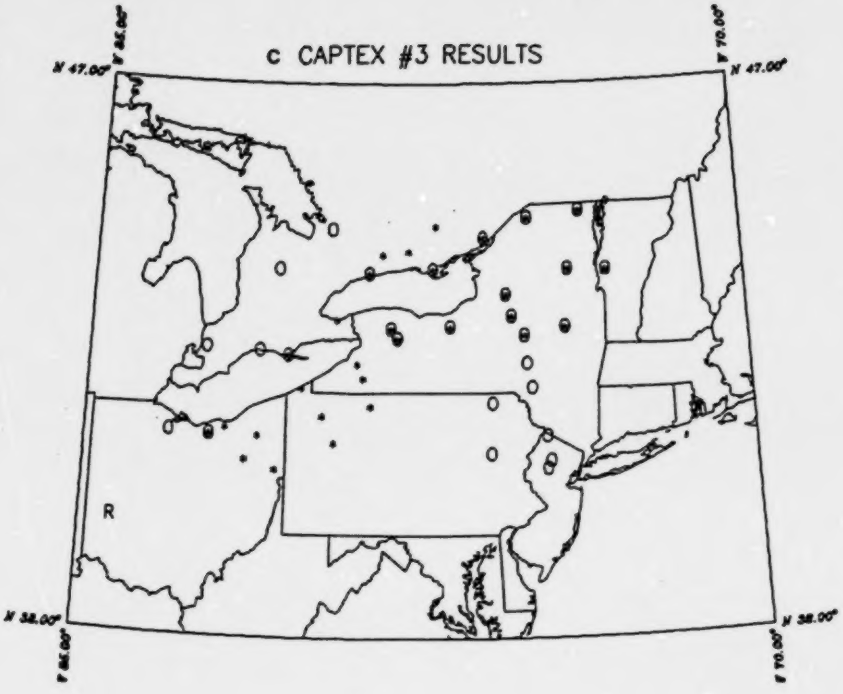
c CAPTEX #3 RESULTS
N 47.00°
W 85.00°
W 70.00°
N 47.00°
R
N 38.00°
W 85.00°
N 38.00°
W 70.00°

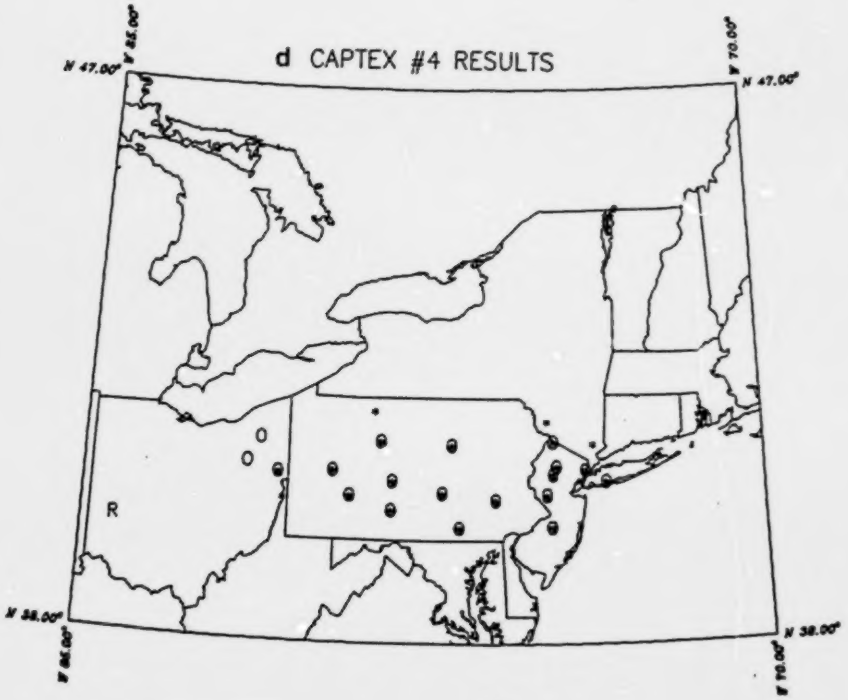
d CAPTEX #4 RESULTS
N 47.00°
W 85.00°
W 70.00°
N 47.00°
R
N 38.00°
W 85.00°
N 38.00°
W 70.00°

Figure 11. Same as 11a-b, except for c) CAPTEX #3 and d) CAPTEX #4.

during #3, as the bulk of it apparently traveled over extreme northwestern Ohio. Clearly, the best overall spatial agreement between the plumes existed during CAPTEX #4. Results of analysis of winds to be shown later will indicate that vertical wind direction shear was comparatively smaller on this case than in the other Dayton episodes.

Figures 11e-f show the plume patterns during CAPTEX #5 and #7 for the Sudbury releases. There was an interesting difference between these cases as the modeled plume traveled to the right (clockwise looking downwind) of the observed plume during CAPTEX #5 and to the left (counterclockwise) of the observed plume during #7. There is also evidence that the spatial separation between the respective plumes increased with distance downwind for these two cases. However, no firm conclusions can be reached about the relative spatial agreement between the plumes at any particular time period within an experiment from Figure 11a-f since each showed only the overall spatial 'footprint' of the modeled and observed plumes over a particular experimental episode. Individual graphical maps of the concentration distributions, too numerous to display herein, are needed to demonstrate the patterns of the observed and modeled plumes at each time period.

Another analysis technique that has emerged to assess spatial displacements between modeled and observed plume patterns relies on plume centroid positions. With this technique, the difference in relative plume positions and plume separation can be explored. A centroid location of a plume is defined herein as the density-weighted maximum concentration coordinate position (X_c, Y_c). The plume centroid positions for the modeled and observed plumes were determined at each time period from concentrations at sites with Eq. (8).

$$X_c(t) = \Sigma\, x_j \bullet C_j \;/\; \Sigma\, C_j \quad , \qquad (8a)$$

$$Y_c(t) = \Sigma\, y_j \bullet C_j \;/\; \Sigma\, C_j \qquad (8b)$$

In Eq. 8, x_j-y_j are the latitude-longitude coordinates of each site (j) with a nonzero concentration (C), where C represents either an observed or modeled concentration over a particular time period (t). The summation is performed over all sites separately with the observed and modeled plumes. Using the results of Eq. 8, the downwind distances of the observed (D_o) and predicted (D_p) plume centroid locations with respect to the particular release site were determined. In addition, the results of Eq. (8) were also applied in order to compute the separation distance (D_s) between the observed and modeled plume centroid positions.

These distance parameters have been advocated by Clark et al. (1988) in an assessment of long range model performance. For example, the statistical and test results presented earlier may not be able to distinguish between the performance of two different models in situations where both calculate zero concentrations at the same sites. That is, one model's plume pattern may slightly miss sampling sites, while the plume from another model may be displaced by a much greater distance from the same measurement sites. With these plume distance parameters, the downwind distance ratio

(D_p/D_o) and a normalized separation distance ratio (D_s/D_o) can be applied to more rigorously assess and distinguish between the performance of different models. For example, values of D_p/D_o that are greater than unity indicate the modeled plume traveled faster than the observed plume, while ratios less than unity signify the modeled plume was transported slower than the observed plume. On the otherhand, the values of D_s could implicate the speed and/or direction components of transport. However, if both plumes were the same distance downwind (i.e. D_p/D_o=1), a separation between the respective plumes would be entirely attributable to directional errors by the model.

The results of these ratios for each CAPTEX episode are presented in Figure 12a-f. Values have been plotted at the mid-point in time of each sampling interval. Focusing on the CAPTEX #1-4 (Fig. 12a-d), most of the values of D_p/D_o are less than 1, which reveals the modeled plumes traveled slower than the observed plumes. In particular, the evidence in some of these cases showed that the modeled plume tended to travel more slowly than the actual plume during the first overnight period. The sign convention adopted for the ratio of D_s/D_o in these figures specifies whether the modeled plume centroid was to the left (minus) or to the right (positive) of the observed tracer plume. The most dramatic shifts in D_s/D_o also occurred during the nocturnal hours of the first night. During the stable night hours, large vertical shears in both speed and direction are expected to develop in association with the nocturnal low level jet. In addition, graphical maps of plume concentration patterns during the morning periods of the second day in these cases also verified that the leading edge of the observed plume was impacting sites along arcs considerably farther downwind than the modeled plume.

An examination of the MESOPUFF II code revealed that the modeled plume was always transported by the lower wind field (mixed layer averaged) even during the nocturnal hours. Transport of the modeled plume was not switched to the upper layer wind field because with a surface-based nonbouyant release as in this application, Z_p always remained less than Z_i. Thus, even though the mixed layer depth dropped to relatively low values at night, Z_i continued to be greater than Z_p. Plume transport by the mixed layer averaged field, which at night is representative of the wind flow over a relatively shallow layer, also explains why the observed tracer probably outpaced the modeled plume during the nocturnal period. At night when significant vertical shears in speed and direction are prevalent, the mixed layer averaged winds were certainly slower than upper level wind speeds which more likely advected the observed tracer plume. In addition, plume separation was also magnified because larger differences in wind direction between these layers often exist during stable conditions at night. Examinations of nocturnal wind profiles during the CAPTEX episodes revealed notable vertical shears in both speed and direction, although there was variability from among the cases.

The results for the two Sudbury cases where the releases were at night under moderate winds behind cold fronts differed somewhat from the previous cases and each other. The results for CAPTEX #5 in Figure 12e were closer to ideal as higher winds and smaller vertical shears were responsible for transporting the rather narrow plumes rapidly off the U. S. east coast (see Figure 8e for plume patterns). Results for CAPTEX #7 in Figure 12f are

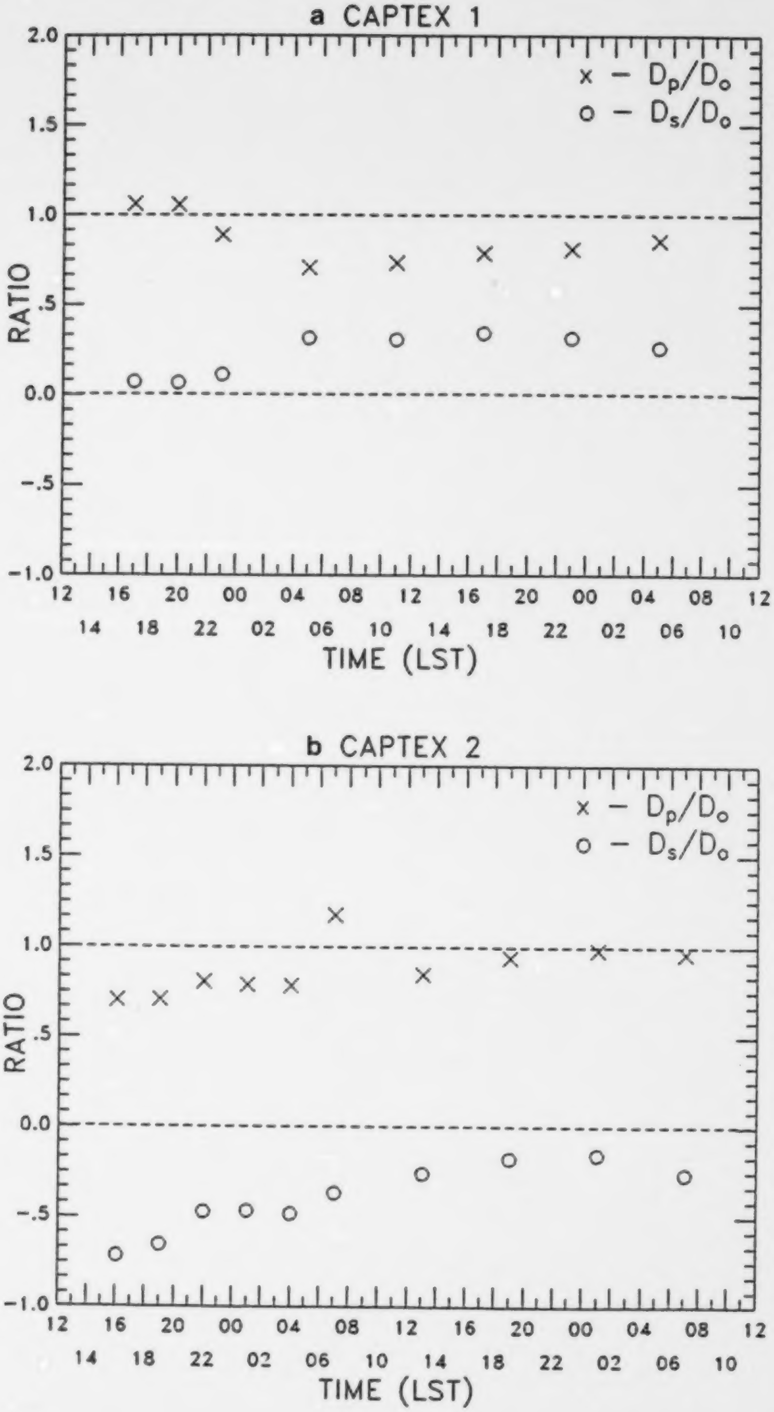

Figure 12. Ratios of downwind distances of the model and observed plume centroid locations (D_p/D_o) and separation distance between centroid positions to the observed downwind distance (D_s/D_o) versus time of day starting from the day of release. Negative and positive values for D_s/D_o denote the model plume position is to the right and left of the observed plume, respectively. a) CAPTEX #1 and b) CAPTEX #2 results.

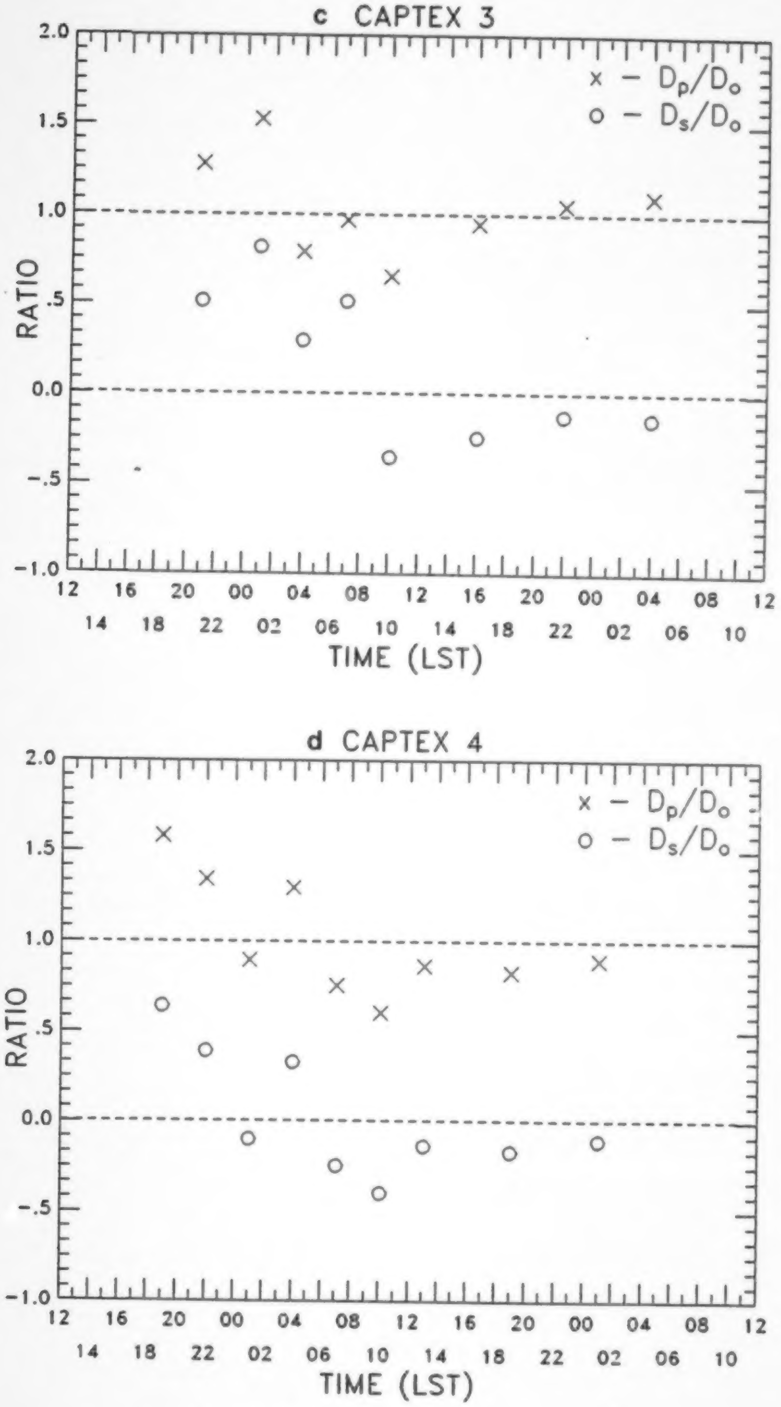

Figure 12. Same as 12a-b, except for c) CAPTEX #3 and d) CAPTEX #4.

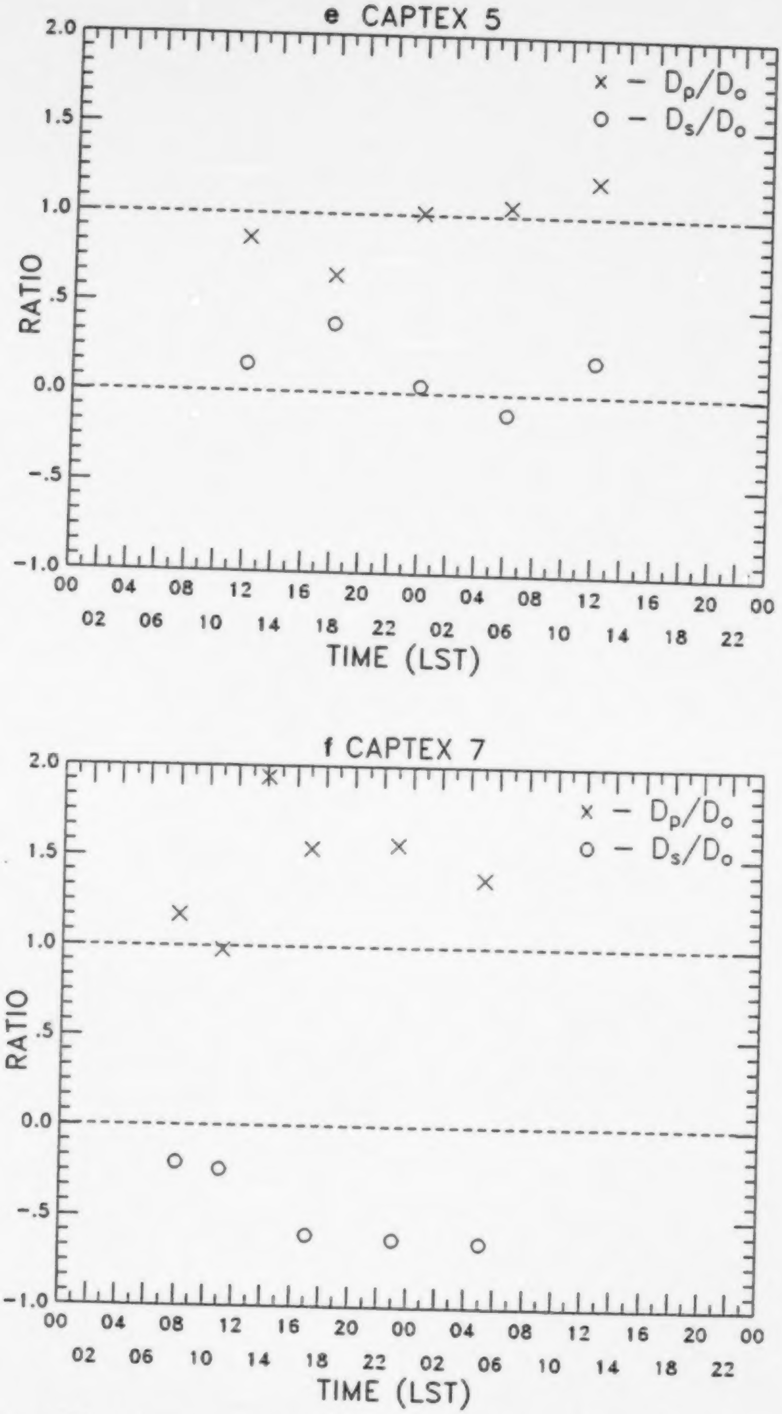

Figure 12. Same as 12a-b, except for e) CAPTEX #5 and f) CAPTEX #7.

in agreement with the overall plume patterns shown earlier in Figure 11f as the modeled plume traveled to the left (looking downwind) of the observed plume and at a faster pace, which was a departure from the other cases.

The non-normalized values of these parameters are presented in Figure 13 to show the actual difference between D_p and D_o and the magnitude of D_s. The results have been plotted against time after release for all episodes. A notable feature is that the largest differences in downwind distance between the respective plume centroid locations appeared from 12-24 hours after releases with values around 200 km. This time frame also coincided with the nocturnal period for the Dayton cases. The largest values of D_s were also found during this time period as values near 300 km occurred among these cases. Some caution must be exercised when interpreting the results for the later time periods because the bulk of the observed plume probably already moved beyond the sampling domain. Consequently, greater uncertainty exists with these points as some values may not accurately reflect the true differences between the respective plumes as the observed plume centroids were derived from plume remnants still being sampled at the farthest arcs from the release locations. Nevertheless, these results have provided valuable quantitive information about the magnitude of spatial plume displacements and helped focus on the probable causes for deviations in plume transport by the model.

DIAGNOSTIC TEST RUN RESULTS

Additional processor and model runs were conducted in order to exercise some of the optional selections for the wind field and dispersion methods and to compare these results with those already obtained from the operational default model runs. It was decided to conduct the diagnostic runs for the Dayton cases only with the emphasis in the analysis on the peak concentration results at the 300 km arc. This test strategy was selected in order to uncover the extent of the differences in the plume impact location and timing for the various wind fields and to identify the cause of the model overpredictions of peak concentrations which were pronounced at the 300 km arc sites. A single optional feature was exercised in each of the diagnostic runs while all other default parameters and methods remained unchanged. The input surface and upper air data files were identical to those in the default runs.

Although MESOPAC II contains options for several different wind fields, it was decided to limit the diagnostic runs to two alternative wind fields; single-level wind fields for the surface and the 850 mb levels. Either of these wind flows might be selected in certain model applications. Winds at the 850 mb level are generally representative of the flow at the top of the daytime mixing layer, and it is expected to provide a strong contrast from the transport provided by a surface wind flow. MESOPAC II processor runs were performed to produce meteorological files for each case with these wind field selections.

Of particular interest are differences in the location and travel time for the peak concentration and its magnitudeat the 300 km arc for the different wind fields and how the results compare with those of the observed plume. Tables 20-23 present the comparative results for CAPTEX #1-4,

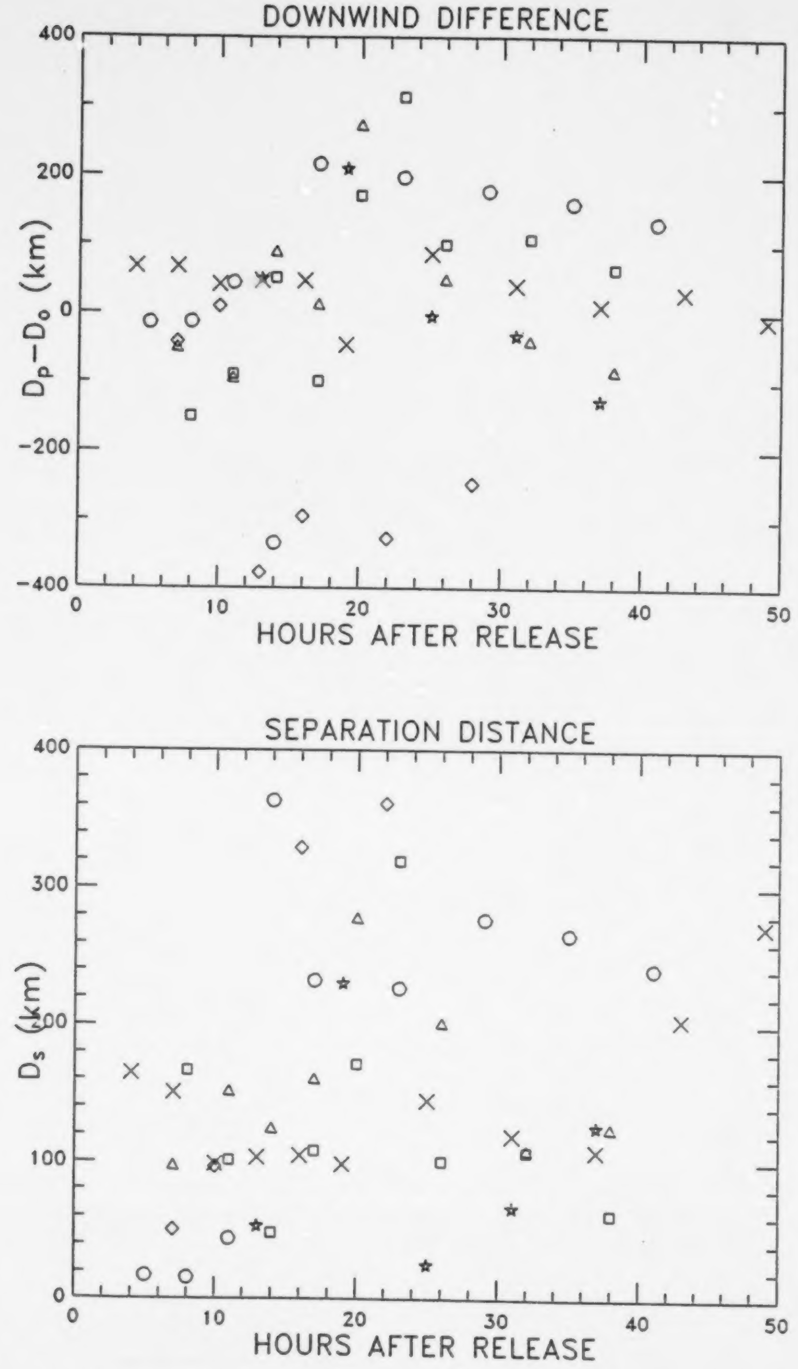

Figure 13. a) Difference in the downwind distances of the centroid positions of the modeled (D_p) and observed (D_o) plume patterns versus time after release. b) Separation distance (D_s) between modeled and observed plume centroid locations versus time after release. Symbols in both figures denote events for each experiment; CAPTEX #1 (O), #2 (X), #3 (triangles), #4 (squares), #5 (stars), and #7 (diamonds).

respectively. The individual results will be discussed separately in this section. The azimuth angle of each site with respect to true north are also given to help quantify the angular difference in the relative positions of plume impacts with the different wind fields. The position of each site in these tables is consistent with the configuration of this arc, as shown earlier in Figure 2, with site numbers increasing from right (east) to the left (west).

Table 24 presents the hourly NWS surface wind observations and results of certain parameters from the operational model runs for the release period. This table is provided with the intention of giving supplemental information for the interpretation of the model results. Surface winds in Table 24 do indeed show that the Dayton releases all occurred under primarily southwesterly wind flows. Consequently, for this wind flow and with the configuration of the sampling arc, a modeled plume impacting a site to the right (left) of the observed plume location on the 300 km arc would indicate a greater influence by a more westerly (southerly) component in the wind field.

The results in Table 20 for CAPTEX #1 indicate that the location and timing of impact of the peak concentration with the mixed layer (default) wind field compares favorably with the observed results. Site 316 was the location of impact for both the observed and model default peak concentration and the transport times were also the same at 5 h after the start of release. In contrast, the surface wind field caused the modeled peak concentration to occur much later and at a site slightly to the left of the observed results. The 850 mb winds transported the modeled plume at about the same speed as the observed plume but directed it to the right of the observed peak concentration location. These results are to be expected when wind direction becomes more westerly with height which was evident from the rawinsonde profiles; the wind flow at 850 mb had a greater westerly component than the surface winds. It appears that winds averaged over the mixed layer simulated the observed transport very well during the afternoon period in this case.

The results in Table 21 for CAPTEX #2 are certainly somewhat different from the CAPTEX #1 in the relative positions of plume impact. During this experiment the model default peak concentration intercepted the arc much faster and to the left of the location of the observed peak value. In fact, several 'model-specific' sampler sites were included in the model run in an effort to better define the modeled plume position in this case. The default peak occurred at a site about 25° to the west (left) of the observed peak. Mixed layer averaged wind directions at Dayton in Table 24 were indeed more southerly than the surface winds, which indicated why the modeled plume moved to the left of the observed plume position, but this did not explain why the mixed layer averaged wind possessed a greater southerly component. However, the afternoon and the regular evening (00 GMT) wind profiles at Dayton in Figure 14 appeared to show why the modeled plume behaved in this manner. The 00 GMT profile ,which was used to determine the modeled winds, revealed that wind direction backed with height from 230° at the surface to 250° near 1000, while the sounding at 18 GMT indicated that wind direction displayed the more typical veering with height during the release period. Consequently, $d\theta$ derived from the surface and layer-averaged directions was positive from the 00 GMT profile, which produced the stronger southerly component found in the mixed

TABLE 20

COMPARATIVE RESULTS FOR DIFFERENT WIND FIELDS ON PEAK CONCENTRATION/PLUME TRANSPORT AT THE 300 KM ARC FOR CAPTEX #1

RELEASE - 9/18 (1200 - 1500 LST)

	SITE NUMBER					
	320	318	316	314	312	310
AZIMUTH (^{o})	(24.5)	(36.2)	(42.5)	(45.3)	(55.4)	(60.5)
O_{max}	1	425	1586	197	0	0
DAY/TIME$	18/1700	18/1700	18/1700	18/1700		
TRAVEL TIME*(h)	5	5	5	5		
MODEL WIND FIELD						
DEFAULT	0	116	2367	1568	0	0
		18/1700	18/1700	18/1700		
		5	5	5		
SURFACE	176	4456	752	163	0	0
	18/2300	18/2000	18/2300	19/0200		
	11	8	11	14		
850 mb	0	0	0	0	1961	642
					18/1700	18/1700
					5	5

$ TIME IS THE START HOUR OF THE SAMPLING INTERVAL

* TIME INTERVAL FROM THE START OF RELEASE AND TO BEGINNING OF OF SAMPLING INTERVAL

TABLE 21

COMPARATIVE RESULTS FOR DIFFERENT WIND FIELDS ON PEAK CONCENTRATIONS/PLUME TRANSPORT AT THE 300 KM ARC FOR CAPTEX #2

RELEASE - 9/25 (1205-1505 LST)

	SITE NUMBER									
	324*	323*	322*	321*	320	318	316	314	312	310
AZI.(^{o})	(-1.5)	(4.7)	(10.8)	(16.7)	(24.5)	(36.2)	(42.5)	(45.3)	(55.4)	(60.5)
C_{max}	-	-	-	-	64	1575	768	407	12	10
DAY/TIME					26/04	26/02	26/04	26/01	26/04	26/04
TRAVEL TIME (h)					16	14	16	13	16	16
MODEL WIND FIELD										
DEFAULT	9 26/01 13	320 25/16 4	2767 25/16 4	1430 25/19 7	390 25/22 10	20 26/04 16	0	0	0	0
SURFACE	12 26/07 19	79 26/07 19	286 26/07 19	459 26/10 22	1106 26/10 22	1324 26/13 25	873 26/13 25	656 26/16 28	92 26/19 31	74 26/19 31
850 mb	0	0	0	0	0	0	533 25/19 7	1002 25/22 10	303 25/22 10	0

* 'Model-specific' sites only

TABLE 22

COMPARATIVE RESULTS FOR DIFFERENT WIND FIELDS ON PEAK CONCENTRATIONS/PLUME TRANSPORT AT THE 300 KM ARC FOR CAPTEX #3

RELEASE - 10/02 (1400-1700 LST)

	SITE NUMBER							
	320	318	316	314	312	310	308	306
AZI. (^{o})	(24.5)	(36.2)	(42.5)	(45.3)	(55.4)	(60.5)	(68.8)	(74.4)
O_{max} DAY/HR TIME (h)	304 02/2200 8	0	2 03/0100 11	0	0	0	0	0
MODEL WIND FIELD								
DEFAULT	0	0	102 02/2200 8	38 02/2200 8	1416 03/01 11	524 02/2200 8	8 03/0100 11	0
SURFACE	258 03/0400 14	10 03/0400 14	3 03/0700 17	11 03/0700 17	0	0	0	0
850 mb	0	0	0	0	0	14 03/0100 11	754 03/0100 11	1357 03/0100 11

TABLE 23

COMPARATIVE RESULTS FOR DIFFERENT WIND FIELDS ON PEAK CONCENTRATIONS/PLUME TRANSPORT FOR THE 300 KM ARC FOR CAPTEX #4

RELEASE - 10/14 (1100-1400 LST)

	SITE NUMBER									
	320	318	316	314	312	310	308	306	304	302
AZI.(°)	24.5	36.2	42.5	45.3	55.4	60.4	68.8	77.4	83.9	93.1
Omax	0	0	0	0	9	1350	33	0	M	M
DAY/HR					15/19	14/19	14/19			
TRAVEL TIME (h)					8	8	8			
MODEL WIND FIELD										
DEFAULT	0	0	0	0	0	0	1448 14/19 8	145 14/16 5	0	0
SURFACE	65 15/07 20	799 15/01 14	1859 15/01 14	1492 15/04 17	231 15/04 17	119 15/04 17	0	0	0	0
850 mb	0	0	0	0	0	0	0	0	626 14/16 5	81 14/19 8

M - missing measurements

TABLE 24

SELECTED METEOROLOGICAL OBSERVATIONS AND MODEL RESULTS AT THE RELEASE SITE OF EACH CAPTEX EXPERIMENT

		SFC OBS.		MODEL ML WINDS$				
SITE-DATE	HR (LST)	WS (m/s)	WD (Degx10)	SPEED (m/s)	DIR (Deg)	PGT CLASS	TEMP (°F)	CLOUD COVER (tenths)
(DAY-9/18)								
#1	12	7.7	22	13.4	224.4	4	86	0
	13	9.3	24	16.0	245.0	4	87	4
	14	8.8	21	15.3	216.7	4	89	4
	15	8.2	22	14.3	224.8	4	89	4
(DAY-9/25)								
#2	12	4.1	24	9.4	230.1	3	66	10 (250)*
	13	5.2	20	12.8	189.5	4	68	10 (250)*
	14	6.2	22	15.6	206.6	4	70	10 (250)*
	15	3.6	22	10.1	205.2	4	69	10 (100)*
(DAY-10/2)								
#3	14	7.2	24	17.3	266.0	4	81	0
	15	5.7	22	13.7	248.7	4	82	0
	16	4.1	23	10.1	258.5	3	81	0
	17	5.2	23	12.4	257.6	4	81	0
(DAY-10/14)								
#4	11	7.7	25	14.8	269.4	4	49	0
	12	7.2	26	14.5	280.9	4	51	0
	13	7.2	24	14.9	264.2	4	53	0
	14	8.2	25	16.3	271.9	4	55	0
(SUD-10/25-26)								
#5	23	4.6	32	4.6	319.9	4	37	8 (11)*
	00	3.6	32	3.6	319.9	4	37	8 (16)*
	01	5.2	33	5.2	329.8	4	39	8 (18)*
	02	5.7	31	5.6	310.0	4	39	8 (13)*
(SUD-10/29)								
#7	01	8.2	33	17.9	326.8	4	32	4
	02	6.2	33	13.0	326.9	4	32	8 (30)*
	03	3.1	33	8.8	339.7	4	30	8 (24)*
	04	6.2	33	13.0	326.9	4	30	4

$ Mixed layer (ML) averaged winds at the grid point nearest release site
* Ceiling height in hundreds of feet above ground

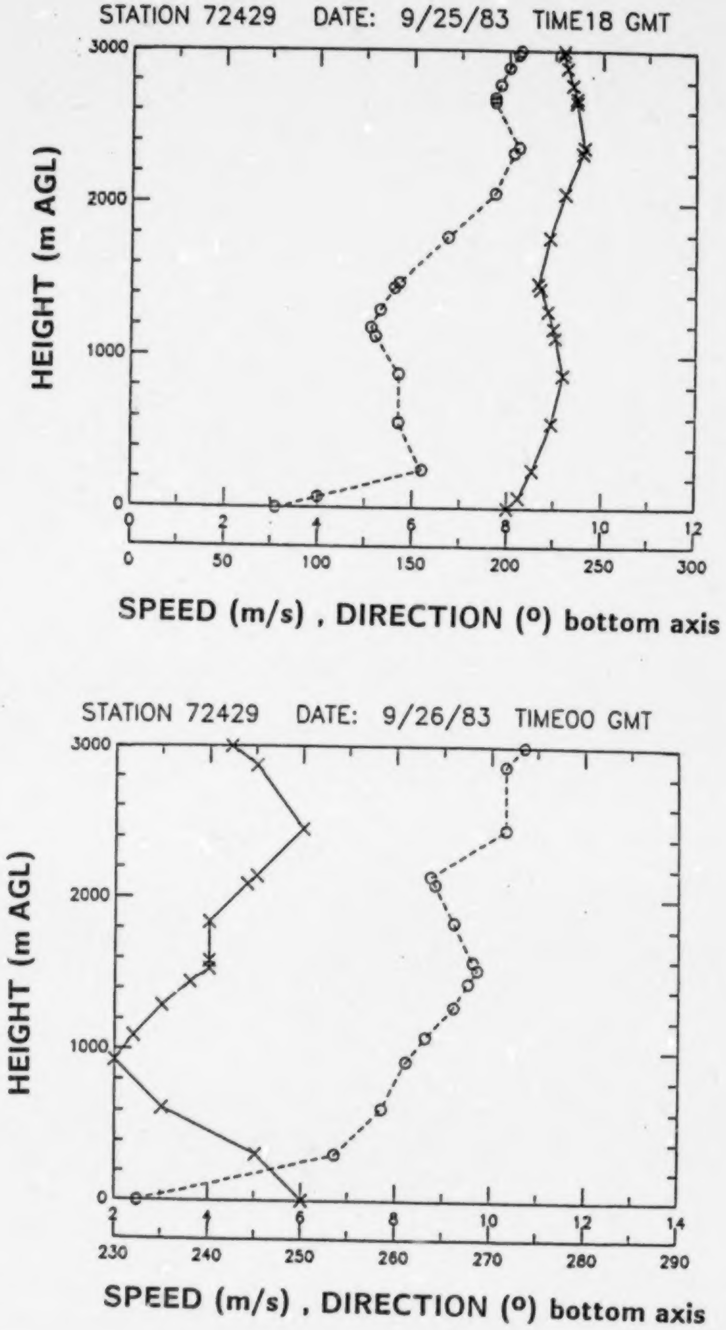

Figure 14. Upper air wind speed (O) and wind direction (X) profiles at a) 18 GMT (i.e. 13 LST) and b) 00 GMT for CAPTEX #2.

layer averaged wind directions in Table 24 for this case. Another wind profile from a rawinsonde launch at 20 GMT was also very similar to the 18 GMT profile, so the vertical variation in wind direction exhibited in the 00 GMT sounding did not occur during the time period of the tracer release. This case demonstrated the impact on model results when the upper air data were not representative of the conditions at an earlier time. It is apparent that better model results might have been obtained if one of the upper air profiles taken during the release period was substituted for the 00 GMT profile, or if the model was capable of using rawinsonde data at more frequent time intervals.

The largest spatial difference in the location of plume impact between the observed plume and modeled plume with the mixed layer averaged winds occurred in CAPTEX #3 (Table 22). The exact location and magnitude of the actual tracer peak concentration could not be accurately judged in this case since the bulk of the tracer plume definitely traveled to the west of this arc. Some of the tracer plume impacted site 320 located on the western end of the arc. It is estimated from Table 22 results that the peak concentration location from the model default run was shifted at least 30° to the right of the position where the observed plume may have passed at this downwind distance. The 00 GMT wind profile at Dayton in Figure 15 reveals that significant vertical shear in direction existed within the mixed-layer in this case, as wind directions varied from 200° at the surface to almost 270° at Z_i. This large vertical variation in direction also explains the large differences in plume impact time and location between the model runs with surface and 850 mb wind fields. The release period for #3, being slightly later in the afternoon compared to the other Dayton releases, may also have contributed to the variations in the plume's trajectory and dispersion. In particular, tracer gas emitted near the end of the release period at 17 LST had much less time to be mixed through the boundary layer as convective turbulence is already less vigorous and is rapidly decreasing during the late afternoon hours.

Tracer measurements from aircraft flights provided additional valuable information about the impact of vertical direction shear coupled with the timing of the release for CAPTEX #3 on the transport and dispersion of the tracer plume. An aircraft flight leg was conducted across northern Ohio at 1500 m around midnight. A tracer plume was discovered at this level with the highest concentration being 1466 fl l^{-1} in the same relative position as modeled peak concentration from the mixed layer wind fields. However, the real suprise occurred from the tracer measurements from aircraft flight legs over southeastern Pennsylvania during the afternoon of the next day, October 3. The vertical cross-section in Figure 16 showed evidence of a coherent tracer plume aloft with a concentration as high as 2961 fl l^{-1}. Clearly, this portion of the tracer plume was transported by westerly winds which existed in the upper part of the boundary layer. Additionally, for concentrations to be so high, this plume section had experienced little boundary layer-based turbulent activity, which would have dispersed it and fumigated it to the surface. Surface sampling sites measured zero concentrations in this area. The multi-layer Lagrangian model by Davis et al. (1987), which contained seven vertical layers up to nearly 3000 m, displayed much greater success in simulating the broad spread and decoupling of the tracer plume pattern due to the large vertical shears during this episode.

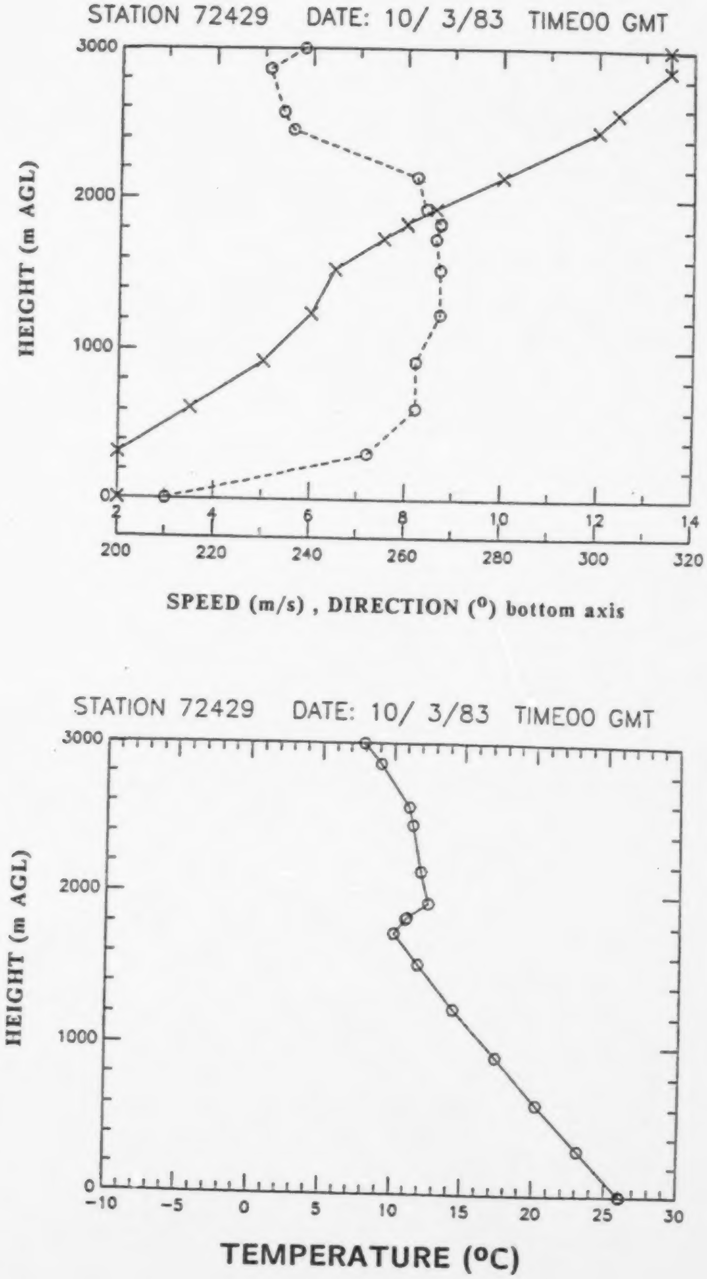

Figure 15. a) Wind speed (O) and wind direction (X) profiles and
b) temperature profile at Dayton, Ohio from CAPTEX #3.

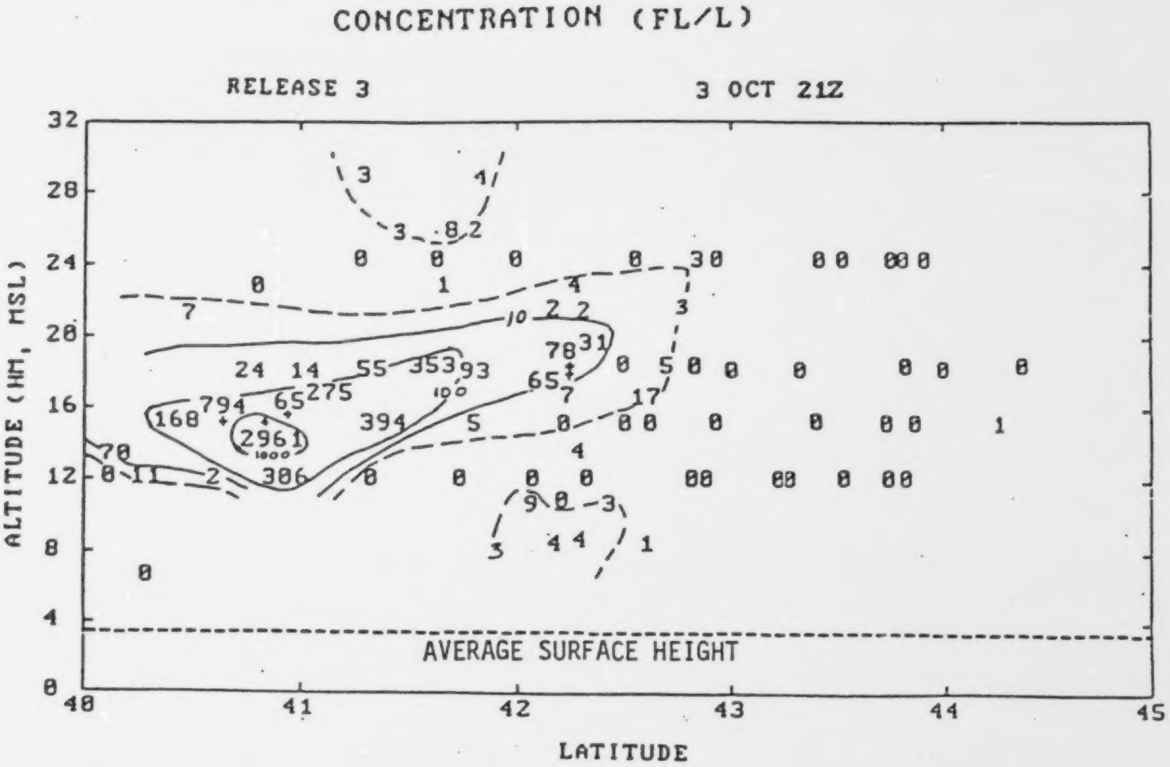

Figure 16. Tracer concentration pattern from aircraft flight legs at different levels during the afternoon of October 3, 1983 during CAPTEX #3. (Ferber et al., 1986)

The results for CAPTEX #4 in Table 23 reveal that the default model plume exhibited relatively good correspondence in time and position with the observed peak concentration. The modeled peak occurred within 10° to the right of site where the observed plume impacted and the respective travel times were in agreement. Both results also show that the tracer plume was narrow in this case. The results for the single layer wind fields were similar to those in #1 and #2; the modeled plume using surface wind fields traveled to the right and slower than the observed plume and the 850 mb winds caused the modeled plume to impact to the right of the observed peak concentration position.

Although the experiments from Sudbury were not examined in these model test runs, it is of interest to assess the plume impact locations for these two cases, especially on the north side of Lake Ontario. For CAPTEX #5, the observed and modeled plumes (Figure 8e) impacted sites 752 and 652, respectively, which were both about 400 km from Sudbury and just north of Lake Ontario (Figure 2). More importantly, the difference in azimuth angle with respect to Sudbury between these sites was about 8°. In CAPTEX #7, the observed plume traveled to the right of the modeled plume (Figure 11f) and the angle difference in azimuth angle for the sites in this case was about 13°. Interestingly, in these cases and in some of the Dayton cases the angular separation of the respective plumes was comparable to the resolution of the surface wind direction observations.

The upper air wind profile data collected during the release periods and at the regular 00 GMT launch time were analyzed to further explore reasons why modeled speeds and directions differed from those inferred from the actual tracer plume measurements out to the 300 km arc. The results in Table 25 were determined from profiles at Dayton and for Buffalo (BUF) to represent the Sudbury cases. The notable values are the ratio of the mixed-layer averaged to surface wind speeds (WS_{ml}/WS_o) and difference between the wind directions. In particular, most of the afternoon wind speed ratios were lower than values at 00 GMT. Wind direction differences in Table 25 also tended to be larger at 00 GMT than in the earlier profiles. Stronger turbulent mixing in the afternoon period likely reduced vertical shears in speed and direction within the mixing layer, however, vertical variations appeared to become stronger by evening. The changes over the time period of these profiles were also consistent with the results reported by Shreffler (1982). From analysis of a large wind profile data base, he found that the diurnal variations of wind speed ratio and wind direction difference over the mixed layer exhibited minimum values during the afternoon period with gradual increases during the evening to maxima at night. Thus, the mixed layer averaged fields computed by the model are believed to be slightly overestimating transport speeds during the daytime period, however, this feature was difficult to assess with the 3-h averaging period for these cases. On the otherhand, there was some evidence of an effect on wind direction in the model as the previous results indicated that the default model plumes were shifted slightly to the right of the observed plumes in CAPTEX #4 (Table 23) and CAPTEX #1 (Table 20).

The other important feature to be examined is the significant model overprediction of peak concentrations reported earlier. The same dispersion method, as outlined in Section 2, was applied in these model runs with the

TABLE 25

RESULTS OF ANALYSIS OF OBSERVED UPPER AIR WIND PROFILES FROM THE CAPTEX RELEASE DAYS

EXPT	SITE	DATE-TIME (MM/DD-GMT)	WS_{ml} (m/s)	WD_{ml} (Deg)	$\frac{WS_{ml}}{WS_o}$	WD_o-WD_{ml} (Deg)	WD_o-WD_{Zi} (Deg)	Z_i (m)
1	DAY	9/18-1800	12.5	229.0	2.4	1.0	-12.0	1254
		9/18-2000	13.1	239.0	2.0	-19.0	-27.0	1855
		9/19-0000	12.7	221.5	1.8	-11.5	-22.0	1675
2	DAY	9/25-1800	5.3	220.0	1.7	-20.0	-21.6	1294
		9/26-0000	7.5	237.9	3.0	12.1	11.8	1439
3	DAY	10/2 -1800	4.9	258.3	1.1*	-26.0*	-39.0*	1808
		10/3 -0000	7.3	226.4	2.4	-26.4	-55.0	1732
4	DAY	10/14-2000	9.2	249.2	1.5	-9.2	-30.6	1217
		10/15-0000	8.0	239.8	2.0	-19.8	-38.6	972
5	BUF	10/26-1800	9.8	290.1	1.4	9.9	12.4	2293
		10/27-0000	11.7	315.0	1.7	-25.0	-30.0	2070
7	BUF	10/29-1800	8.5	335.5	1.2	14.5	6.5	1254
		10/30-0000	6.2	330.5	3.1	-0.5	-8.1	1175

NOTE:

WS_{ml} - mixed-layer mean wind speed from observed profile data
WD_{ml} - mixed-layer mean wind direction from observed values
WS_o - surface observed wind speed at the rawinsonde site
WD_o - surface observed wind direction at the rawinsonde site
WD_{Zi} - observed wind direction at the mixing height
Z_i - observed mixing height; winds averaged up to this level

* Missing observed surface wind; values at next higher level applied; this result may slightly underestimate the actual condition.

different fields. In the three Dayton cases where the peak concentration was readily resolved (Tables 20, 21, and 23), model predictions with the default wind scheme were greater than observed peak values by varying amounts. Since dispersion is dependent on travel time after 100 km in the model, modeled peak values differed for the various wind fields. Focusing on the default model results in Tables 20-23, the overpredictions were smaller for #1 (Table 20) and #4 (Table 23) where model transport times agreed with observed values. The most sizeable overprediction of the peak concentration by the default model run occurred in CAPTEX #2 (Table 21) as the modeled plume arrived much earlier than the observed plume.

Differences in the width of modeled and observed plumes were difficult to assess even for the site spacing of this network, however, the results at 300 km suggested that modeled and observed plumes exhibited comparable horizontal spread. Nevertheless, the consistent model overprediction strongly implied that dispersion was greater for the observed plumes. Since puff growth is controlled by dispersion parameters, whose variations are dependent on stability class, the results for PGT class in Table 24 are illustrative of a possible cause for the model overpredictions. Neutral stability (PGT class 4) was often found during these afternoon hours when unstable conditions might be expected, although based on the observed wind speeds the specification of a neutral stability class appears appropriate. A further examination of processor output revealed stability class 4 was indeed prevalent at the grid points in Ohio during the afternoon hours. Consequently, the initial growth of the model plume, particularly in the vertical dimension, was much more limited due to the significantly slower increase in the dispersion parameters under neutral stability when compared to that under the unstable PGT classes (Turner, 1970). In particular, the coefficients of the power law curve for σ_z for neutral stability in the model were derived from a fit to the so-called D2 curve in Pasquill (1974), which is the neutral curve for the vertical dispersion parameter in Turner (1970). However, greater vertical dispersion in the model would have been produced under the D1 curve for neutral stability in Pasquill (1974). In any event, the principal cause for overprediction by the model in this application was attributed to underestimation of vertical dispersion. More evidence to support this explanation will be given next from additional model test runs.

Diagnostic model test runs were also performed to assess the impact on peak concentrations by applying optional variations to the default dispersion method or selecting the uniform vertical mixing feature in the model. Results in Table 26 for CAPTEX #1 were representative of those found in model runs for the other Dayton cases. The peak concentrations at the plume centerline with the uniform vertical mixing option were lower than values from the default model run. Since the observed peak concentration was 1586 fl l^{-1} in CAPTEX #1 (see Table 20), the peak value using the vertical mixing option was certainly more comparable and suggested that distributing the plume vertically over the depth of the mixed layer was more representative in this case. In fact, a further examination of operational model output indicated that σ_z was much less than Z_i at the 300 km arc, which revealed the modeled plume had not yet become well-mixed even out at this distance. Thus, it is evident that more rapid growth of σ_z in the model would have provided an improvement in the prediction of peak concentrations.

TABLE 26

PEAK CONCENTRATIONS FOR CAPTEX #1 USING VARIOUS DISPERSION OPTIONS

MODEL RUN	SITE NUMBER 320	318	316	314	312
DEFAULT METHODS*	0	116	2367	1568	0
UNIFORM VERTICAL MIXING OPTION@	0	69	1446	980	0
CROSSOVER DISTANCE# AT 50 km	0	133	2586	1722	0
CROSSOVER DISTANCE# AT 10 km	0	126	3075	2020	0

* PGT dispersion curves applied out to 100 km, time dependent growth according to Heffter (1965) at greater distances.
@ Puffs vertically distributed over the mixed-layer after release instead of σ_z growth.
# Downwind distance where puff dispersion changes from PGT curves to time dependent method.

TABLE 27

COMPARISON OF OBSERVED AND MODELED MIXING HEIGHTS

	ALL PAIRS		$0 < CC \leq 8/10$		$0 < CC \leq 4/10$	
TIME (GMT)	18	00	18	00	18	00
N	59	73	38	49	18	28
Z_{io} (m)	1456. ±533.	1479. ±496.	1368. ±437.	1369. ±431.	1300. ±453.	1307. ±409.
Z_{ip} (m)	1145. ±317.	1166. ±326.	1244. ±270.	1191. ±339.	1355. ±324.	1313. ±331.
d (m)	311.	312.	124.	177.	-56.	-6.
AAR (m)	468.	471.	336.	402.	283.	340.
R	0.22	0.15	0.35	0.22	0.56	0.34
O>P (%)	66.1	67.1	57.9	59.2	44.4	39.3
F2 (%)	84.7	89.0	92.1	95.9	88.9	100.

CC = cloud cover
F2 = percent of observed and modeled values within a factor of 2

Additional results in Table 26 revealed that reducing the crossover distance caused even higher peak concentrations compared to the default distance (i.e. 100 km). Clearly, these results indicated that the time dependent dispersion formulas provided even slower growth than that offered by PGT class 4 in this application.

Since it was noted earlier that accurate specification of Z_i was also important to both transport and dispersion in this model, a brief examination of the modeled mixing height is warranted. The diurnal variation of Z_i at the grid point closest to Dayton over the two day period of CAPTEX #1 is depicted in Figure 17 to illustrate the typical temporal behavior and magnitude of mixing height derived by the MESOPAC II processor. The most dramtic change in Z_i occurred around sunset when a switch in methods takes place. Mechanical Z_i's at night were generally much lower than the daytime convective Z_i's which were primarily controlled by the variation in the sensible heat flux. However, the term containing the thermal gradient aloft in Eq. 1 also appears to be counteracting the surface sensible heat flux term in this case. This effect is attributed to the gradual decreases in Z_i in the late afternoon hours prior to the substantial drop observed at sunset.

Of particular interest is how well the modeled mixing heights compare to observed values. Therefore, a data set of observed and modeled Z_i's was developed. An observed Z_i, defined as the height of the elevated temperature inversion base, was paired against a modeled value from the closest grid point to a rawinsonde site at the same hour. Observed values were easily obtained from the temperature profiles because a strong inversion was present during the CAPTEX episodes (e.g. Figure 15). Statisitical results were computed for Z_i pairs at 18 and 00 GMT. For the latter time, however, it was decided that the modeled convective Z_i at 23 GMT was appropriate to compare with an observed value since sunset had already occurred by 00 GMT at some sites.

The results in Table 27 contain the results for both time periods for separate categories of cloud cover. The model performed best under clear to partly cloudy conditions which generally prevailed, as the bias (d) was smaller and the correlation was higher than for the mostly cloudy cases. It is apparent that the underpredicted Z_i for the few cases when overcast conditions prevailed. Finally, no strong conclusions about the general applicability of this method to model Z_i should be drawn because the data set was relatively small and represented a rather limited set of temporal cases and meterological conditions.

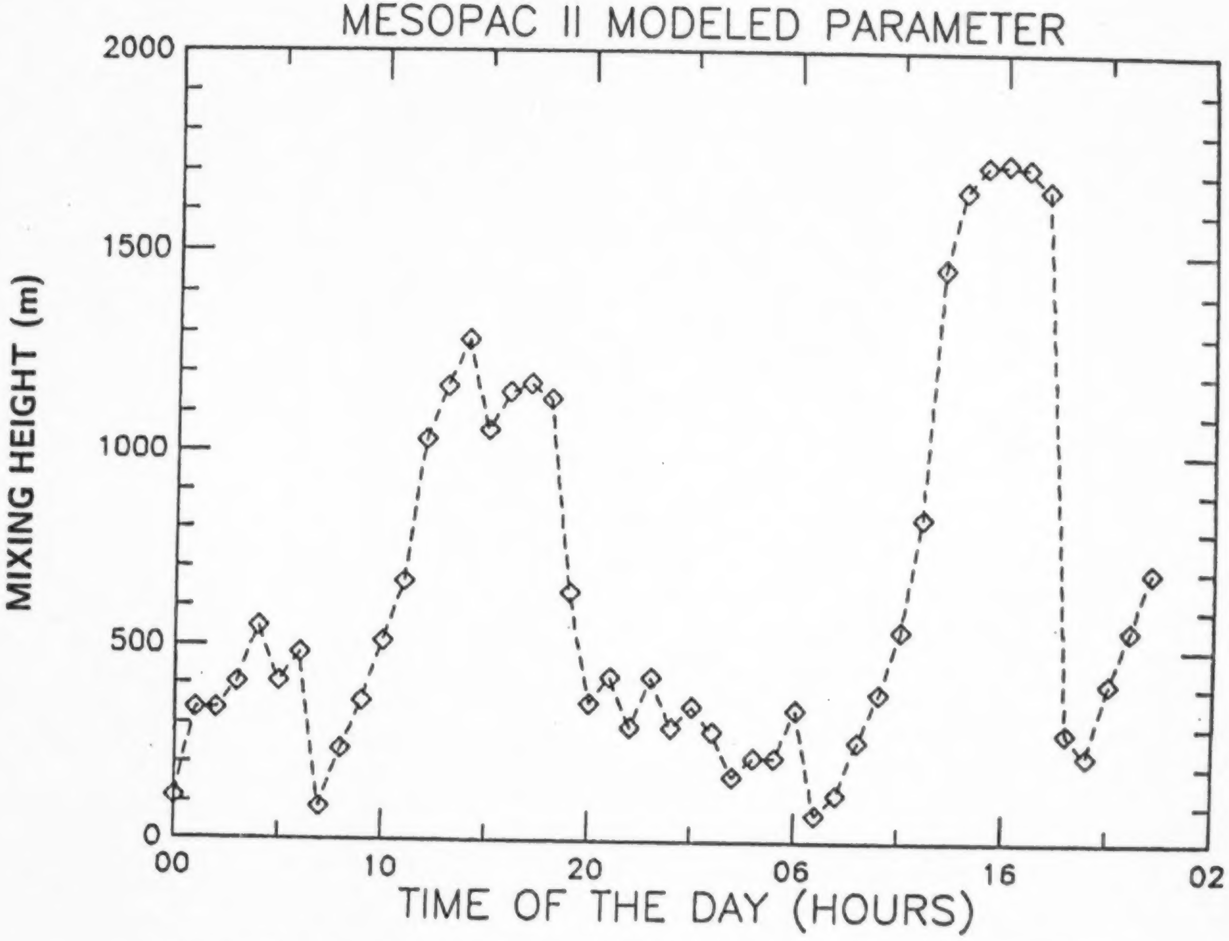

Figure 17. Hourly variation of mixing height (Z_i) from the MESOPAC II for Dayton, Ohio for September 18-19, 1983 of CAPTEX #1.

SECTION 5

MODEL SENSITIVITY RESULTS

Flexibility built into the design of model code can be advantageous to the testing of various model components. MESOPUFF II contains considerable flexibility which allows certain changes in methods or variations in technical parameters to occur through input values (Scire et al., 1984b). Nevertheless, the intent of this testing effort was not to conduct a comprehensive sensitivity study of the various model components. Practical considerations of time and computer costs necessitated a limit to the number of model test runs for selected model components. It was decided to place major emphasis of this sensitivity analysis on the dry deposition and chemical transformation algorithms, which were not exercised in the CAPTEX evaluation effort. Furthermore, no evaluation of the methods for these processes was possible during the development effort that led to this version of the model. Finally, there was a desire to report for the first time the impact from some of the options in this model.

The main purpose of this sensitivity effort was to investigate the impact on surface concentrations for a typical short-term averaging period (i.e. 24 h) from selected changes in methods available in the model or from differences in particular key technical parameters involved in the two model components. Differences in concentrations between the test cases and a model base case are emphasized herein because Morris et al. (1988) already examined the responses of deposition velocity and transformation rates of the modeled pollutant species to ranges in atmospheric parameter variations, land use types, and for differences in technical parameters involved in these model components.

Although various types of sensitivity methods are available (Gelinas and Vayk, 1979), the test procedure adopted for this effort consisted of varying a single option or parameter in a model test run while holding all other inputs and model features the same as those in a base case. This testing strategy permitted a comparative assessment of the relative impact of the variation in each test run to the base case results. Consequently, all model test runs were performed with the same input meteorological fields; namely, the gridded results produced by MESOPAC II in the default mode for CAPTEX #1.

The identical source characteristics and emissions from a single realistic elevated point source were input to each model run. Table 28 contains the source information and emission rates used in all model runs. The location of this single source was set to the same grid coordinates as the Dayton tracer release site. The elevated source height and strong buoyancy of the plume also exercises plume rise and fumigation methods in the model. A single source was chosen because the analysis and interpretation of the effects on ground-level concentrations from one point source are more straightforward and model runs are less expensive than for multiple sources. These test runs focused on computing SO_2 and sulfate (SO_4) concentrations with the emission rates specified in Table 28.

TABLE 28

SOURCE CHARACTERISTICS AND EMISSION RATES FOR ALL MODEL SENSITIVITY TEST RUNS

Point source location - Grid coordinates of Dayton tracer release site

Stack height - 304 m AGL

Stack diameter - 8 m

Exit velocity - 22 m/s

Exit temperature - 407 K

SO_2 emission rate - 7064 g/s

SO_4 emission rate - 53 g/s

Several other aspects of the model base case and test runs should also be identified. All model runs commenced at midnight and model execution continued for a 48 h period. Source emissions in Table 28 were continuous over the 2-day simulation period, which was of sufficient duration for the source plume to travel across the entire model domain while being subjected to the various physical processes. Additionally, pollutant concentrations were computed at grid points on the model sampling grid which was set to the same size as the meteorological grid in the CAPTEX application. It was desireable to analyze concentrations on the denser, uniform model grid in order to take advantage of the capabilities of the MESOFILE II postprocessor program. Computational procedures were specially designed into this program to perform various analyses on different gridded concentration fields from independent model runs.

The methods described in Section 2 for dry deposition and chemical transformation were applied in the model base case run. The 24-h average concentration fields of SO_2 from the model base case run for Day 1 and 2 are displayed in Figures 18a and 18b, respectively. The results in Figure 18a show that the plume had reached the eastern edge of the model grid by the end of Day 1. The 24-h average plume patterns on both days are similar because of prevailing southwesterly winds within the mixed-layer with stronger westerly winds in the upper layer field. The highest SO_2 concentrations are found close to the source and values generally decrease with distance downwind due to the dispersion, and both deposition and transformation processes reducing SO_2 levels in the plume.

The 24-h sulfate concentration patterns for the two simulation days from the base case run in Figure 19a and 19b are identical to those for SO_2, except SO_4 concentration levels are considerably lower. However, in contrast to the results for SO_2, highest sulfate concentrations are found several hundred kilometers downwind of the source on both days. This is a consistent feature for some pollutants, such as sulfate, which is primarily formed from chemical reactions during transport across a region.

Since the plume patterns from all model test runs were also identical to the base case distributions because the same transport and dispersion conditions were applied in all cases, concentration differences were examined from the set of grid points defining the plume pattern. Thus, analyses by the postprocessor was restricted to the grid points with nonzero concentrations. The results consist of percent deviations of a test case concentration (C_t) from a corresponding model base case value (C_b).

The results of peak and plume average concentrations for SO_2 and SO_4 over the two 24-h periods from initial model test runs are given in Table 29. The peak concentration was defined as the highest value found from the entire gridded plume pattern over the time period, while average plume concentrations were computed from all nonzero values. These initial test runs were conducted to examine the impact on concentrations when one of these physical processes was not modeled, which represents an extreme situation. The results in Table 29 show minor differences in peak SO_2 concentrations when either deposition or transformation processes were omitted. This is to be expected since peak SO_2 concentrations were generally found close to the source where these processes have not yet had much

```
DATA READ FROM MESOPUFF OUTPUT FILE -- UNIT:  20  RUNSTREAM:    1
     VERSON=  4.0  LEVEL=870421  NSYR=83  NSDAY=261  NSHR= 0  NADVTS=   48  IAVG=    1  NPUF=  4  NSAMAD=  4  IELMET=30  JELMET=19
     DGRID=  37000.0  IASTAR= 1  IASTOP=30  JASTAR= 1  JASTOP=19  ISASTR= 1  ISASTP=30  JSASTR= 1  JSASTP=19  MESHDN= 1  NPTS=   1
     NAREAS=   0  NREC=   0  IPRINF=   2  LGAUSS=T  LCHEM=T  LDRY=T  LWET=F  LPRINT=T  L3VL=T  LVSAMP=T  WSAMP=   4.00  LSGRID=T
     NSPEC= 2
     XREC=
     YREC=

GRIDDED RECEPTOR CONCENTRATIONS                                     YEAR: 83  DAY: 262  ENDING HOUR:  0  POLLUTANT:  1

MULTIPLY ALL VALUES BY 10 **  -3

19 \     0     0     0     0     0     0     0     0     0     0     0     0     0     0     0     0     0     0     0     0     0     0     0     0     0     0     0     0     0     0
   \     +     +     +     +     +     +     +     +     +     +     +     +     +     +     +     +     +     +     +     +     +     +     +     +     +     +     +     +     +     +
18 \     0     0     0     0     0     0     0     0     0     0     0     0     0     0     0     0     0     0     0     0     0     0     0     0     0     0     0     0     0     0
   \     +     +     +     +     +     +     +     +     +     +     +     +     +     +     +     +     +     +     +     +     +     +     +     +     +     +     +     +     +     +
17 \     0     0     0     0     0     0     0     0     0     0     0     0     0     0     0     0     0     0     0     0     0     0     0     0     0     0     0     0     0     0
   \     +     +     +     +     +     +     +     +     +     +     +     +     +     +     +     +     +     +     +     +     +     +     +     +     +     +     +     +     +     +
16 \     0     0     0     0     0     0     0     0     0     0     0     0     0     0     0     0     0     0     0     0     0     0     0     0     0     0     0     0     0     0
   \     +     +     +     +     +     +     +     +     +     +     +     +     +     +     +     +     +     +     +     +     +     +     +     +     +     +     +     +     +     +
15 \     0     0     0     0     0     0     0     0     0     0     0     0     0     0     0     0     0     0     0     0     0     1     5    19    23     7     0     0     0     0
   \     +     +     +     +     +     +     +     +     +     +     +     +     +     +     +     +     +     +     +     +     +     +     +     +     +     +     +     +     +     +
14 \     0     0     0     0     0     0     0     0     0     0     0     0     0     0     0     0     0     0     9    24    40    76   122   180   150    43     5     0     0     0
   \     +     +     +     +     +     +     +     +     +     +     +     +     +     +     +     +     +     +     +     +     +     +     +     +     +     +     +     +     +     +
13 \     0     0     0     0     0     0     0     0     0     0     0     0     0     0     0    13    75   213   356   408   367   363   320   301   199    60     9     1     0     0
   \     +     +     +     +     +     +     +     +     +     +     +     +     +     +     +     +     +     +     +     +     +     +     +     +     +     +     +     +     +     +
12 \     0     0     0     0     0     0     0     0     0     0     0     0     1    51   223   516   829  1027   897   603   349   232   147   131   113    70    29    13     6     2
   \     +     +     +     +     +     +     +     +     +     +     +     +     +     +     +     +     +     +     +     +     +     +     +     +     +     +     +     +     +     +
11 \     0     0     0     0     0     0     0     0     0     0     0     9   292   941  1272  1257   766   441   281   180   130   129   146   181   207   183   120    78    32     9
   \     +     +     +     +     +     +     +     +     +     +     +     +     +     +     +     +     +     +     +     +     +     +     +     +     +     +     +     +     +     +
10 \     0     0     0     0     0     0     0     0     0     0    97  1015  1461  1697  1170   428   174   225   164    91   235   429   505   590   605   467   283   155    69    19
   \     +     +     +     +     +     +     +     +     +     +     +     +     +     +     +     +     +     +     +     +     +     +     +     +     +     +     +     +     +     +
 9 \     0     0     0     0     0     0     0     0     0   344  1622  1753  1950   678   195   295   178   105    45   370  1519  2017  1401  1085   873   552   281   140    62    18
   \     +     +     +     +     +     +     +     +     +     +     +     +     +     +     +     +     +     +     +     +     +     +     +     +     +     +     +     +     +     +
 8 \     0     0     0     0     0     0     0     0   299  2051  1975  1249  1258   471   157    77   114   164   595  1999  3419  2775  1234   618   404   228   106    52    24     8
   \     +     +     +     +     +     +     +     +     +     +     +     +     +     +     +     +     +     +     +     +     +     +     +     +     +     +     +     +     +     +
 7 \     0     0     0     0     0     0     0     0  5364  2780  2415  1108   528   920  1339  1618  2086  2687  2904  2644  1775  1049   395   123    61    33    15     8     4     2
   \     +     +     +     +     +     +     +     +     +     +     +     +     +     +     +     +     +     +     +     +     +     +     +     +     +     +     +     +     +     +
 6 \     0     0     0     0     0     0     0  6123  5138  2851   815   666   707  1259   628  1219  2959  2570  1371   749   470   287    80     9     2     1     1     0     0     0
   \     +     +     +     +     +     +     +     +     +     +     +     +     +     +     +     +     +     +     +     +     +     +     +     +     +     +     +     +     +     +
 5 \     0     0     0     0     0     0  8950  1366   686     0     0     0     0     4    14   593  1958   504   503   360   143    50     8     0     0     0     0     0     0     0
   \     +     +     +     +     +     +     +     +     +     +     +     +     +     +     +     +     +     +     +     +     +     +     +     +     +     +     +     +     +     +
 4 \     0     0     0     0     0  1999    46     0     0     0     0     0     0     0     0    21   159   148   324    55     4     0     0     0     0     0     0     0     0     0
   \     +     +     +     +     +     +     +     +     +     +     +     +     +     +     +     +     +     +     +     +     +     +     +     +     +     +     +     +     +     +
 3 \     0     0     0     0     0     0     0     0     0     0     0     0     0     0     0     0     0     6    14     0     0     0     0     0     0     0     0     0     0     0
   \     +     +     +     +     +     +     +     +     +     +     +     +     +     +     +     +     +     +     +     +     +     +     +     +     +     +     +     +     +     +
 2 \     0     0     0     0     0     0     0     0     0     0     0     0     0     0     0     0     0     0     0     0     0     0     0     0     0     0     0     0     0     0
   \     +     +     +     +     +     +     +     +     +     +     +     +     +     +     +     +     +     +     +     +     +     +     +     +     +     +     +     +     +     +
 1 \     0     0     0     0     0     0     0     0     0     0     0     0     0     0     0     0     0     0     0     0     0     0     0     0     0     0     0     0     0     0
   \     +     +     +     +     +     +     +     +     +     +     +     +     +     +     +     +     +     +     +     +     +     +     +     +     +     +     +     +     +     +
    ------------------------------------------------------------------------------------------------------------------------------------------------------------------------------------

         1     2     3     4     5     6     7     8     9    10    11    12    13    14    15    16    17    18    19    20    21    22    23    24    25    26    27    28    29    30
```

Figure 18. Average 24-h SO_2 concentration fields from the model base case run for a) Day 1 and b) Day 2. All values in units of μg m^{-3}.

```
GRIDDED RECEPTOR CONCENTRATIONS                          YEAR: 83  DAY: 263  ENDING HOUR:  8  POLLUTANT:  1

MULTIPLY ALL VALUES BY 10 **  -2

19 \     0    0    0    0    0    0    0    0    0    0    0    0    0    0    0    0    0    0    0    0    0    0    0    0    1    3    5    6    5    2
18 \     0    0    0    0    0    0    0    0    0    0    0    0    0    0    0    0    0    0    0    0    0    0    0    1    8   17   21   20   15    8
17 \     0    0    0    0    0    0    0    0    0    0    0    0    0    0    0    0    0    0    0    0    0    0    1    9   28   40   41   37   26   14
16 \     0    0    0    0    0    0    0    0    0    0    0    0    0    0    0    0    0    0    0    0    0    0    4   27   51   51   53   47   33   19
15 \     0    0    0    0    0    0    0    0    0    0    0    0    0    0    0    0    0    0    0    0    0    0   10   45   55   47   55   47   36   22
14 \     0    0    0    0    0    0    0    0    0    0    0    0    0    0    0    0    0    0    0    0    0    1   17   48   41   39   47   41   38   26
13 \     0    0    0    0    0    0    0    0    0    0    0    0    0    0    0    0    0    0    1    3    6   14   37   46   32   36   39   42   45   31
12 \     0    0    0    0    0    0    0    0    0    0    0    0    0    2    2    1    2   10   23   34   41   45   53   44   40   48   55   65   67   45
11 \     0    0    0    0    0    0    0    0    0    0    0    2   16   22   17   25   54   86   94   88   79   70   65   65   78   97  108  111  104   70
10 \     0    0    0    0    0    0    0    0    0    0    7   63   63   47   87  124  140  130  110   96   88   84   83   93  119  153  163  153  133   88
 9 \     0    0    0    0    0    0    0    0    0    7  180   95   26   78  180  262  218  160  132  122  117  125  139  156  166  174  164  138  110   69
 8 \     0    0    0    0    0    0    0    0    2  286  153   42  101  307  365  355  283  231  229  265  260  261  271  261  199  139  101   73   81   30
 7 \     0    0    0    0    0    0    0    0  353  171  108  273  440  379  310  302  321  359  420  434  367  305  271  222  135   68   37   22   13    7
 6 \     0    0    0    0    0    0    0  398  251  229  366  319  329  277  282  305  329  320  242  159  114   95   89   71   40   17    7    4    2    1
 5 \     0    0    0    0    0    0  795  365  309  121  196  225  171  152  123   89   58   33   16    7    5    7    9    8    4    1    0    0    0    0
 4 \     0    0    0    0    0 1376    2    0    0    0    0    0    0    1    0    0    0    0    0    0    0    0    0    0    0    0    0    0    0    0
 3 \     0    0    0    0    0    0    0    0    0    0    0    0    0    0    0    0    0    0    0    0    0    0    0    0    0    0    0    0    0    0
 2 \     0    0    0    0    0    0    0    0    0    0    0    0    0    0    0    0    0    0    0    0    0    0    0    0    0    0    0    0    0    0
 1 \     0    0    0    0    0    0    0    0    0    0    0    0    0    0    0    0    0    0    0    0    0    0    0    0    0    0    0    0    0    0
    \
     -------------------------------------------------------------------------------------------------------------------------------------------------------
         1    2    3    4    5    6    7    8    9   10   11   12   13   14   15   16   17   18   19   20   21   22   23   24   25   26   27   28   29   30
```

Figure 18b. Same as 18a, except for Day 2.

```
DATA READ FROM MESOPUFF OUTPUT FILE -- UNIT:  20  RUNSTREAM:    1
    VERSON=  4.0  LEVEL=870421  NSTR=83  NSDAY=261  NSHR= 0  NADVTS=   48  IAVG=    1  NPUF=  4  NSANAD=  4  IELMET=30  JELMET=19
    DGRID=  37000.0  IASTAR= 1  IASTOP=30  JASTAR= 1  JASTOP=19  ISASTR= 1  ISASTP=30  JSASTR= 1  JSASTP=19  MESHDN= 1  NPTS=   1
    NAREAS=   0  NREC=   0  IPRINF=   2  LGAUSS=T  LCHEM=T  LDRY=T  LWET=F  LPRINT=T  L3VL=T  LVSAMP=T  VSAMP=   4.00  LSGRID=T
    NSPEC= 2
    XREC=
    YREC=

GRIDDED RECEPTOR CONCENTRATIONS                                        YEAR: 83  DAY: 262  ENDING HOUR:  0  POLLUTANT:  2

MULTIPLY ALL VALUES BY 10 **  -6

19 \    0    0    0    0    0    0    0    0    0    0    0    0    0    0    0    0    0    0    0    0    0    0    0    0    0    0    0    0    0    0
   \    +    +    +    +    +    +    +    +    +    +    +    +    +    +    +    +    +    +    +    +    +    +    +    +    +    +    +    +    +    +
18 \    0    0    0    0    0    0    0    0    0    0    0    0    0    0    0    0    0    0    0    0    0    0    0    0    0    0    0    0    0    0
   \    +    +    +    +    +    +    +    +    +    +    +    +    +    +    +    +    +    +    +    +    +    +    +    +    +    +    +    +    +    +
17 \    0    0    0    0    0    0    0    0    0    0    0    0    0    0    0    0    0    0    0    0    0    0    0    0    0    0    0    0    0    0
   \    +    +    +    +    +    +    +    +    +    +    +    +    +    +    +    +    +    +    +    +    +    +    +    +    +    +    +    +    +    +
16 \    0    0    0    0    0    0    0    0    0    0    0    0    0    0    0    0    0    0    0    0    0    0    0    1    1    0    0    0    0    0
   \    +    +    +    +    +    +    +    +    +    +    +    +    +    +    +    +    +    +    +    +    +    +    +    +    +    +    +    +    +    +
15 \    0    0    0    0    0    0    0    0    0    0    0    0    0    0    0    0    0    0    0    0    0    4   18   51   57   16    1    0    0    0
   \    +    +    +    +    +    +    +    +    +    +    +    +    +    +    +    +    +    +    +    +    +    +    +    +    +    +    +    +    +    +
14 \    0    0    0    0    0    0    0    0    0    0    0    0    0    0    0    0    0    0   16   54  132  233  330  443  352   99   11    0    0    0
   \    +    +    +    +    +    +    +    +    +    +    +    +    +    +    +    +    +    +    +    +    +    +    +    +    +    +    +    +    +    +
13 \    0    0    0    0    0    0    0    0    0    0    0    0    0    0    0   21  125  331  561  744  680  896  767  685  437  133   20    2    0    0
   \    +    +    +    +    +    +    +    +    +    +    +    +    +    +    +    +    +    +    +    +    +    +    +    +    +    +    +    +    +    +
12 \    0    0    0    0    0    0    0    0    0    0    0    0    1   62  279  793 1365 1475 1252  906  634  463  321  294  263  178   89   48   26    7
   \    +    +    +    +    +    +    +    +    +    +    +    +    +    +    +    +    +    +    +    +    +    +    +    +    +    +    +    +    +    +
11 \    0    0    0    0    0    0    0    0    0    0    0    8  304 1043 1585 1896 1156  592  385  291  258  293  361  475  572  543  398  257  123   36
   \    +    +    +    +    +    +    +    +    +    +    +    +    +    +    +    +    +    +    +    +    +    +    +    +    +    +    +    +    +    +
10 \    0    0    0    0    0    0    0    0    0    0   80  939 1386 1876 1397  535  267  434  336  207  603 1138 1363 1613 1704 1397  935  563  263   74
   \    +    +    +    +    +    +    +    +    +    +    +    +    +    +    +    +    +    +    +    +    +    +    +    +    +    +    +    +    +    +
 9 \    0    0    0    0    0    0    0    0    0  255 1274 1443 1866  726  270  475  314  202   93  884 3750 5138 3687 2894 2389 1403  904  502  234   71
   \    +    +    +    +    +    +    +    +    +    +    +    +    +    +    +    +    +    +    +    +    +    +    +    +    +    +    +    +    +    +
 8 \    0    0    0    0    0    0    0    0  189 1465 1597 1010  849  482  227  112  169  273 1149 4291 7909 6827 3222 1650 1100  655  339  186   91   30
   \    +    +    +    +    +    +    +    +    +    +    +    +    +    +    +    +    +    +    +    +    +    +    +    +    +    +    +    +    +    +
 7 \    0    0    0    0    0    0    0    0 3126 1743 1067  486  470  931 1423 1877 2741 4174 5348 5353 3993 2581 1042  339  172   96   50   29   16    6
   \    +    +    +    +    +    +    +    +    +    +    +    +    +    +    +    +    +    +    +    +    +    +    +    +    +    +    +    +    +    +
 6 \    0    0    0    0    0    0    0 2594 2596 1280  376  419  521 1011  594 1193 3699 3969 2431 1444 1031  495  208   26    8    4    2    2    1    1
   \    +    +    +    +    +    +    +    +    +    +    +    +    +    +    +    +    +    +    +    +    +    +    +    +    +    +    +    +    +    +
 5 \    0    0    0    0    0    0 2372  349  109    0    0    0    0    3   12  590 2261  487  697  581  287  115   19    0    0    0    0    0    0    0
   \    +    +    +    +    +    +    +    +    +    +    +    +    +    +    +    +    +    +    +    +    +    +    +    +    +    +    +    +    +    +
 4 \    0    0    0    0    0  262    5    0    0    0    0    0    0    0    0   20  168  144  381   75    7    0    0    0    0    0    0    0    0    0
   \    +    +    +    +    +    +    +    +    +    +    +    +    +    +    +    +    +    +    +    +    +    +    +    +    +    +    +    +    +    +
 3 \    0    0    0    0    0    0    0    0    0    0    0    0    0    0    0    0    0    6   15    0    0    0    0    0    0    0    0    0    0    0
   \    +    +    +    +    +    +    +    +    +    +    +    +    +    +    +    +    +    +    +    +    +    +    +    +    +    +    +    +    +    +
 2 \    0    0    0    0    0    0    0    0    0    0    0    0    0    0    0    0    0    0    0    0    0    0    0    0    0    0    0    0    0    0
   \    +    +    +    +    +    +    +    +    +    +    +    +    +    +    +    +    +    +    +    +    +    +    +    +    +    +    +    +    +    +
 1 \    0    0    0    0    0    0    0    0    0    0    0    0    0    0    0    0    0    0    0    0    0    0    0    0    0    0    0    0    0    0
   \    +    +    +    +    +    +    +    +    +    +    +    +    +    +    +    +    +    +    +    +    +    +    +    +    +    +    +    +    +    +
    ----------------------------------------------------------------------------------------------------------------------------------------------------

        1    2    3    4    5    6    7    8    9   10   11   12   13   14   15   16   17   18   19   20   21   22   23   24   25   26   27   28   29   30
```

Figure 19. Average 24-h sulfate concentration fields from the model base case run for a) Day 1 and b) Day 2. All values in units of $\mu g\ m^{-3}$.

```
GRIDDED RECEPTOR CONCENTRATIONS                                    YEAR: 83  DAY: 263  ENDING HOUR: 0  POLLUTANT: 2

MULTIPLY ALL VALUES BY 10 **  -6

19 \     0     0     0     0     0     0     0     0     0     0     0     0     0     0     0     0     0     0     0     0     0     0     0     1    22    72   124   147   116    42
   \     +     +     +     +     +     +     +     +     +     +     +     +     +     +     +     +     +     +     +     +     +     +     +     +     +     +     +     +     +     +
18 \     0     0     0     0     0     0     0     0     0     0     0     0     0     0     0     0     0     0     0     0     0     0     0    28   158   357   467   473   359   197
   \     +     +     +     +     +     +     +     +     +     +     +     +     +     +     +     +     +     +     +     +     +     +     +     +     +     +     +     +     +     +
17 \     0     0     0     0     0     0     0     0     0     0     0     0     0     0     0     0     0     0     0     0     0     0    12   153   519   784   858   812   623   366
   \     +     +     +     +     +     +     +     +     +     +     +     +     +     +     +     +     +     +     +     +     +     +     +     +     +     +     +     +     +     +
16 \     0     0     0     0     0     0     0     0     0     0     0     0     0     0     0     0     0     0     0     0     0     0    67   444   892   956  1078  1021   813   518
   \     +     +     +     +     +     +     +     +     +     +     +     +     +     +     +     +     +     +     +     +     +     +     +     +     +     +     +     +     +     +
15 \     0     0     0     0     0     0     0     0     0     0     0     0     0     0     0     0     0     0     0     0     0     4   155   712   942   899  1151  1109   992   679
   \     +     +     +     +     +     +     +     +     +     +     +     +     +     +     +     +     +     +     +     +     +     +     +     +     +     +     +     +     +     +
14 \     0     0     0     0     0     0     0     0     0     0     0     0     0     0     0     0     0     0     0     0     1    18   251   736   745   855  1121  1182  1249   897
   \     +     +     +     +     +     +     +     +     +     +     +     +     +     +     +     +     +     +     +     +     +     +     +     +     +     +     +     +     +     +
13 \     0     0     0     0     0     0     0     0     0     0     0     0     0     0     1     0     0     1    28    63    94   185   520   723   696   945  1159  1428  1639  1181
   \     +     +     +     +     +     +     +     +     +     +     +     +     +     +     +     +     +     +     +     +     +     +     +     +     +     +     +     +     +     +
12 \     0     0     0     0     0     0     0     0     0     0     0     0     6    35    42    20    44   199   437   604   635   626   738   780  1004  1428  1780  2204  2372  1684
   \     +     +     +     +     +     +     +     +     +     +     +     +     +     +     +     +     +     +     +     +     +     +     +     +     +     +     +     +     +     +
11 \     0     0     0     0     0     0     0     0     0     0     0    28   220   366   319   382   814  1404  1612  1488  1256  1052  1016  1292  2000  2830  3359  3647  3547  2471
   \     +     +     +     +     +     +     +     +     +     +     +     +     +     +     +     +     +     +     +     +     +     +     +     +     +     +     +     +     +     +
10 \     0     0     0     0     0     0     0     0     0     0    78   650   805   688  1175  1867  2274  2174  1863  1658  1580  1612  1885  2543  3640  4815  5316  5134  4494  2978
   \     +     +     +     +     +     +     +     +     +     +     +     +     +     +     +     +     +     +     +     +     +     +     +     +     +     +     +     +     +     +
 9 \     0     0     0     0     0     0     0     0     0    70  1439  1052   630  1287  2982  3731  2844  2182  2006  2097  2414  3200  4387  5444  6162  6302  5895  4968  3851  2367
   \     +     +     +     +     +     +     +     +     +     +     +     +     +     +     +     +     +     +     +     +     +     +     +     +     +     +     +     +     +     +
 8 \     0     0     0     0     0     0     0     0     5  1392  1420   734  1576  3993  4743  4196  3399  2914  3564  4810  5676  7008  8901  9757  7843  5527  3994  2842  1930  1087
   \     +     +     +     +     +     +     +     +     +     +     +     +     +     +     +     +     +     +     +     +     +     +     +     +     +     +     +     +     +     +
 7 \     0     0     0     0     0     0     0     0  1465  1512  1454  1048  4362  3174  2540  2864  3529  4580  6389  7775  7815  8020  8750  8212  5406  2860  1582   942   553   277
   \     +     +     +     +     +     +     +     +     +     +     +     +     +     +     +     +     +     +     +     +     +     +     +     +     +     +     +     +     +     +
 6 \     0     0     0     0     0     0     0  1421  1708  2315  3225  1960  1983  1757  2079  2552  3147  3550  3274  2782  2490  2614  2949  2687  1654   763   349   178    87    35
   \     +     +     +     +     +     +     +     +     +     +     +     +     +     +     +     +     +     +     +     +     +     +     +     +     +     +     +     +     +     +
 5 \     0     0     0     0     0     0  2025  2221  1231   809  1668  1860  1263  1115   918   695   490   318   181   118   131   204   314   322   197    65    22     8     0     0
   \     +     +     +     +     +     +     +     +     +     +     +     +     +     +     +     +     +     +     +     +     +     +     +     +     +     +     +     +     +     +
 4 \     0     0     0     0     0  2074     5     0     0     0     0     0     3     4     2     0     0     0     0     0     0     0     2     2     0     0     0     0     0     0
   \     +     +     +     +     +     +     +     +     +     +     +     +     +     +     +     +     +     +     +     +     +     +     +     +     +     +     +     +     +     +
 3 \     0     0     0     0     0     0     0     0     0     0     0     0     0     0     0     0     0     0     0     0     0     0     0     0     0     0     0     0     0     0
   \     +     +     +     +     +     +     +     +     +     +     +     +     +     +     +     +     +     +     +     +     +     +     +     +     +     +     +     +     +     +
 2 \     0     0     0     0     0     0     0     0     0     0     0     0     0     0     0     0     0     0     0     0     0     0     0     0     0     0     0     0     0     0
   \     +     +     +     +     +     +     +     +     +     +     +     +     +     +     +     +     +     +     +     +     +     +     +     +     +     +     +     +     +     +
 1 \     0     0     0     0     0     0     0     0     0     0     0     0     0     0     0     0     0     0     0     0     0     0     0     0     0     0     0     0     0     0
   \     +     +     +     +     +     +     +     +     +     +     +     +     +     +     +     +     +     +     +     +     +     +     +     +     +     +     +     +     +     +
    ---------------------------------------------------------------------------------------------------------------------------------------------------------------------------------------

         1     2     3     4     5     6     7     8     9    10    11    12    13    14    15    16    17    18    19    20    21    22    23    24    25    26    27    28    29    30
```

Figure 19b. Same as 19a, except for Day 2.

TABLE 29

RESULTS OF MODEL SENSITIVITY RUNS: COMPARISONS WITH 24-HOUR BASE CASE PEAK AND MEAN CONCENTRATIONS

MODEL RUN	VARIATION IN PEAK SO_2 $(C_b - C_t)/C_b$ (%)		VARIATION IN PLUME AVERAGE SO_2 $(C_b - C_t)/C_b$ (%)	
	DAY 1	DAY 2	DAY 1	DAY 2
BASE CASE	----	----	----	----
No Dep. only	-1.6	-0.6	-15.5	-24.6
No Transf. only	-1.2	-0.5	-7.2	-8.8
No Vert. Gauss. Distribution*	-168.5	-97.7	3.2	25.9
1-layer mode*	-0.1	0.0	-2.4	-2.9
	PEAK SO_4 $(C_b - C_t)/C_b$ (%)		PLUME AVERAGE SO_4 $(C_b - C_t)/C_b$ (%)	
BASE CASE	----	----	----	----
No Dep. only	-8.4	-28.5	-8.6	-17.4
No Transf. only	91.3	89.3	93.1	94.0
No Vert. Gauss. Distribution*	22.6	21.5	14.7	26.5
1-layer mode*	0.0	0.0	-1.7	-1.9

NOTE: C_b - base case concentration
C_t - test case concentration
* Both deposition and transformation applied as in default mode

impact on SO_2. However, there was a greater effect on the average SO_2 concentrations since these values were derived over the entire plume pattern. For example, in the model run where no deposition was permitted, the average plume concentration on Day 2 was nearly 25% higher than the base case concentrations. The results in the case with no SO_2 loss by chemical transformation indicated that the mean plume concentrations were less than 10% greater than the base case. On the otherhand, it is evident from Table 29 that transformation has a much greater impact on SO_4, as peak concentrations without transformation were around 90% lower than those in the base case. In this simulation, the peak SO_4 concentrations were located from 500-700 km downwind of the source position.

Other results in Table 29 are from the model test run with no vertical Gaussian dispersion (i.e. uniform vertical mixing). In this case, peak SO_2 concentrations were particularly sensitive to the type of vertical dispersion technique. Peak values were substantially higher than those in the base case using the Gaussian vertical dispersion parameter because the plume became distributed immediately through the entire mixed-layer under this optional method. Since this option feature produced higher peak concentrations and slightly greater deposition near the source, lower mean plume concentrations were obtained. For Day 2, the impact on the mean concentration is comparable, except in an opposite sense to the results without deposition. Peak and mean SO_4 concentrations were reduced under this dispersion option. In particular, the peak SO_4 concentration for both days was more than 20% lower than the base case values. In contrast, there appeared to be little impact on peak and mean concentrations in the 1-layer model mode where the source depletion method for dry deposition was applied as pollutant mass over the entire vertical extent of the plume was subjected to dry removal.

Additional model test runs were performed to determine the impact of prescribed changes in r_s for SO_2 and sulfate. The processor results indicated that PGT class 4 (neutral) was often determined to represent the stability during the afternoon periods. The surface resistances for SO_2 for the various land use categories is 100 s/m for the unstable classes and 300 s/m for neutral stability. During the daytime period, r_s is generally the dominant resistance to pollutant uptake since the sum of the two atmospheric resistances are often much less than r_s. A model run was performed with r_s redefined to be 100 s/m for neutral class, which essentially was an attempt designate these cases as being unstable in the model. However, the results in Table 30 show that the effects of this change are rather small on the peak and plume average concentrations of SO_2 and SO_4. On the otherhand, the results for a test run where the default value of r_s for SO_4 was modified from its default value of 1000 s/m to 100 s/m reveal comparable impacts on peak and mean SO_4 concentrations. No differences occurred in SO_2 values, but the peak and plume average SO_4 concentrations for this model run were between 15-20% lower than base case values. The current default r_s value limits the maximum V_d for sulfate to 0.1 cm s^{-1}, which might be too low based on some experimental results and the analysis reported by Morris et al. (1988). Thus, a refinement in the formulation for r_s for SO_4 appears to be warranted.

The background ozone concentration (O_{3bg}) is an important parameter

TABLE 30

RESULTS OF SENSITIVITY RUNS FROM VARIATIONS IN SELECT KEY TECHNICAL PARAMETERS IN THE MODEL

MODEL RUN	VARIATION IN PEAK SO_2 $(C_b - C_t)/C_b$ (%)		VARIATION IN PLUME AVERAGE SO_2 $(C_b - C_t)/C_b$ (%)	
	DAY 1	DAY 2	DAY 1	DAY 2
BASE CASE	----	----	----	----
modified r_s (SO_2)	1.8	0.01	4.5	4.4
modified r_s (SO_4)	0	0	0	0
O_{3bg} = 40 ppb	-0.3	-0.2	-1.5	-1.7
O_{3bg} = 120 ppb	0.3	0.1	1.2	1.4
stack z_s = 150m	-147.7	-210.3	-37.2	-20.3
	PEAK SO_4 $(C_b - C_t)/C_b$ (%)		PLUME AVERAGE SO_4 $(C_b - C_t)/C_b$ (%)	
BASE CASE	----	----	----	----
modified r_c(SO_2)	1.2	2.7	1.4	2.3
modified r_s(SO_4)	17.0	18.2	15.8	18.5
O_{3bg} = 40 ppb	19.0	18.0	19.1	18.2
O_{3bg} = 120 ppb	-16.0	-15.0	-16.1	-15.2
stack z_s = 150 m	21.0	30.1	1.1	4.4

NOTE: O_{3bg} - background ozone concentration
r_s - surface resistance
z_s - height above ground of stack top

in the determination of the transformation rate (k). Clearly, ozone generally exbihits a strong diurnal variation and large differences in ozone levels occur between air masses. Consequently, model test runs were conducted to assess concentration differences to a ±50% variation in $O_{3_{bg}}$ from its current default value of 80 ppb. In fact, k is larger by a factor of two when $O_{3_{bg}}$ = 120 ppb compared to 40 ppb with all other parameters being equal (Morris et al., 1987). The results for these model runs in Table 30 reveal little effect on SO_2, however, the changes in SO_4 peak and mean concentrations are more important. Rather clean and polluted air masses are represented by $O_{3_{bg}}$ being 40 and 120 ppb, respectively. Peak and plume average SO_4 concentrations in the test cases appeared to be equally affected, as results with $O_{3_{bg}}$ = 40 ppb were 18-19% lower and those with $O_{3_{bg}}$ = 120 ppb were 15-16% higher than base case values. Thus, the sulfate concentration levels were fairly sensitive to variations in $O_{3_{bg}}$ values with this transformation method, Therefore, representative ozone levels from measurements made within the model domain should be input for particular applications.

The height of a pollutant release has a strong influence on the ground-level concentrations; the rationale for higher stacks during the past two decades was that peak concentration reductions would be produced with higher stack heights (z_s). A model run was performed with z_s = 150 m, which is approxiately one-half the height of the stack used in the base case. The final results shown in Table 30 reveal that peak SO_2 concentrations indeed were considerably higher on both days compared to base case values, while increases in the plume mean SO_2 concentrations were not as dramatic. A notable result with the lower stack, however, is that peak sulfate values were 21% and 30% lower than base case peak values on Day 1 and 2, respectively. Thus, the change in stack heights may also have had an impact on secondary pollutant levels.

It is recognized that these results represent only a small subset of a much larger group of possible model test runs which could explore the effects more features and variations in the numerous parameters incorporated into the current model. However, these limited set of model runs present a clearer picture of the impact on modeled concentrations when an important process is excluded or when certain key technical parameters in the dry deposition and chemical transformation methods are modified. More evaluation and testing efforts of this modeling system are certainly advocated.

SECTION 6

SUMMARY AND CONCLUSIONS

The MESOPUFF II regional Lagrangian model has been evaluated and tested with measurements from six full-scale CAPTEX episodes to assess its ability to simulate long-range transport and dispersion of an inert, non-depositing tracer plume. A neutrally-buoyant tracer gas was released over a 3-hour period from ground-level during four cases from Dayton, Ohio and during two cases from Sudbury, Ontario under fair weather conditions.

The results revealed that the model overpredicted both mean and peak concentrations. The overpredictions were most pronounced for the Dayton releases at the first two sampling arcs. Since differences in horizontal plume spread were not evident during the first day of transport, it was concluded that the primary cause for the model overpredictions was an underestimation of vertical plume growth for neutral stability, which was the stability class most often specified during the afternoon release periods. It is suggested that a different dispersion formula for the Gaussian vertical dispersion parameter for neutral conditions (the D1 curve established by Pasquill (1974)) be incorporated and tested within the current framework of the model. This revision would provide for more rapid vertical plume spread with the default Gaussian dispersion distance-dependent scheme under neutral conditions, a stability class frequently selected from the widely-used methodology by this model and others.

The statistical results also showed that large scatter and low correlations occurred between modeled and observed concentrations paired in time and space for both mean and peak values. This reflected the inability of this model, like other similar models, to accurately replicate the speed and/or direction of the tracer plume. Thus, the large concentration differences where observed and modeled plumes did not overlap were primarily attributed to trajectory errors. However, the statistical analyses did not provide sufficient information for an assessment of the causes for model errors in transport.

Graphical displays and a technique to determine plume centroid positions, which indicated the size of the spatial plume differences, greatly assisted in characterizing model trajectory errors. Spatial displacements of varying amounts were evident from graphical maps of modeled and observed plume patterns with time. Plume centroid positions, derived as the concentration-weighted locations from non-zero values at 6-hour intervals, were used in quantifying differences in the downwind distance and the separation distance between observed and modeled plumes. Specifically, results from MESOPUFF II indicated that the observed plume moved faster and/or along a different path during the nocturnal period and was generally found further downwind of the modeled plume by the second daytime period in these episodes. The plume separation distance, the difference in centroid locations between the observed and modeled plumes, ranged from 100-300 km during these cases at downwind distances of 500-1000 km. The most rapid increase in plume separation also occurred during the nocturnal periods.

The CAPTEX tracer emissions consisted of non-buoyant, ground-level releases. For this source type, puff heights in MESOPUFF II were always less than the mixing height which caused modeled plumes to be continually transported by the lower layer wind field. This feature is believed to be a shortcoming of the model design, especially during the nocturnal period when greater vertical shears in speed and direction often prevail. It was concluded from analyses of the plume centroid positions that the modeled plumes must have been advected by slower winds derived over the shallow mixed layer at night, while observed plumes had been transported along a different trajectory by faster winds at higher levels. In the case of an elevated source emitting a buoyant plume which rises to even higher levels, the model would have switched the plume transport at night to the upper layer wind field when the mixing height dropped below the height of the puff center. Based on these results, model applications for multi-day simulations of ground-level, non-buoyant point emissions are not recommended. The model's treatment for this source type could be improved if the height of the puff center after release was redefined to be one-half of its vertical dimension and this revised puff center height reached a limit when vertical puff growth extended up to the mixing height.

Four other regional-scale models have also been applied on two or all of the CAPTEX episodes with results being reported in the literature. These models contained greater sophistication in transport (e.g. more vertical layers) and different dispersion techniques. Unfortunately, comparable statistical measures and plume displacement parameters were not reported for three of the four models and an extensive comparison could not be made. Nevertheless, the available results for the other models also displayed large variabilities when observed and modeled concentrations were compared and concentration differences were primarily attributed to spatial discrepancies in plume patterns due to trajectory errors.

The most extensive results with CAPTEX data were reported by Draxler (1987) who tested a Lagrangian puff model which utilized several wind layers and permitted puff splitting. Observed-modeled plume separation distances with this model appeared to be smaller than those for MESOPUFF II, especially for the cases exhibiting the greatest speed and directional shears. However, plumes simulated by MESOPUFF II appeared to be displaced to the same side with respect to the observed plumes (i.e. either to the right or left) as those with the multi-layer model. Draxler (1987) reported that average spatial displacements for the 24-42 hour period after each release varied from 90-189 km among the CAPTEX episodes, while individual separation distances with MESOPUFF II were found to be 100-300 km as noted above. It must be noted, however, that Draxler's model runs included rawinsonde profile data obtained at 6-hour intervals during CAPTEX. Better temporal resolution of flow fields was translated into reduced trajectory errors when the more frequent upper-air profile data and higher spatial resolution of observed data were included in his model simulations. These supplemental profiles were not used in the MESOPUFF II model simulations since they are not available on a routine basis for model applications.

Qualitatively, the results from MESOPUFF II appeared to be competitive with those of the other models. Therefore, radical changes of MESOPUFF II and its processors are probably not warranted that could eliminate its advantages of being computationally practical and easy to use for single sources. Indeed, the model should be expected to perform better for a ground-level point source if revisions identified earlier are instituted. The feasibility of puff splitting within the current model's framework should also be explored as a step toward better addressing directional shear-induced dispersion.

Any firm judgment of the comparative capabilites of the models for general application was not possible based on the reported CAPTEX results. If conclusions could have been made, they would necessarily be tempered by the rather small number of cases, the specific source characteristics, and the narrow set of meteorological scenarios during CAPTEX. Consequently, a simultaneous evaluation of MESOPUFF II and a hierarchy of other models using an agreed upon set of evaluation measures with a broader data base(s), which should include elevated point source data, is certainly needed to provide definitive evidence of relative model performance. In the interim, the MESOPUFF II model should continue to be considered a useful modeling tool for short-term, regional applications.

Diagnostic tests of optional features in the model provided distinct differences in plume transport and dispersion from the default methods. The mixed-layer averaged wind field (i.e. default lower level wind field) was found to be superior to single level wind fields at the surface or 850 mb height in simulating the impact time and location of the tracer plume at the 300 km arc. Results suggested that it should remain as the preferred wind field for representing boundary layer transport when applying this model. Model test run results with the uniform vertical mixing option indicated that peak concentrations were much closer to observed values than those from the default Gaussian dispersion parameter methods. With the uniform vertical mixing method, puffs are completely dispersed through the entire extent of the boundary layer after release. These test results gave more evidence that modeled plumes required greater vertical mixing during the afternoon release periods. In lieu of the suggested revision to the Gaussian dispersion scheme noted earlier, the selection of this optional dispersion method appears to be an attractive alternative since it produces the desired vertical dispersion when neutral conditions are prevalent.

A limited group of model sensitivity runs was also performed in an effort to examine the impact on 24-h peak and plume average SO_2 and sulfate concentrations from variations in certain key parameters and changes in methods in the dry deposition and chemical transformation components of the model. The model base case and test case runs were exercised with the same meteorological fields from CAPTEX #1 and the same emission rates from a large, elevated point source. Results showed that sulfate concentrations were more sensitive to the selected variation in a parameter or method. In particular, sensitivity run results with differences in the surface SO_4 resistance or ±50% differences in background ozone concentration produced negligible variations in SO_2 peak and mean concentrations; however, the impact on sulfate concentrations was from 15-20%. This finding is particularly relevant to regional model applications since the higher concentration levels for sulfate were found at much greater downwind distances than was SO_2. It follows that SO_4 is influenced to a greater extent by transformation and deposition processes. A more extensive evaluation of these modules is advocated with suitable experimental data.

REFERENCES

Benkley, C. W. and A. Bass, 1979: Development of mesoscale air quality simulation models; Vol. 3. User's guide to MESOPUFF. EPA/600/7-80-058, U.S. Environmental Protection Agency, Available as NTIS PB80-227796.

Brown, R., M. Leach, G. Raynor, and P. Michael, 1985: A summary of the weather documentation for the 1983 Cross-Appalachian Tracer Experiments. Atmospheric Sciences Division, Brookhaven National Laboratory, Upton, New York 11973.

Clark, T. L., R. Cohn, S. Seilkop, R. Draxler, and J. Heffter, 1988: Comparison of modeled and measured tracer gas concentrations during the Across North America Tracer Experiment (ANATEX). Paper at the 17th International Techn. Meeting of NATO-CCMS on Air Poll. Modeling and Its Application, Cambridge, Engl., Sept. 19-22, 1988, 13 pp.

Davis., W. E., A. R. Olson, B.T. Didier, and D. W. Damschen, 1986: A comparison of meso-alpha MLAM model results with observations from CAPTEX. Preprints, Fifth Joint Conf. on Applications of Air Poll. Meteorol., Amer. Meteorol. Soc., Boston, MA., p.69-72.

Draxler, R.R., 1987: Sensitivity of a trajectory model to spatial and temporal resolution of the meteorological data during CAPTEX. J. Clim. and Appl. Meteorol.,26, 1577-1588.

Ferber, G. J., J. L. Heffter, R. R. Draxler, R. J. Lagomarsino, F. L. Thomas, R. N. Dietz, and C. M. Benkovitz, 1986: Cross-Appalachian Tracer Experiment (CAPTEX 83). Final Report NOAA Tech. Memo. ERL ARL-142, Air Resources Laboratory, Silver Spring, MD.

Gelinas, R. J., and J. P. Vayk, 1979: Systematic sensitivity analysis of air quality simulation models. EPA/600/4-79-035. U. S. Environmental Protection Agency.

Hales, J. M., B. B. Hicks, and J. M. Miller, 1987: The role of research measurement networks as contributors to federal assessments of acid deposition. Bull. Amer. Meteorol. Soc.,68, 216-225.

Heffter, J. L., 1965: The variation of horizontal diffusion parameters with time for travel periods of one hour or longer. J. Appl.Meteorol., 4, 153-156.

Kao C. and T. Yamada, 1988: Use of the CAPTEX data for evaluations of a long-range trnasport numerical model with a four-dimensional data assimilation technique. Mon. Wea. Rev., 116, 293-306.

Lagomarsino, R. J., F. L. Thomas, T. J. Weber, and L. R. Greenfield, 1987: Cross-Appalachian Tracer Experiment (CAPTEX 83) Quality Assurance of Surface Samples. Environmental Measurements Lab., EML-462, New York, New York 10014.

Lee, I. Y., 1987: Numerical simulations of Cross-Appalachian transport and diffusion. Boundary-Layer Meteorol., 39, 53-66.

Morris, R. E., R. C. Kessler, S. G. Douglas, and K. R. Styles, 1988: Rocky mountain acid deposition model assessment: Evaluation of mesoscale deposition models for use in complex terrain. EPA/600/3-88-088. U. S. Environmental Protection Agency. Available as NTIS PB88-167 481.

Page, S. H., 1980: National land and land cover inventory. U. S. Environmental Protection Agency, Washington, D.C.

Pasquill, F., 1974: Atmospheric Diffusion (2nd Edition). Ellis Horwood Ltd., Chichester, Engl. 228pp.

Policastro, A. J., M. Wastag, L. Coke, R. A. Carhart, W. E. Dunn, 1986: Evaluation of short-term long range transport models (Vol I, II). EPA-450/4-86-016a, b. U. S. Environmental Protection Agency. Available as NTIS documents PB87-142337, PB87-142345.

Raynor, G. S., R. N. Dietz, and T. W. D'Ottavio, 1984: Aircraft measurements of tracer gas during the 1983 Cross-Appalachian Tracer Experiment. Proc. of Fourth Joint Conf. on Applications of Air Pollution Meteorol., Amer. Meterol. Soc., Boston, MA, 162-165.

Scire, J. S., F. W. Lurmann, A. Bass, S. R. Hanna, 1984a: Development of the MESOPUFF II dispersion model. EPA/600/3-84-057, Environmental Protection Agency, Research Triangle Park, NC. Available as NTIS PB No. 84-183 753.

Scire, J. S., F. W. Lurmann, A. Bass, and S. R. Hanna, 1984b: User's Guide to the MESOPUFF II model and related processor programs. EPA/600/8-84-013, Environmental Protection Agency, Research Triangle Park, NC. Available as NTIS PB No. 84-182 775.

Sheih, C. M., M. L. Wesely, and B. B. Hicks, 1979: Estimated dry deposition velocities of sulfur over the eastern United States and surrounding regions. Atmos. Environ.,13, 1361-1368.

Shreffler, J. H., 1982: Intercomparisons of upper air and surface winds in an urban region. Boundary-Layer Meteorol.,24, 345-356.

Stunder, B. J. B., J. L. Heffter, and R. R. Draxler, 1986: Long range transport model evaluation using CAPTEX aircraft and surface data. Vertical tracer distribution. Preprints, Fifth Joint Conf. on Applications of Air Pollution Meteorol., Amer. Meteorol. Soc., Boston, MA., 65-68.

Turner, D. B., 1964: A diffusion model for an urban area. J. Appl. Meteorol.,3, 83-91.

Turner, D. B., 1970: Workbook of atmospheric dispersion estimates.

Publ. No. AP-26, Office of Air Programs, U. S. Environmental Protection Agency., 84 pp. Available as NTIS PB 191 482.

Walcek, C. J., R. A. Brost, J. S. Chang, and M. L. Wesely, 1986: SO_2, sulfate and HNO_3 deposition velocities computed using regioanl land use and meteorological data. Atmos. Environ.,20, 949-964.

Wilson, W. E., 1981: Sulfate formation in point source plumes: A review of recent field studies. Atmos. Environ., 15, 2573-2590.

APPENDIX A

MODEL TEST RESULTS FOR DIFFERENT PUFF RELEASE/SAMPLING RATES

A series of MESOPUFF II model runs for the CAPTEX #1 case was performed with various puff release and sampling rates. The results presented below were generated from peak tracer concentration values at the initial tracer measurement arc at 300 km where the highest concentrations were found. An average peak concentration value (CAVE) was computed from the results of each model test runs and the individual peak concentrations were normalized by this average value to determine the amount of difference among the test runs. Differences over this set of puff release/sampling rates indicated relatively little sensitivity to the peak concentrations at this distance under the conditions of this experiment. Similar test runs are advocated in other applications to determine sensitivity of modeled concentrations to these rates.

TABLE 1A

DIFFERENCES IN PEAK VALUES AT THE INITIAL ARC
FOR DIFFERENT PUFF RELEASE/SAMPLING RATES

RUN	RELEASE RATE (puffs/h)	SAMPLING RATE (#/h)	$C_{max}/CAVE_{max}$	CPU TIME (s)
1	2	2	0.997	12.7
2	2	4	0.966	22.1
3	4	2	1.020	22.4
4	4	4	0.984	41.0
5	8	2	1.023	41.8
6	12	2	1.024	61.6
7	12	4	0.986	117.6